RSC Advances

ROYAL SOCIETY OF CHEMISTRY

www.rsc.org/advances

Journal Name

ARTICLE

Structure guided drug-discovery approach towards identification of *Plasmodium* Inhibitors

Received 00th January 20xx,
Accepted 00th January 20xx

DOI: 10.1039/x0xx00000x

www.rsc.org/

Babita Aneja[a], Bhumika Kumar[a], Mohamad Aman Jairajpuri[b], Mohammad Abid[a]*

Rapidly increasing resistance to the currently available antimalarial drugs has drawn attention globally for the search of more potent novel drugs with high therapeutic index. The genome sequencing of human malarial parasite *Plasmodium falciparum* has provided extensive information to understand potential target pathways and efforts are being made to develop lead inhibitors with a hope to eliminate the disease. This review is focused on brief description of key biochemical targets identified from the genome sequence of *P. falciparum*. This review also summarized the work undertaken by different scientific groups since last five years to develop inhibitors from natural, semisynthetic or synthetic sources, which will be valuable to the medicinal chemists to develop novel antimalarial agents.

Keywords: *Plasmodium falciparum*; malaria; genome sequence; targets; inhibitors

Introduction

Despite global efforts to control and eradicate malaria, it is one of the most widespread and deadliest parasitic diseases affecting more than 40% of the world's population. [1] World Health Organization (WHO) factsheet for 2014 reveals more than 198 million cases with an estimated 584000 fatalities. The severity of this disease is prevalent in WHO African region with an estimated 90% mortality rate, affecting mainly the children under the age of 5, who account for 78% of all deaths. [2] This disease is mainly attributable to five species of malaria parasite i.e. *Plasmodium* which are known to infect humans - *P. falciparum*, *P. vivax*, *P. ovale*, *P. malariae* and *P. knowlesi.* Out of these, *P. falciparum* and *P. vivax* are biggest threat to public health. While *P. vivax* is widely distributed geographically, *P. falciparum* is reportedly more fatal. [3]

Though a number of antimalarial drugs such as quinine, artemisinin, artemether, artesunate, dihyroartemisinin, atovaquone, chloroquine, cinchonine, chlorproguanil, mefloquine, pyrimethamine, primaquine, piperaquine, sulfadoxine, amodiaquine, lumefantrine (Fig. 1) are available, these drugs are rapidly losing their therapeutic potential due to emerging drug resistance in *Plasmodium*. [4,5] The parasitic mutations associated with resistance to antimalarial drugs primarily contributes to the re-emergence of the disease and its spread to new places and populations. Although artemisinin-based combination therapy has been recommended by WHO as the first-line of treatment for multi-drug resistant *P. falciparum* infection which is non-responsive to quinoline and antifolate based drugs, [6] but the frequent use of artemisinin and its derivatives has also resulted in resistance to this class of drugs and the first signs of resistance have emerged in South-East Asian countries. [2,7] Thus, there is an urgent need to develop new therapeutic agents with novel mode of action to save people from the grasp of this deadly disease and to reduce morbidity and mortality.

Different approaches adopted till now by the scientific communities for antimalarial drug discovery are mainly based upon (a) combination of existing drugs (artemether-lumefantrine, amodiaquine-artesunate, dihyroartemisinin-piperaquine) (b) chemical modification of known drugs and compound classes (mefloquine, primaquine, chloroquine, artesunate) (c) "piggy back approach" for the compounds active against other diseases (antifolates, tetracyclines, atovaquone) (d) use of natural products (quinine, artemisinin) (e) use of drug resistance reversers (verapamil. desipramine, trifluoperazine) [8] (f) *in vitro* whole cell parasitic assay (KAE609 (formerly known as NITD609) and KAF156 under phase II clinical trials). [9] The most recent approach is the identification and validation of novel molecular targets and the development of inhibitors active against these targets. The accessibility of whole genome sequence of *P. falciparum* has facilitated the identification of potential targets for the development of new drugs and also shed light on the mechanism of action of older drugs. The validation of identified target is crucial for this approach and is carried out by repeated antiparasitic activity of different lead compounds against that particular target. Identification of potentially active compounds and their optimization subsequently results in lead candidates that are further taken to pre-clinical and clinical investigations. [10] Since the qualitative information of all the identified lead compounds and potential drug targets imparts impetus to the drug discovery programmes, this review aims to provide the same for antimalarial research boon. In this review, the antimalarial potential of various natural, semi-synthetic as well as synthetic compounds reported during the last 5 years (2010-2015) are compiled and discussed in target-oriented manner, which will provide a stand to medicinal chemists for the development of better antimalarial therapeutics.

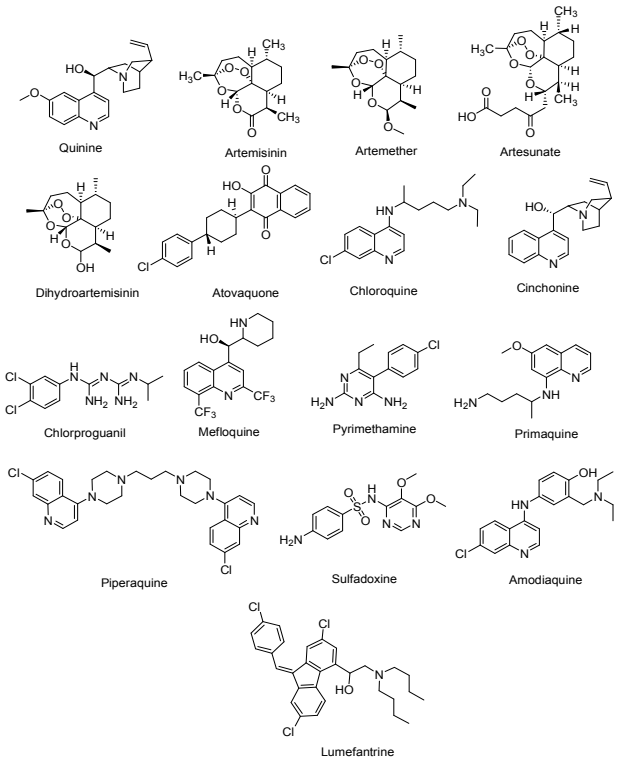

Fig. 1 Structure of commonly used antimalarial drugs

[a] *Medicinal Chemistry Lab, Department of Biosciences, Jamia Millia Islamia (A Central University), Jamia Nagar, New Delhi 110025, India*
[b] *Protein Conformation and Enzymology Lab, Department of Biosciences, Jamia Millia Islamia (A Central University), Jamia Nagar, New Delhi 110025, India*
mabid@jmi.ac.in; (Phone):- +91-8750295095; (Fax): +91-11-26980229

Target insights of antimalarial inhibitors

Drug targets which have been identified and characterized against malaria can be classified on the basis of their locations within the malaria parasite. The enzymes that are crucial for parasite growth and survival are the strategic targets of these inhibitors. Inhibiting either of these may prove lethal to the parasite thus targeting these enzymes will be a powerful strategy in the malaria eradication campaign. The key targets and their inhibitors along with their locations in the parasite are summarised in Table 1.

Table 1 Antimalarial drug targets and their inhibitors along with their location in *P. falciparum*

Target location	Pathway/ mechanism	Target enzyme	Inhibitors	References
Parasite invasion and release	Merozoite invasion	Apical membrane antigen 1(AMA1)	*N*-methylated 20-residue peptide, R1	198
	Merozoite egress	Subtilisin-like protease 1 (*Pf*SUB1)	Chloroisocoumarin JCP104, difluorostatone based inhibitors	199 20
Food vacuole	Hemoglobin degradation	Plasmepsin (PM)	Allophenylnorstatine-based inhibitor	42
		Falcipain (FP)	Cyanopyrimidine based analogues	45
		Aminopeptidase	Bestatin analogues, phosphonic acid arginine mimetics, hydroxamate derivatives	88, 89, 91
		Dipeptidyl aminopeptidase (DPAP)	Dipeptide based analogues	94
Nucleus	Nucleic acid regulation	Histone deacetylase (HDAC)	Apicidin, WR301801, aryltriazolylhydroxamates based derivatives	200, 201 98
		Cyclin dependent protein kinase (CDK)	Oxindole derivatives	202
Mitochondria	Electron transport system	Cytochrome *bc*1 complex	ELQ-300	113
		Dihydroorotate dehydrogenase (DHODH)	Phenyl-substituted triazolopyrimidines	121
		NADH: ubiquinone oxidoreductase (*Pf*NDH2)	SL-2-25	134
Apicoplast	Type II fatty acid biosynthesis	*Pf*FabZ	NAS91	203
		*Pf*FabI	Coumarin-based triclosan analogues	142
		*Pf*FabG	(-)-catechin gallate	204
	Isoprenoid biosynthesis	DOXP reductoisomerase (DXR)	Fosmidomycin, FR-900098	150
	Protein myristoylation	*N*-myristoyltransferase (NMT)	Benzo[*b*]thiophene derivatives	159
Cytosol	Protein synthesis	Heat shock protein 90 (Hsp 90)	Geldanamycin	165
	Glycolysis	Lactate dehydrogenase (LDH)	Gossypol, azole derivatives	205, 206
	Nucleic acid biosynthesis	Purine nucleoside phosphorylase (PNP)	Immucillins	207
	Folate metabolism	Dihydrofolate reductase (DHFR)	Pyrimethamine, cycloguanil	208
		Dihyropteroate synthase (DHPS)	Dapsone, sulphamethaoxazole	209
		Thymidylate synthase (TS)	5-fluoroorotate	210
	Carbon dioxide metabolism	Carbonic anhydrase (CA)	Acetazolamide, sulfanilamide	211
	Oxidative stress	Thioredoxin reductase	5,8-dihydroxy-1,4-naphthoquinone	212
	Pyrimidine biosynthesis	Thymidylate kinase (TMK)	Thymidine derivatives	194

1. Parasite invasion and release

Plasmodium adopts multiple invasive 'zoite' forms to complete their multi-stage development in both the mosquito vector and the human host (Fig. 2). [11] Female *Anopheles* mosquito injects *Plasmodium* sporozoites into the human host which move towards the liver where they invade hepatocytes to start liver stage infection. These intracellular parasites develop into exoerythrocytic merozoites which are released into the blood stream where they invade

erythrocytes initiating disease's symptomatic erythrocyte stage. [12] This process of merozoite invasion is facilitated by the apical membrane antigen 1 (AMA1) which is involved in the formation of moving junction in association with rhoptry neck protein (RON). [13] Being obligate intracellular parasites, merozoites undergo maturation within the erythrocyte and develop cyclically through ring, trophozoite and schizont stage inside parasitophorous vacuole. At the final stage of development, parasite produces 16-32 daughter merozoites due to asexual division (schizogony) which are released upon egress to invade new erythrocytes mediated by cysteine protease dipeptidyl peptidase 3 (DPAP3) and subtilisin family serine protease *Pf*SUB1. [11,14]

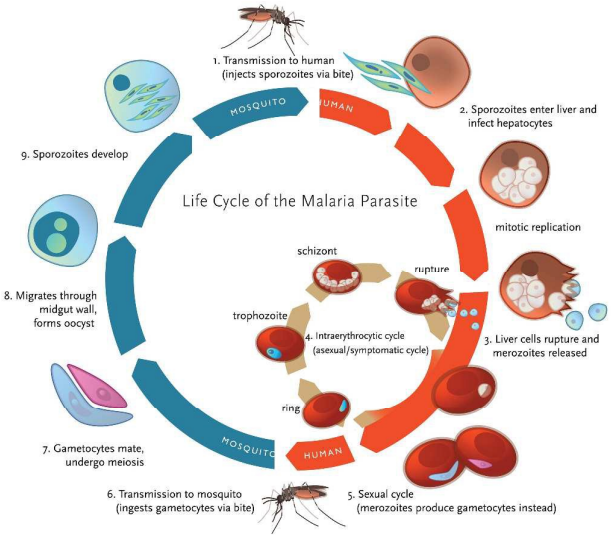

Fig. 2 Life cycle of *Plasmodium falciparum* illustrating the various stages (reproduced with permission from Klein, 2013)

1.1. Apical membrane antigen 1 (AMA1). Apical membrane antigen 1, a 66 kDa type 1 integral membrane protein comprising a short well-conserved cytoplasmic region, is involved in the key interactions with the rhoptry neck protein (RON) complex which forms the moving junction at the time of invasion between the merozoite and the erythrocyte. [13,15] Prior to the invasion, AMA1 is involved in the reorientation of the merozoite on the erythrocyte surface. [16] Conserved hydrophobic cleft present in the AMA1 contains sites for the key interactions with the rhoptry neck protein complex and is targeted by numerous inhibitory peptides and antibodies. [13] This was also revealed by crystallography and NMR studies showing invasion inhibitory peptide R1, which binds to *Pf*AMA1 hydrophobic groove unexpectedly, mimics *Pf*RON2. This has also identified the key residues crucial for the interactions between AMA1 and RON2 in *P. falciparum* which can be exploited for the development of antimalarial chemotherapeutics (Fig. 3). [17] AMA1 can be explored as potential antimalarial drug target because of its uniqueness to *Plasmodium* species and other apicomplexan parasites such as *Toxoplasma gondii*. [15] Absence of AMA1 homologues in human host provide an interesting and safe target for the development of selective inhibitors without affecting the host. Moreover, the presence of AMA1 on the surface of the merozoite stage of the parasite propels inhibitors to target these easily without crossing various membranes surrounding intra-cellular targets. This enables AMA1 inhibitors to develop resistance to parasite-mediated drug efflux mechanism. [13] Thus, inhibitors like peptides, R1 (**1**) which is identified from random peptide libraries using phage display and monoclonal antibodies designed to prevent red blood cell invasion also avert initial liver-stage infections caused by *Plasmodium* parasites. [16] Further, the expression of AMA1 in the sporozoites and blood stage merozoites flaunts its non-stage specific vaccine candidature. [18] Designing of AMA1 inhibitors derived by modification of peptide R1 or small molecule inhibitors using fragment-based ligand design or by screening of diverse libraries have also been reported. [13,16]

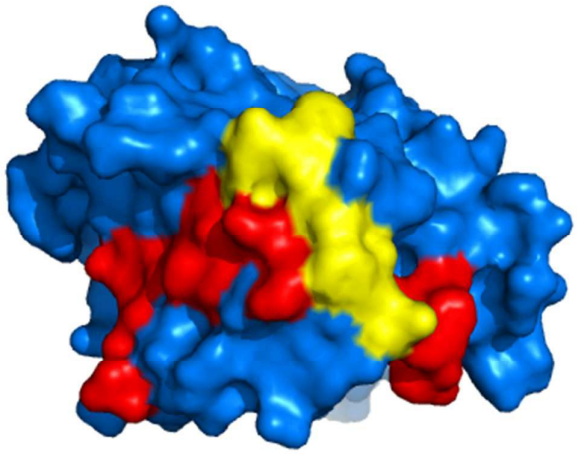

(A)

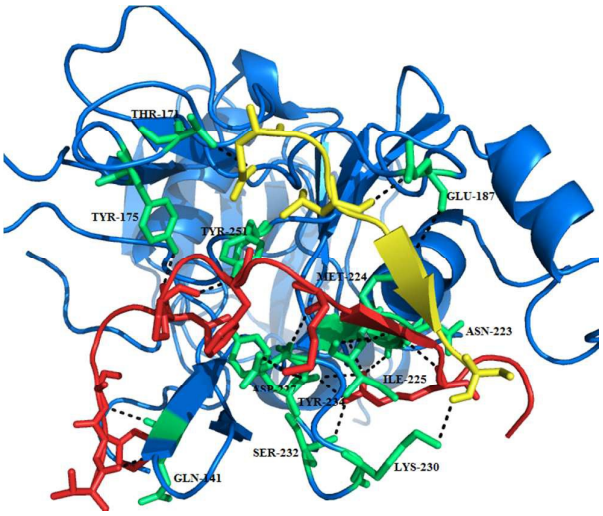

(B)

Fig. 3 Structure of *Pf*AMA1 complexed with R1 peptide. (A) The co-crystal structure of *Pf*AMA1 (blue surface) with R1 shows two bound peptides, R1 major (red) and R1 minor (yellow). (B) Detailed analysis of interactions at the *Pf*AMA1-R1 major, *Pf*AMA1-R1 minor interfaces. The pictures are drawn using PyMol (PDB ID: 3SRJ).

Key binding residues involved in the tight binding of peptide inhibitors to the AMA1 of *P. falciparum* were identified. The structural analogues were based on **1**, a potent inhibitor of parasite invasion of erythrocytes *in vitro*. The importance of residues 5-10 present in the turn-like conformation of **1** (solution structure) for binding to AMA1 was analysed through site-directed mutagenesis and NMR spectroscopy. Both the **1** and modified peptide, R2 (**2**) exhibited similar binding affinities to *Pf*AMA1, having IC_{50} values of 177 and 250 nM. The replacement of Met16 by Leu was not detrimental to the binding affinity of **2** suggesting that this residue is not critical for this interaction. Substitution of Phe5, Pro7, Leu8 and Phe9 with alanine led to significant decrease in the binding affinity (7.5- to >350-fold) for AMA1. Lack of significant changes in the chemical shifts for the backbone amide and $C^{\alpha}H$ resonances of these mutant peptides in comparison to **2** suggests that these mutations caused little effect on the overall solution conformation of **2**. Slightly large differences were observed for residues flanking position 7 in the **2**(P7A). Based on R1 mimetics, the identification of nonpolar region possessing residues critical for AMA1 binding provides a platform for the designing of antimalarial agents. [16]

Fragment-based drug design approach was also employed for the development of small molecule inhibitors of *Pf*AMA1. This approach which employed saturation transfer difference (STD) NMR and Carr-Purcell-Meiboom-Gill (CPMG) experiments identified fragments that bind to the hydrophobic cleft with the overall hit rate of 5%. The high hit rate obtained in this experiment strongly supports the presence of a druggable pocket within the hydrophobic cleft that is capable of binding to small molecules. The hits obtained via R1 competing experiments were reportedly grouped into 2-aminothiazoles and 2-arylfurans series. The R1-competing hits were evaluated against immobilized 3D7 *Pf*AMA1 for estimation of binding affinities. Among 57 NMR hits evaluated, 46 compounds displayed binding in the surface plasmon resonance (SPR) experiments with binding affinities (K_D values) weaker than 1mM except two compounds and the active hits displayed K_D value of 600 µM. The ligand efficiencies (LE) of these compounds were found between 0.2-0.3 kcal mol^{-1} heavy $atom^{-1}$ while fragments with ligand efficiencies of ≥0.3 kcal mol^{-1} heavy $atom^{-1}$ belonged to 2-aminothiazole series. The SAR studies around 4-aryl substituted 2-aminothiazoles revealed that meta substituted methyl, **3** (K_D = 660 µM, LE= 0.33) and methoxy group substituted compound, **4** (K_D = 1.2 mM, LE = 0.28) was responsible for high potency. Although these are weak binders of AMA1 but these may serve as building blocks for the development of potent AMA1 inhibitors with broad strain specificity. [13]

Several small-molecule inhibitors targeting AMA1-RON2 complex were identified by screening a ~21000 member library via AlphaScreen assay by utilizing short RON2 peptide (RON2L). This screen further identified three compounds, NCGC00015280 (**5**), NCGC00014044 (**6**) and NCGC00181034 (**7**) (Fig. 4) that exhibited the tendency to block the interaction of AMA1 and RON2 as well as inhibited merozoite invasion of RBCs with IC_{50} values in the range of 21-29 µM. All the three compounds blocked merozoite invasion of four genetically distinct *Pf* clones with IC_{50} values of 10-14 µM with minimal to no effect on schizont rupture. Chemical modification of **5** led to identification of NCGC00262650 (**8**) and NCGC00262654 (**9**) which exhibited improved inhibition with IC_{50} values of 9.8 µM and 6.0 µM in comparison to resynthesized **5**'s activity of 30 µM. Combination of **5** and **8** with dihydroartemisinin (DHA) reportedly enhanced the efficiency of growth inhibition by simultaneous targeting of intracellular parasites and merozoite invasion. Such combinations provide an excellent strategy to prevent as well as treat artemisinin-resistant parasites. The mode of action of these inhibitors was identified by using SPR and depletion assays which is facilitated through binding to AMA1 and blocking its interaction with RON2 thus preventing the junction formation which leads to the inhibition of merozoite invasion. Molecular docking within the hydrophobic cleft also proposed the presence of two

potential interaction sites (hotspots) for the small molecule inhibitors. One hotspot was located near the flexible loop region where a well-formed hydrophobic pocket is present adjacent to DII loop and is involved in extensive van der Walls and aromatic interactions with compounds **5**, **8** and **9,** resulting in prevention of AMA1-RON2 interaction**.** Other binding mode was present at a more open and rigid region along the hydrophobic groove which plays an important role in the RON2 peptide binding. Thus, the identification of these hotspots provides insights for the development of next generation AMA1-RON2 inhibitors. [19]

To address the issues such as low solubility, high clog *P* and low LLE_{AT} values related to small molecule inhibitors of *Pf*AMA1 reported previously by Srinivasan *et al.* [19], a critical evaluation was carried out for these compounds by Devine *et al.* [15] by using their own method for monitoring AMA1 ligand binding. Compounds **5** and **9** exhibited extensive aggregation in comparison to **8** which was evidenced from the presence of very weak signals obtained in the ^{1}H-NMR spectra. The evaluation of binding affinity of **8** to AMA1 by surface plasmon resonance (SPR) revealed unambiguous over-binding at higher concentrations while inconsistency was observed at lower concentrations with an affinity for AMA1 tighter than ~1mM. IC_{50} for compound **8** was found 9.8 μM as reported by Srinivasan *et al.*[19]. This discrepancy observed suggests that this series of compounds caused effects on host cell invasion by some other mechanism than direct inhibition of AMA1. To resolve the issues of solubility, another series of pyrrolo[2,3-d]pyrimidine-4-amines was synthesized and reportedly possess clog *P* values of 0.93-2.35 with reduced aggregation behavior. These compounds were reported as weak inhibitors of *Pf*AMA1 with K_D values of ≥1 mM but displayed substantial inhibition of parasite growth suggesting alternate mechanism of action for these compounds. The best analogue **10** among the series displayed IC_{50} value of < 31 μM. (Fig. 4)

	1 5 10 15 20
1	NH_2-VFAEFLPLFSKFGSRMHILK-COOH
1(s)	H-ALLRKESEMELVIPFGKSLH-NH2
2	NH_2-VFAEFLPLFSKFGSR**L**HILK-COOH
2(F5A)	NH_2-VFAE**A**LPLFSKFGSR**L**HILK-COOH
2(P7A)	NH_2-VFAEFL**A**LFSKFGSR**L**HILK-COOH
2(L8A)	NH_2-VFAEFLP**A**FSKFGSR**L**HILK-COOH
2(F9A)	NH_2-VFAEFLPL**A**SKFGSR**L**HILK-COOH
2(F5A+F9A)	NH_2-VFAE**A**LPL**A**SKFGSR**L**HILK-COOH

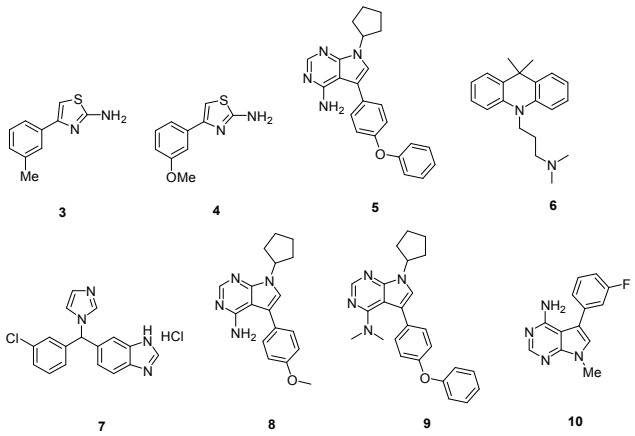

Fig. 4 Chemical structures of AMA1 inhibitors

1.2. Subtilisin-like Protease 1 (SUB1). *P. falciparum* SUB1, a serine protease has been identified as a key enzyme involved in two essential processes of life cycle of the parasite: merozoite egress from red blood cells (RBCs) and invasion. [20] During the symptomatic asexual erythrocytic phase, parasite undergoes invasion and multiplication within RBCs successively transforming through ring, trophozoite and schizont stages which eventually produces mature merozoites. [21] These merozoites upon egress invade new RBCs by rupturing of both the parasitophorous vacuole (PV) membrane and the RBC membrane (Fig. 2). [20] Just prior to egress, *Pf*SUB1 facilitates the proteolytic activation of a family of protease-like proteins called serine repeat antigen family (SERA) in the PV space. Further, *Pf*SUB1 is involved in processing of merozoite surface proteins (MSPs) thus enabling the merozoite for the subsequent invasion step. [21] As the inhibition of *Pf*SUB1 prevents maturation of SERA proteins and egress, *Pf*SUB1 may serve as potential target for the development of promising antimalarial chemotherapeutics. [20,22] Active site of *Pf*SUB1 as identified by crystallography studies consist of conserved S1-S4 subsites where S4 pocket is hydrophobic in nature, S2 pocket is constricted and S1 pocket is highly polar. In addition to this, an extended, basic S' pocket is playing an important role in substrate stabilisation. This crystal structure analysis has also shed light on the calcium dependence of SUB1 and presence of solvent-exposed redox-sensitive disulphide bridge acting as regulator of protease activity in the parasite. [23]

Molecular modelling approach was utilised along with existing understanding of SUB1 substrates and recombinant expression and characterization of additional *Pf*SUB1 orthologues to investigate active site architecture and the substrate specificity of *P. falciparum*,

and its orthologues from the two other major human malaria pathogens *P. vivax* and *P. knowlesi*, as well as from the rodent malaria species, *P. berghei*. The results disclosed the presence of the unusual features of SUB1 substrate binding cleft together with the requirement of interaction with both the prime and non-prime side residues of the substrate recognition motif thus supporting the observation obtained by crystallography studies. SUB1 catalysed the cleavage of conserved parasite substrates in all the parasites species which is well supported by the species-specific co-evolution of protease and substrates. To target *Pf*SUB1, peptidyl alpha-ketomides (Fig. 5) based on authentic *Pf*SUB1substrate were designed and compound **11** completely inhibited the substrate hydrolysis, thus acting as fast-binding inhibitor of *Pf*SUB1with IC_{50} value of ~6.0 µM and the IC_{50} values for r*Pv*SUB1 and r*Pk*SUB1 inhibition were ~12 µM and ~6.0 µM respectively. The inhibitory potency was found to be increased by incorporating the carboxyl moiety to introduce prime side interactions with protease as exemplified by **12** possessing IC_{50} against *Pf*SUB1 and *Pk*SUB1 of ~1.0 µM, and an IC_{50} against *Pv*SUB1 of ~2.0 µM. Thus, the development of these selective inhibitors based on *Pf*SUB1 substrates which also exhibited inhibition of both r*Pv*SUB1 and r*Pk*SUB1, raises the prospect of developing broad-spectrum antimalarial agents targeting SUB1. [22]

Quinolylhydrazone, **13** was identified as hit compound for *Pf*SUB1 (IC_{50} = 20 µM) through high-throughput screening of proprietary library of compounds. SAR studies of this set of compounds suggested the dependence of inhibitory activity on the hydrazone moiety attached to an aromatic ring possessing a strong electron withdrawing group. The mechanism of inhibition of the enzyme was reported to be either competitive or covalent reversible. [24]

Based on the previously reported hexapeptidic ketomide **14** inhibitor of *Pf*SUB1, [20,22] peptidic α-ketomides as *Pf*SUB1 inhibitors were synthesised. SAR analysis was carried out to predict the crucial interactions that are beneficial for increasing the enzymatic activity. The SAR predictions revealed the dependence of inhibitory activity over serine trap (ketoamide) and on P_1'-P_1-P_4 amino acids which determine the enzyme binding interactions. The studies clearly showed the preference for charged β-aminoalanine in the P_1' position while small size substituents like ethyl group is preferred in the P_1 position. P_2 position craves for glycine amino acid over alanine while threonine is required at P_3 position to provide a solvent-exposed hydrophilic side chain to minimize solvation penalty. Isoleucine present at P_4 position is desired to make crucial hydrophobic interactions for improved inhibitory activity. This optimization of side chain led to the pentapeptidic α-ketoamide **15** (Fig. 5) which is less polar than the parent hexapeptidic analogue **14** that exhibited IC_{50} of 0.9 µM similar to the compound **14**. Thus, this compound can be explored further to develop as a lead against *Pf*SUB1. [25]

In order to address the issue of low potency, lack of selectivity or poor cell permeability associated with reported inhibitors, [22,24] rational drug-design approach was used for the synthesis of novel difluorostatone based inhibitors and evaluated them for inhibition of *Pf*SUB1. The enzymatic assay led to the identification of compounds **16**, **17** as potent *Pf*SUB1 inhibitors (IC_{50} = 0.6 µM) possessing selectivity over mammalian proteases (Fig. 5). The homology model built for analysing the binding poses of the compounds were found to be in good agreement with crystal structure of *Pf*SUB1. The docking results clearly revealed that both the potent compounds exhibits a series of interactions with the key residues present in the binding cleft of the enzyme. The enzyme/inhibitor interaction pattern proposed in the study will guide for the future optimization of this novel class of potent *Pf*SUB1 inhibitors. [20]

SAR was further carried out on the previously identified inhibitors [20] and reported novel and potent inhibitors of *Pf*SUB1 based on rational drug designing approach. Compounds, **18** and **19** bearing non-natural amino acids (Fig. 5) were found to be most potent inhibitors reported to date with IC_{50} values of 0.25 and 0.28 µM respectively. Docking study carried out on the compound, **18** clearly fulfilled the key structural prerequisites outlined previously which are important for achieving inhibitory activity: presence of difluorostatone moiety, terminal carboxylic group at the P1' site and three residues (P2-P4) at the non-prime side of the inhibitor. Furthermore, compound **20** with only two amino acid residues on the P-side, characterized by reduced peptidic character provide an efficient strategy for the development of inhibitors possessing decreased peptidic character. [21]

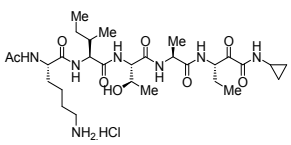

11

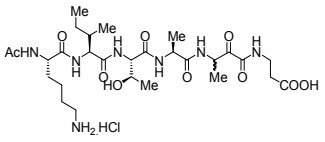

12

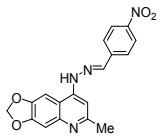

13

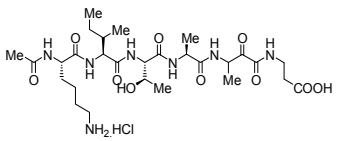

14

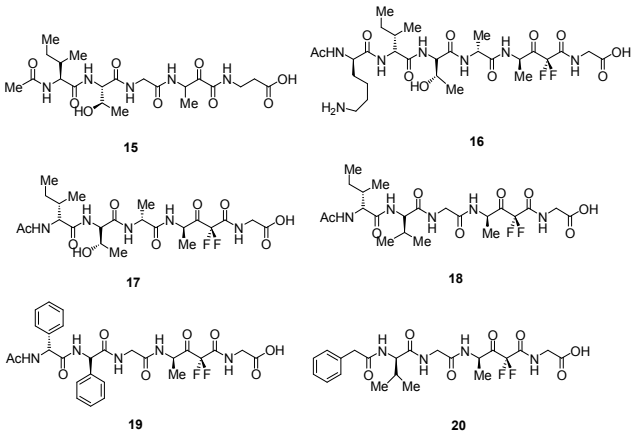

Fig. 5 Chemical structures of SUB1 inhibitors

2. Food vacuole

P. falciparum digestive food vacuole plays a central role in the metabolism of the parasite where hemoglobin is degraded in the acidic environment to yield heme which is polymerized into insoluble hemozoin pigment and globin which is further degraded into individual amino acids. [26] The whole process of globin digestion is carried out by various endo- and exo-peptidases in the specialized organelle, food vacuole. [14] These constitute an important target since they are crucial for the survival of parasite.

2.1. Hemoglobin digestion Hemoglobin digestion is one of the key metabolic processes essential for the survival and propagation of *Plasmodium* in human. Proteases belonging to classes: aspartic, cysteine and metalloproteases ingest the hemoglobin in specialized organelles, the food vacuole, at pH 5.0 into individual amino acids which are used by the parasite for protein biosynthesis. [27] This degradative process also helps in maintaining intracellular osmolarity during parasite growth as well as for making space for growth. [14] Since the inhibition of this proteolytic pathway is lethal to the parasite both in culture and in animal models making it a very attractive target for malaria chemotherapy.

2.1.1. Aspartic proteases inhibitors Plasmepsins (PMs) are pepsin like aspartic proteases found in *P. falciparum* which are involved in hemoglobin digestion occurring in digestive vacuole during the intra-erythrocytic phase of infection.[28] The *P. falciparum* genome encodes ten PMs out of which PM I, PM II, PM III known as histo-aspartic protease (HAP) and PM IV reside in acidic vacuole and degrades hemoglobin whereas others present outside digestive vacuole supposed to play different roles. [29] Various inhibitors have been reported in the literature and more potent are being developed with better pharmacokinetic profile.

A new class of copper(II) nanohybrid solids **21** and **22** was reported (Fig. 7) and evaluated for their *in vitro* antimalarial potential against *P. falciparum* chloroquine-sensitive isolate (MRC 2). These nanohybrids exhibited activity with IC_{50} values of 0.032 µg/ml and 0.025µg/ml respectively which is quite similar to standard drug chloroquine (IC_{50} = 0.020 µg/ml). Moreover, Lineweaver–Burk plots for the inhibition of PM II by both the solids revealed the competitive inhibition with respect to the substrate. The selectivity over human cathepsin D (hCatD) and non-toxicity make them excellent leads to be developed as antimalarial compounds. Modelling experiments on PM-II further established that both nanohybrid based compounds interacts with active site Asp214 which is part of the catalytic dyad. Benzimidazole group of **21** binds hydrophobically to the S1-S3 subsites.[30]

A series based on pyrrolidine scaffold, synthesised originally as HIV-1 protease inhibitors, was also evaluated for PM II and IV inhibition potential. Some of the inhibitors were found to be active in nanomolar range against both the isoforms. Compound **23** exhibited inhibition with *Ki* values of 0.10 and 0.09 µM against PM-II and PM-IV, respectively. Although the compounds were active in nanomolar range but the selective inhibition of PM over hCatD was not addressed for the most active compounds. [31]

Hydrazide and hydrazine derivatives were also identified as novel aspartic protease inhibitors through virtual screening of an in-house library followed by enzyme inhibition. This screening process identified five virtual hits which exhibited inhibition of both hCatD and *P. falciparum* PM II with IC_{50} in the low micromolar range of 1-2.5 µM but still a lot of work need to be done to discover lead molecules with high potency and selectivity towards PM II over hCatD. [32]

Four peptidomimetic analogues designed to act as mechanism based inhibitors of PM II were also evaluated. Three of these derivatives **25**, **26** and **27** exhibited potent irreversible inhibition of the enzyme with IC_{50} values in the low nanomolar range (Fig. 7). Compounds **26** and **27** displayed antiparasitic activity with IC_{50} values of 7.7 and 9.2 µM while compound **25** was found to be poor inhibitor in growth assay suggesting the importance of activatable propargyl group in order to retain its antiparasitic activity. Although these compounds did not demonstrate reasonable selectivity of PM II over hCatD, optimization studies need to be carried out to increase their selectivity. [33]

Three nitrophenacyl derivatives of *N*-methyl-4-hydroxy piperidine were synthesized and evaluated for its enzyme inhibition potential. The compound 1-methyl-1-(4'-nitrophenacyl)-4-hydroxypiperidinium bromide with *p*-nitro group (**28**) was reported most active at the conc. of 1.0 µM with 22% inhibition in comparison to 100% inhibition by standard compound pepstatin.[34] New potent inhibitors of *P. falciparum* CQ resistant W2 strain were developed by adopting dual drug strategy. 7-chloro-4-aminoquinoline ring system was introduced in the statine double drugs in order to improve the accumulation of PM inhibitors inside the food vacuole. These compounds were tested against *Pf*PM II, *Pf*, *Po*, *Pv* and *Pm*PM IV and against D10 (CQ sensitive) and W2 (CQ resistant) *P. falciparum* strains. Although compound **29** showed potent inhibition against *Pf*PM II, *Pf*PM IV and *Po*PM IV but it showed moderate inhibition against *P. falciparum* strains. Based on enzymatic activity as well as growth inhibition assay, compound **30** with high selectivity over hCatD can be considered as potential antimalarial candidate. [35]

The selectivity towards PM II over hCatD was also improved by synthesizing novel benzimidazole derivatives. Enzyme inhibition data revealed that compounds **31** and **32** (Fig. 7) exhibited three times more selectivity towards PM II (IC_{50} = 10 µM) in comparison to hCatD. In the series, the compound **33** was found to be most potent and selective inhibitor of hCatD with IC_{50} = 2.0 µM and it exhibited highest antiparasitic activity with IC_{50} = 0.16 µM. The antiplasmodial data for this series laid emphasis on the importance of phenyl and a chlorine group at the para position. [28]

Non-peptide inhibitors of PM II from chemical databases of Specs and MayBridge were identified on the basis of structure-based virtual screening. Five novel non-peptide inhibitors with moderate potencies having IC_{50} in the range from 4.62 to 9.47 µM were identified. The lead compound, **34** displayed 68% inhibition of PM II with IC_{50} value of 4.62 µM. [29] Several docking and molecular modelling studies on PM II showed interactions (H-bonds) with the important catalytic residues (Asp34 and Asp214) and also with other key residues such as flap residue Val78, residues Ser218 and Gly36 in close proximity to the catalytic dyad with compounds **25**, **33** and **34**. [28,29,33]

Structure based design of substituted 7-azanorbornenes was reported that was synthesised by hydroformylation reaction of substituted 7-azabicyclo[2.2.1]heptane core. The main concern behind this synthetic step was to introduce a new vector which could occupy S1' pocket. The *in vitro* evaluation of these derivatives revealed high potency against three plasmepsins: PM I, II and IV in the nanomolar IC_{50} range and good selectivity over hCatD and E. The molecular modelling studies clearly depicted the importance of occupation of cycloalkylaminomethyl substituent at 6th position in S1' pocket which increases the binding affinity and selectivity particularly in the case of PM IV. [36]

SAR analysis and optimization studies of aminohydantoins were performed to identify potent nanomolar range inhibitors of PM-II and PM IV. The presence of cyclohexyl group on the *N*-3 position of aminohydantoin displayed improved antimalarial potential while inhibition of human aspartic proteases (BACE) was reduced. Thus, compound **43** can be further optimized for antimalarial drug development on the basis of low molecular weight, modest lipophilicity and oral bioavailability. [37]

Structurally simplified analogues **44** and **45** of potent hydroxyethylamine-based PM IV inhibitor **1*SR*** (TCMDC-134674), **46** were identified in a GlaxoSmithKline cell based screening campaign. X-ray crystal structure of PM II bound with **46** shed light on the interaction between the hydroxyethylamine core of **46** and the PM II catalytic dyad Asp34−Asp214, thus provided structural insight for the design of potent and selective inhibitors (Fig. 6). SAR studies revealed that importance of R-configuration of the central hydroxyl-bearing stereo centre is crucial for plasmepsin inhibition. Further replacing 2-(1,2-thiazinane-1,1-dioxide) moiety by nonplanar hydrophobic groups such as piperidinyl and cyclohexyl resulted in increased potency against PM I and II due to the favorable interaction with Val78, while planar and more compact groups were responsible for PM IV inhibition, possibly, due to favorable flap-closing interactions, indicating selectivity for PM IV over CatD inhibition. [38]

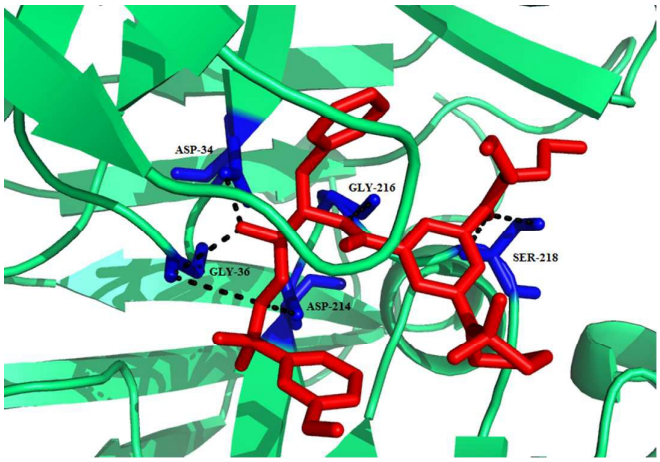

Fig. 6 A ribbon diagram of PM II with inhibitor **46** shown in stick presentation (red). Active site residues (Asp34 and Asp214) and residues in vicinity to these (Ser218, Gly216 and Gly36) are depicted as blue sticks. The

plausible hydrogen-bonding interactions are shown as black broken lines. The figure was made on PyMol using crystal structure coordinates of PM II bound to **46** (PDB ID: 4CKU).

Inhibitory potential for some dietary flavonoids was investigated against *P. falciparum* FP-2 and PM II and identified two flavonol compounds, myricetin (**47**) and fisetin (**48**) as the dual inhibitors (Fig. 7). Compound **47** exhibited IC_{50} value of 1.5 and 7.2 µM while **48** displayed IC_{50} value of 4.9 and 7.8 µM against FP-2 and PM II, respectively. Kinetic investigation and molecular docking were carried out on these flavonoids to explore the inhibitory mechanisms which depicted that **47** and **48** are well docked in the active grooves of the enzymes through a number of hydrophobic as well as polar interactions. These dual inhibitors which act on multiple targets are supposed to possess synergistic activity thus prevent the emergence of drug resistance during malaria treatment. [39]

Plasmepsin inhibition potential was improved further by substituting 2-aminoethylamino groups to allophenylnorstatine-containing plasmepsin inhibitors that were identified previously [40,41] and their *in vitro* antimalarial activity was investigated. On exploring SAR of the methyl or ethyl substituents on the amino groups, compounds **49** (KNI-10743) and **50** (KNI-10742) were found to be highly potent PM II inhibitors ($Ki < 0.1$ nM). These peptidomimetics reportedly exhibit antiplasmodial activity with EC_{50} of 0.36 and 0.46 µM, respectively. One of the peptidomimetics **51** (KNI-10740) was found to have highest antimalarial activity with EC_{50} of 0.19 µM. Binding model of compound **49** with PM II (PDB ID, 1SME) predicted a new hydrogen bonding interactions between 2-aminoethylamino groups with Asp130, present outside the enzyme active site, which may enhance PM II inhibitory potential.[42]

Inhibitor (KNI-10740) **51** was optimised to avoid drug resistance mechanism of multi-drug resistant TM91C235 strain of *P. falciparum*. The PM inhibitor, **51** exhibited 5-fold reduced activity against this resistant strain. A hypothesis was stated that reduction in inhibition potential is due to the structural similarity between 2-aminoethylamino substituent of **51** and chloroquine. To prove the hypothesis, moiety was modified which led to the identification of **52** (KNI-10823) that counters drug-resistant mechanism of TM91C235 strain. [43] A series of short peptide based compounds was evaluated against D6 and W2 strains of *P. falciparum* which showed potent antiplasmodial activity with IC_{50} in the range 1.4-4.7 µg/ml. The high potency of these peptides against drug resistant strain indicated their efficacy in the treatment of drug-resistant malaria parasites. The selected compounds were further evaluated for PM II inhibition and the most potent compound, **53** was found to have maximum inhibition of 25%. These were reported non-cytotoxic making them suitable antimalarial candidate (Fig. 7). [44]

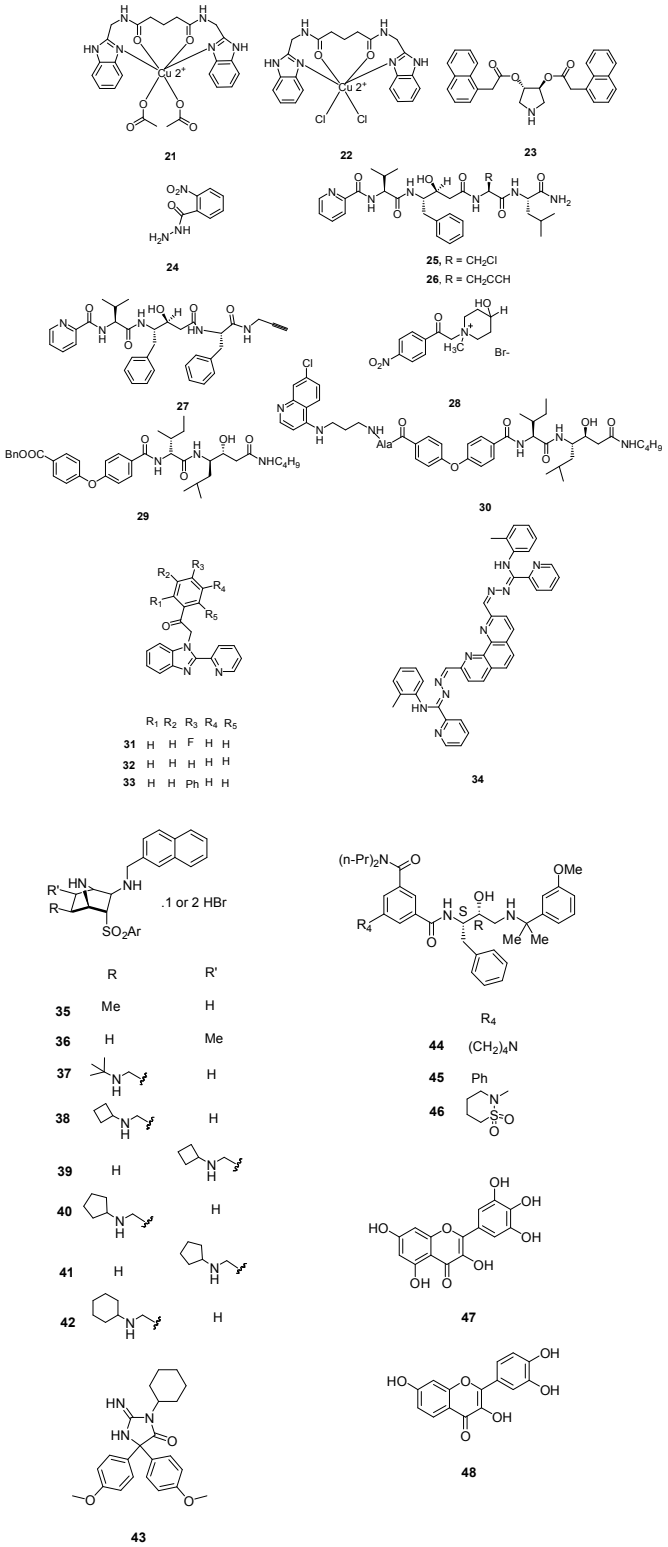

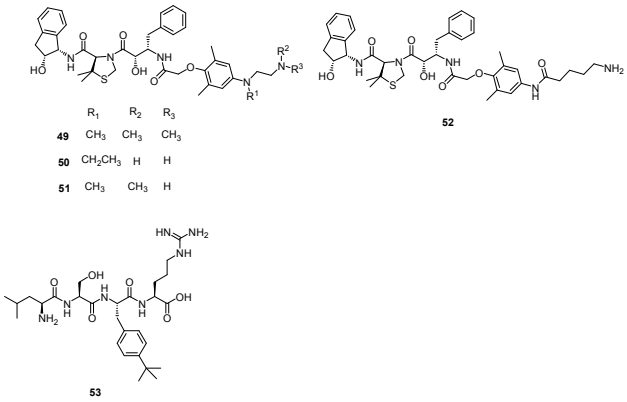

Fig. 7 Chemical structures of plasmepsin inhibitors

2.1.2. Cysteine protease inhibitors *P. falciparum* encodes four cysteine proteases from the papain family called falcipains (FPs): FP-1, FP-2, FP-2', FP-3. Out of these, FP-2 and FP-3 have been identified as potential therapeutic targets where both contribute to degradation of host hemoglobin in the digestive vacuole. [45] This proteolytic process generates amino acids which are utilized by erythrocytic malaria parasites for protein synthesis thus aids in parasite survival and development. [31] FP-2 is also involved in erythrocyte rupture by the cleavage of cytoskeletal elements such as ankyrin and band protein 4.1, required for the stability of red blood cell membrane. [46] Since hemoglobin digestion is crucial for the survival of malaria parasite, the inhibition of FP-2 and FP-3 is the promising way to effectively treat the disease.[47] Several groups have characterized and validated FP-2 and FP-3 as potential drug targets so simultaneous inhibition of both FPs will be a powerful strategy to achieve parasite death. The FP inhibitors reported so far, have been grouped into different classes: peptides-based, peptidomimetics and non-peptidic inhibitors depending on their core structural features.

I. Peptide based inhibitors

Azadipeptide nitriles were reported as potent inhibitors of FP-2 and FP-3 as displayed by inhibition of parasite's hemoglobin-hydrolysing cysteine-proteases. These have also showed structure-dependent antimalarial effect against chloroquine-sensitive (3D7) and chloroquine-resistant (Dd2) lines of cultured *P. falciparum* malarial parasites. Compounds **54** and **55** (Fig. 8) both possessing phenylalanine in P^2 and phenylethyl and pentyl in P^1, respectively, exhibited the most potent activity against *P. falciparum* parasites, with IC_{50} values of ~4.0 and ~3.0 µM, respectively suggesting the importance of P^1 substituents as well as azadipeptide nitrile scaffold for antimalarial activity. The compound **56,** bearing a Leu side chain in the P^2 position, was found to be potent inhibitor of FP-2 exhibiting an IC_{50} value of 59 nM. While compound **55** having phenylalanine at P^2 and pentyl group at P^1 displayed potent inhibitory activity with IC_{50} value of 110 nM against FP-3. These results suggested that there existed a correlation of enzyme inhibitory and antimalarial activity in this series of compounds but differences exist when comparing structure-activity relationship between isolated enzyme and parasite suggesting the synergistic action of a combination of hemoglobinases on the inhibition of parasite growth. This new class of antimalarial compounds provides greater structural variety into P^1 position, which is quite feasible. [48]

Small peptides were synthesised mimicking the protein-protein interactions between FP-2 and chicken egg white cystatin (CEWC) which were designed based on the co-crystal structure of FP-2/CEWC. Three regions were identified in CEWC primary sequence through molecular modelling studies which made contacts with FP-2 active site: the N-terminal sequence (^{6}RLLGAPV^{12}), a β -hairpin loop (^{52}RQLVSGI^{58}) which is in close contact with FP-2 and another β-hairpin loop (^{103}PW^{104}) which is involved in minor interactions with FP-2. The peptide based mimics were designed taking into consideration these interacting motifs which contained different linkers: γ-aminobutyric acid (GABA), cis-4-aminocyclohexane carboxylic acid (cis-ACHC), a macrocycle formed by GABA and two cysteines joined by a disulfide linkage. The effect of the synthesized peptides was evaluated on FP-2 activity which revealed that peptides bearing the cis-ACHC were found to be more active than peptides containing GABA residue. Some of the compounds inhibited FP-2 in the micromolar range and produced morphological abnormalities in the food vacuole. Compound **57** emerged as most active compound with *Ki* value of 2.0 µM. Though the potency of these peptides are lower than cystatin, but the tendency to alter the food vacuole and the capacity to cross membranes may be beneficial in developing a new class of anti-malarial drugs. [49]

A new acyltetrapeptide, falcitidin, **58** was identified from methanolic extract from a myxobacterium *Chitionophaga* sp. Y23 which was isolated from soil collected in Singapore. Biological evaluation of this peptide against FP-2 showed IC_{50} value of 6.0 µM while it is ineffective against PM II (IC_{50} = 50 µM in FRET assay) and serine protease, tryptase (IC_{50} > 90 µM). Low yield and inconsistent production of the peptide led to the total synthesis of the **58** whose structure was confirmed as isovaleric acid-D-His-L-Ile-L-Val-L-Pro-NH_2. **58** is different from other peptide-based inhibitors as it does not possess reactive groups like halomethyl ketones, vinyl sulfones, aldehydes, α-ketoamides and aziridines, which covalently

bind to cysteine in the active site. [50] In the search of more potent inhibitor of FP-3, Rathi *et al.* reported novel peptide based self-assembled nanostructures possessing hydroxylamine isostere. Spherical nanostructures **59** and **60** were screened against anti-malarial target, FP-3, involved as a major hemoglobinase of *P. falciparum* (Fig. 8). Hemoglobin hydrolysis assay data strongly indicated that **60** can completely inhibit FP-3 activity at an effective conc. of 1.5 μM as evidenced from its inability to act on hemoglobin, its natural substrate. Thus, bis hydroxethylamine based peptide nanostructures exhibit excellent inhibitory activity against malarial cysteine proteases. [47]

Analogues of natural product gallinamide A, **61** were reported as potent inhibitors of falcipain cysteine proteases. Some of the analogues (**62** and **63**) exhibited potent inhibition of FP-2 and FP-3 as well as potent antiplasmodial activity strongly suggesting the presence of olefinic functional group within *α, β*-unsaturated imide moiety along with *N*-acylpyrrolinone unit for the potent inhibition. Some of the analogues with alike peptide backbone but with variation in the side chain of pyrrolinone unit and in the substitution of the enol of pyrrolinone exhibited equipotent inhibition as that of chloroquine against 3D7 strain and high potency against Dd2 parasite as well. [51]

Various analogues were synthesised based on the structure of pseudotripeptide designed using *in silico* screening tools and three dimensional structures of cysteine proteases like FP-2, FP-3 and papain. Out of 23 compounds, 8 compounds exhibited submicromolar inhibition of FP-2 with *Ki* value being in the range 0.2 μM to 0.8 μM while five compounds showed inhibitory activity against *P. falciparum* 3D7 cultures with IC_{50} less than 10 μM. Three compounds, **64**, **65** and **66** selected on the basis of enzyme inhibition and antiparasitic activity were evaluated against Dd2 and MCamp (Malayan patient isolate with an unknown drug resistance profile) revealing compound **64, 65** to be the most potent inhibitor against both the isolates (Fig. 8). [52]

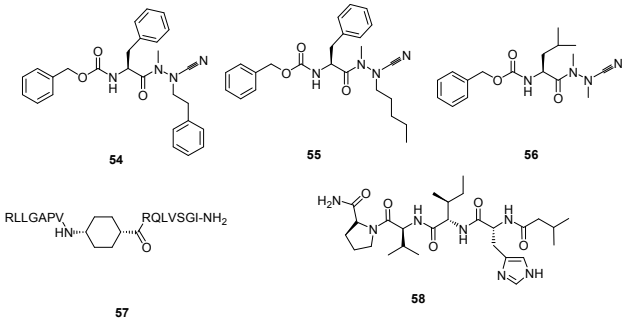

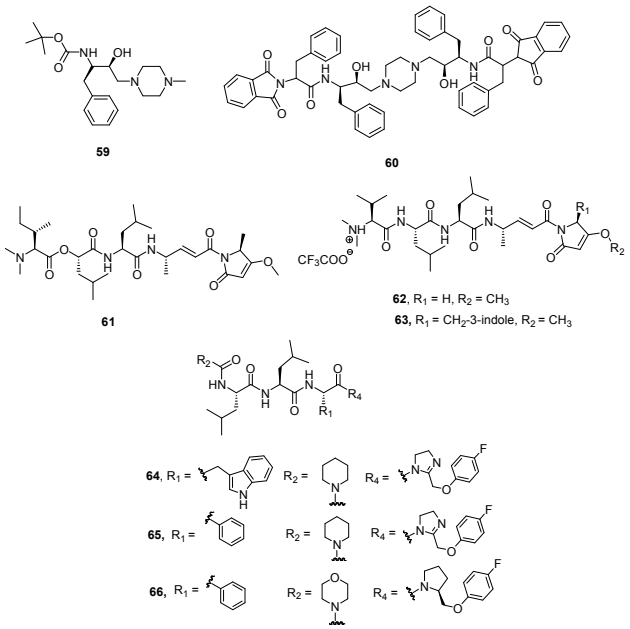

Fig. 8 Chemical structures of peptide based falcipain inhibitors

II. Peptidomimetics

Constrained peptidomimetics were reported based on benzodiazepine scaffold serving as mimic of fragment D-Ser-Gly and endowed with vinylester warhead. These derivatives were structurally related to previously reported irreversible inhibitor of FP-2, compound **67**. Structural variations in the P1 site and substitution at the aromatic rings of benzodiazepine moiety were not a suitable design for constructing a favourable motif. Introduction of bulkier group, adamantyl at the side chain of serine at P3 site produced potent inhibitor, **68** (Fig. 9) with remarkable inhibition potential against FP-2 (*K*i = 0.014 μM) and rhodesain (*K*i = 0.0026 μM) as well as good selectivity over human cysteine proteases. [53]

Peptidomimetic nitriles as selective inhibitiors of FP-2 were synthesised based on the structure-based molecular modelling approach. The designing of these inhibitors were mainly focused on the optimal occupation of the selectivity-determining subpockets. The biological potential of this series of compounds containing nitrile as head group was assessed in order to gain insights into the binding site properties of the target enzyme. The compounds designed based on lead compound **69** exhibited covalent, reversible inhibition of the target enzyme with inhibitory affinities found in the nanomolar range (*K*i = 17.2-2.1 μM). The carbamate analogue **70** showed *K*i value of 1.2 μM. The most active compound, **71** (Fig. 9) bearing aldehyde group exhibited *K*i value of 0.065 μM which may be due to high reactivity of this functionality as compared to the nitrile group but it also binds to both cathepsin B and L. Majority of

the synthesized compounds displayed selectivity over human cathepsin B and L, and the serine protease α-chymotrypsin. Thus, the enzyme inhibition results clearly emphasised the optimal electrophilicity of the nitrile group as well as perfectly occupied selectivity-determining S2 pocket. [54] Lipophilicity of 1,4-benzodiazepine scaffold was further improved by incorporating protected aspartyl aldehyde warhead which yielded the novel peptidomimetics, thioacylals and acylals. Trans diastereomers **72** and **73** (Fig. 9) exhibited potent enzyme inhibition in reversible manner with a *Ki* value of 8.2 μM and 8.9 μM, respectively almost equipotent to its parent compound **74** (*Ki* = 4.0 μM). The ability of both the derivatives to inhibit *Plasmodium* growth significantly increased as compared to the parent compound due to increased lipophilicity (IC_{50} = 28.5 and 49.5 μM). The compound **72** may also be developed as antiprotozoal agent as it emerged as a potent rhodesain inhibitor (*Ki* = 0.7 μM) and this also possessed potent trypanocidal activity with an IC_{50} value of 14.2 μM. [55]

Weldon *et al.* synthesised and reported a new series of peptidomimetic pseudo-prolyl-homophenylalanylketones and evaluated them for FP-2 and FP-3 inhibition as well as antiparasitic effect. Among the 22 compounds, **75** possessing homophenylalanine-based *α*-hydroxyketone linked Cbz-protected hydroxyproline emerged as the most potent inhibitor with IC_{50} values of 80 nM, 60 nM and 7.70 μM against FP-2, FP-3 and W2 strain of *Plasmodium*, respectively. *In silico* studies carried on these peptidomimetics shed light on important protein-ligand structural insights and role of water molecules in the active sites of these protease isoforms by utilizing WaterMap study. Thus, the pseudo-dipeptide and its analogues offered an interesting aspect to be carry forward for the design of competitive inhibitors of falcipains for antimalarial therapy. [56]

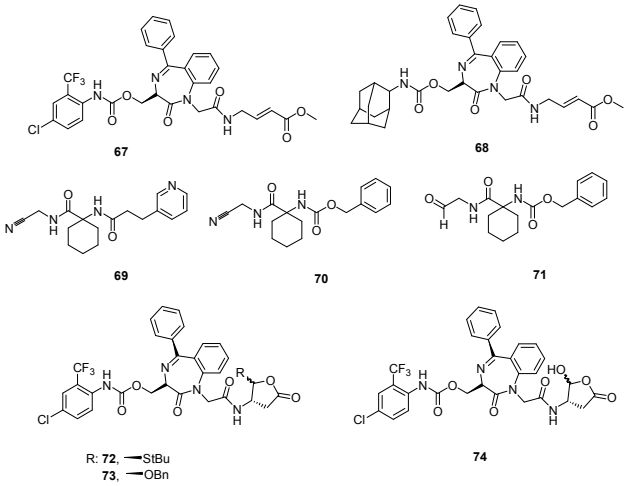

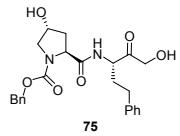

Fig. 9 Chemical structures of peptidomimetics based falcipain inhibitors

III. Artemisinin derivatives

A series of 10-substituted artemisinin derivatives was synthesised by incorporating (thio)semicarbazone and evaluated them for FP-2 inhibition potential (Fig. 10). Most of the compounds displayed potent inhibition in low micromolar range and compounds **76** and **77** incorporating thiosemicarbazone and semicarbazone, respectively, were found to be the most effective with IC_{50} value of 0.46 μM. Molecular docking studies performed with the most active inhibitor, **76** predicted the plausible binding mode as well as binding affinity. It is involved in the hydrogen bonding interactions with Gly83, Leu172 and Asp234. [57]

Another series of dihydroartemisinin derivatives was developed based on (thio)semicarbazone scaffold and evaluated them against FP-2 enzyme. The enzyme assay showed that most of the synthesised compounds displayed significant inhibition with IC_{50} values in the range of 0.29-10.63 μM and **78** presented IC_{50} value of 0.29 μM against FP-2, the most potent among them, formed hydrogen bonds with Cys42 and Gly83 as predicted by molecular docking studies. [58]

Further a series comprising 4-quinolylhydrazone and artemisinin cores was synthesised and evaluated for FP-2 inhibitory activity. The enzymatic assay revealed that all the compounds exhibited excellent potential against recombinant FP-2 (IC_{50} = 0.15–2.28 μM). The best inhibitor **79** of this series exhibited IC_{50} value of 0.15 μM. Molecular modelling study further indicated formation of hydrogen bonds as well as hydrophobic contacts with key residues of the receptor pocket. [59]

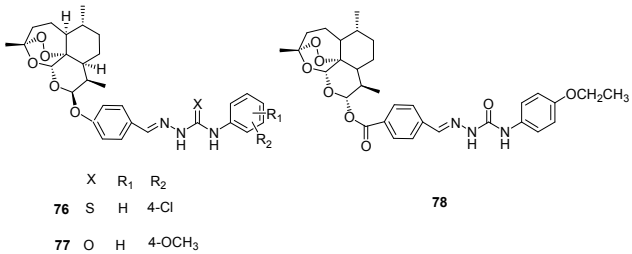

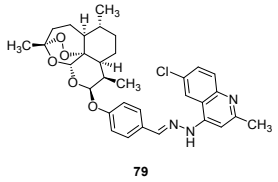

79

Fig. 10 Chemical structures of artemisinin based falcipain inhibitors

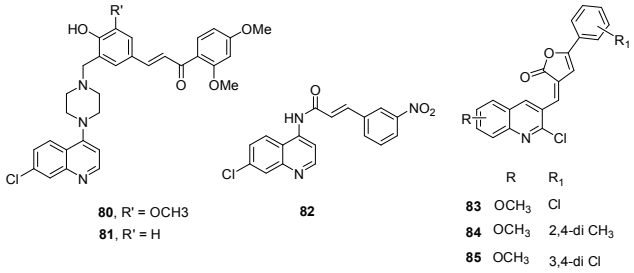

80, R' = OCH3
81, R' = H

82

	R	R_1
83	OCH_3	Cl
84	OCH_3	2,4-di CH_3
85	OCH_3	3,4-di Cl

Fig. 11 Chemical structures of quinoline based falcipain inhibitors

IV. Quinoline based analogues

Guantai *et al.* designed and synthesized enone- and chalcone-chloroquinoline hybrid analogues based on the previously reported promising antimalarial leads (Fig. 11). [60] These analogues were developed with the aim to improve solubility and antimalarial potential. *In silico* predictions provided favourable results in terms of improved solubility at low pH as well as permeability properties but indicated susceptibility to hepatic metabolism which was very well supported by *in vitro* results. Compounds **80** and **81** were reported as the most potent leads with the mechanism predicted to be FP-2 inhibition. But the primary mechanism underlying the potency of other compounds was inhibition of hemozoin formation as suggested by biochemical studies. [61]

Novel cinnamic acid/4-aminoquinoline conjugates linked through a retro-enantio dipeptide were developed as dual action drugs. These derivatives (with or without spacer) were assessed for their ability to inhibit hemozoin growth, FP- 2/3 inhibition as well as blood stage *P. falciparum* growth. The results did not exhibit correlation between blood stage growth and enzyme inhibition as hybrids with dipeptide were active against blood stage *P. falciparum* and hemozoin growth while compounds lacking spacer were found to be better FP-2 inhibitors, thus suggesting different mechanism of action. One of the compounds, **82** was found to be the best inhibitor with IC_{50} value of 14.2 µM. The results clearly indicated that this dipeptide plays a critical role in inhibiting *P. falciparum* growth and hemozoin formation and this is more preferable to its counterparts with L-amino acids. [62]

Quinoline-substituted furanone derivatives were synthesised and evaluated their antimalarial potential. The compounds **83**, **84** and **85** displayed excellent antiparasitic activity with IC_{50} in the range of 0.50-0.72 µg/mL. A preliminary SAR emphasised on the presence of electropositive character for enhancing antimalarial activity. The FP-2 enzymatic assay on these three selected compounds suggested that **83** and **84** exhibited 58% and 62% inhibition of FP-2, respectively and could be developed as selective FP-2 inhibitors. [63]

V. Natural product based analogues

Allicin, **86** main biologically active component of garlic extracts, and its derivative **87** having large lipophilic groups were identified as inhibitor of cysteine proteases FP-2 (Fig. 12). These compounds inhibited FP-2 and other cysteine proteases rhodesain, cathepsin B and L in low nanomolar range. These derivatives displayed potent antiplasmodial and antitrypanosomal activities in micromolar range. The SAR study emphasized on the presence of primary carbon atom in vicinity to the thiosulphinate sulphur atom for improved enzyme activity. Since compound **87** bearing dihexyl group is more stable in solution, so it can be taken further as lead molecule for designing allicin derivatives with enhanced affinities. [64]

Wang *et al.* isolated catharoseumine, **88** a monoterpenoid indole alkaloid having a peroxy bridge moiety from the whole plant of *Catharanthus roseus*. It exhibited potential inhibition of FP-2 with IC_{50} value of 4.06 µM. [65] Stolze *et al.* synthesized some analogues of natural product symplostatin 4 (Sym4), **89** reported to be potent nanomolar growth inhibitor of malaria parasite *P. falciparum* with EC_{50} = 0.7µM. The effect of **89** was seen in the form of red food vacuole defect which indicated the blockage of initial stages of hemoglobin degradation. This effect was found due to FP-2, 2' and 3 inhibition at low nanomolar conc. (1.5 nM). Sym4 exhibited different potencies towards these cysteine proteases as FP-2/2' were inhibited more potently than FP-1 and FP-3. The critical importance of unusual methylmethoxypyrrolinone (mmp) group of Sym4 was established by the low potency of synthesised analogues of Sym4 which suggested that the compounds bearing mmp motif can be considered for the development of antimalarial FP inhibitors (Fig. 12). [66]

A fraction was isolated from the Caribbean coral *Plexaura homomalla* that was enriched in tight-binding protease inhibitors and evaluated for its antiparasitic effect against *P. falciparum* and *T. cruzi.* The inhibitor-enriched fraction displayed *Ki* values of 1.99 nM

and 4.81 nM for FP-2 and cruzipain from *P. falciparum* and *T. cruzi,* respectively. The antiparasitic results showed reduced growth of chloroquine-resistant *P. falciparum* strain Dd2 with IC_{50} value of 0.46 µM. This fraction also resulted in the reduction of Vero cells infection by *T. cruzi* trypomastigotes at sub-micromolar conc. [67]

Ten natural compounds were identified as FP-2 inhibitors through structure-based virtual screening of an in-house Natural Product Database (NPD) that exhibited good potencies against FP-2 with IC_{50} in the range of 3.18 to 68.19 µM. Among them, compounds **90** and **91** exhibited promising potential with IC_{50} value of 3.18 and 3.77 µM, respectively. Some of the inhibitors were evaluated for their antiparasitic effect and compound **92** inhibit chloroquine sensitive (3D7) and resistant strain (Dd2) in low nanomolar range (IC_{50} = 5.54 µM and 4.05 µM against 3D7 and Dd2, respectively). Compound **90** was further assessed to have various hydrogen bonds and hydrophobic interactions with active site residues.[68]

Two compounds 2,3,6-trihydroxy benzoic acid (**93**) and 2,3,6-trihydroxy methyl benzoate (**94**) were extracted based on activity-guided fractionation from the air-dried fruits of *Sorindeia juglandifolia*. The collected fractions were tested for inhibition potential against *P. falciparum* W2 strain and FP-2. Nine fractions showed inhibitory activity with IC_{50} value in the range 2.3-11.6 µg/ml for W2 and 1.1-21.9 µg/ml for FP-2. These were also active against the field isolates of *P. falciparum.* Purified compounds **93** and **94** (Fig. 12) also displayed potent inhibition against W2 (IC_{50} =16.5 µM and 13 µM) and FP-2 (IC_{50} = 35.4 and 6.1 µM). *In vivo* assessment of compound **93** showed activity as well as safety in rodent malaria model thus can be further investigated for the development of antimalarial candidate. [69]

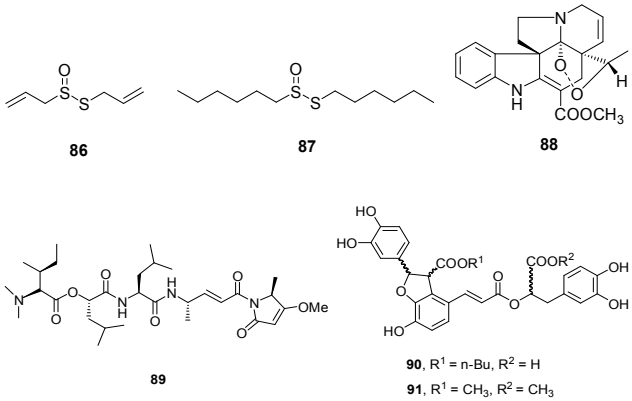

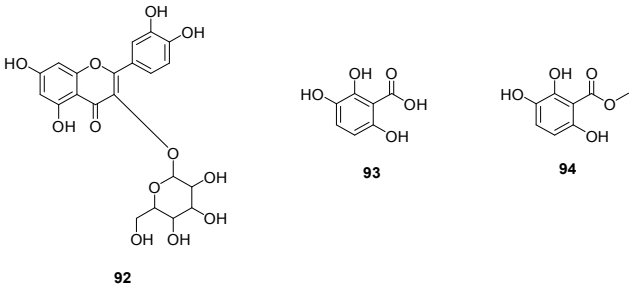

Fig. 12 Chemical structures of natural product based falcipain inhibitors

VI. Pyrimidine based analogues

Coterón *et al.* reported various heteroarylnitrile derivatives, among them, 5-substituted-2-cyanopyrimidine emerged as most promising series (Fig. 13). Sequential optimization of this series, considering different positions present in the parent scaffold, led to the identification of potent FP- 2 and FP-3 inhibitors with nanomolar and subnanomolar range inhibition. Identified inhibitors exhibited activity in whole cell assay in micromolar range. Introduction of different substituents bearing amines at P_3 position in the structure of lead compounds led to the improved enzymatic activities in the picomolar to low nanomolar range with antiparasitic activity in the low nanomolar range. [45]

To further support the observation that pyrimidine nitrile motifs could accommodate a variety of substituents at P_3 position without significantly affecting enzyme inhibition, tetraoxane-pyrimidine nitriles with peroxide moiety at P_3 position were developed (Fig. 13). These derivatives were evaluated against blood and liver stages of malaria as well as FP-2 enzyme. All the derivatives exhibited potent nanomolar activity against the three strains of *P. falciparum* and FP-2 in comparison to their vinyl sulphone counterpart. The most potent compound **96** displayed excellent FP-2 inhibition with IC_{50} = 3.4 nM as well as low cytotoxicity and good activity in the liver stage assay *in vivo*. Nitriles inhibit cysteine proteases by forming hydrogen bonds with catalytic residues, Cys42 and Gln36. Additional interactions were detected with Gly83 and Asn81. [70] Pyrido[1,2-*a*]pyrimidin-4-ones were evaluated for FP-2 inhibition potential which displayed fairly good activity. The excellent FP-2 inhibition by compounds **97** and **98** with IC_{50} values of 6.0 and 7.0 µM, respectively emphasized the presence of urea moiety to enable the compounds to be potent FP-2 inhibitor (Fig. 13). [71]

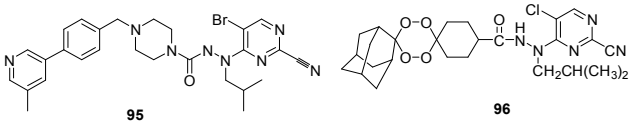

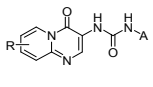

97, R = 8-CH_3, A = $(CH_2)_2$-OCH_3
98, R = 7-Cl, A = $(CH_2)_2$-(4-morpholine)

Fig. 13 Chemical structures of pyrimidine based falcipain inhibitors

VII. Chalcone based analogues

A series of β-amino alcohol thiolactone-chalcone and isatin-chalcone hybrids was developed and evaluated for growth inhibitory activity against W2 chloroquine-resistant strain of *P. falciparum* and its inhibitory activity against recombinant FP-2. The results for a 36-member β-amino alcohol triazole library showed that the thiolactone-chalcones displayed promising antiplasmodial activity, with IC_{50} values ranging from 0.68 to 6.08 μM, than the isatin-chalcones with IC_{50} of 14.9 μM or less. While isatin-chalcones hybrids exhibited FP-2 inhibitory activity with meta substitution preferred compound, thiolactone-chalcones lacked FP-2 inhibitory activity suggesting that these compounds act via impairment of other parasite pathways or targets. [72]

A library of 88 chalcones were synthesised as analogues of natural antimalarial agents, medicagenin, **101** and munchiwarin, **102**. These derivatives were evaluated for their *in vitro* antimalarial potential, and compounds **103**-**107** were found with good antiparasitic activity, low cytotoxicity and good selectivity index (Fig. 14). *In vivo* results demonstrated rapid parasite clearance (71-98%) with increased survival time. The inhibitory potential of these compounds against FP-2 showed that the compound **107** inhibited FP-2 with IC_{50} of 4.6 μM. Docking study of chalcone based inhibitor, **107** with FP-2 showed formation of hydrogen bonds with S1' and S1 subsites (Tyr206 Gln36, Cys39, Cys42 and His174). Alkenyl group of **107** formed hydrophobic contacts with Leu84 (S2) and Ile 85 (S3). [73]

An in-house library consisting of (*E*)-chalcones, (*E*)-*N'*-benzylidene-benzohydrazides and alkylesters of gallic acid against FP-2 were developed. Among these, (*E*)-chalcones were found to possess lower IC_{50} value with compound **108** emerged as potent FP-2 inhibitor displaying non-competitive inhibition with IC_{50} value as 4.9 μM. [74]

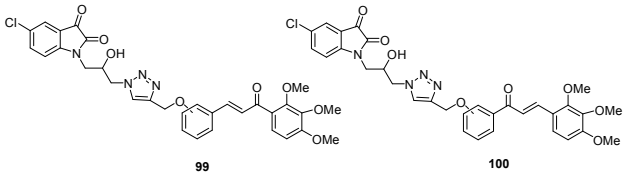

99 **100**

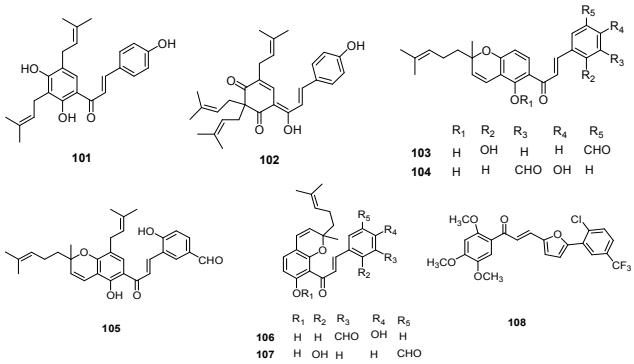

	R_1	R_2	R_3	R_4	R_5
103	H	OH	H	H	CHO
104	H	H	CHO	OH	H

	R_1	R_2	R_3	R_4	R_5
106	H	H	CHO	OH	H
107	H	OH	H	H	CHO

101 **102** **105** **108**

Fig. 14 Chemical structures of chalcone based falcipain inhibitors

VIII. 1,4-diazepan based analogues

A new class of FP-2 inhibitors was designed and synthesised using ligand based approach. The 2-(4-(substituted benzoyl)-1,4-diazepan-1-yl)-*N*-phenylacetamide derivatives were evaluated for FP-2 inhibition. Out of all the compounds, five compounds displayed >60% inhibition at 10 μM conc. while **109** was found to be most potent compound with 72% inhibition at the same conc. and forms several hydrophobic and hydrogen-bond interactions with active site residues as indicated by modelling studies.[75]

Novel antiprotozoal agents containing 1,4-benzodiazepine scaffold were developed through an optimization study of previously reported inhibitors. [76] The novel compounds were synthesized by modifying or even removing the side chain attached at C3 position of the benzodiazepine scaffold. The nature and length of the spacer connecting the benzodiazepine ring and 3-bromoisoxazoline moiety was also considered. These derivatives were evaluated against rhodesain and FP-2 which displayed single-digit micromolar or sub-micromolar activity against one or both enzymes. Among these, the most potent FP-2 inhibitor was found to be **110** with *Ki* value 0.23 μM even more potent than the model compounds **111** and **112** exhibiting *Ki* value of 5.48 and 6.0 μM, respectively (Fig. 15). [47]

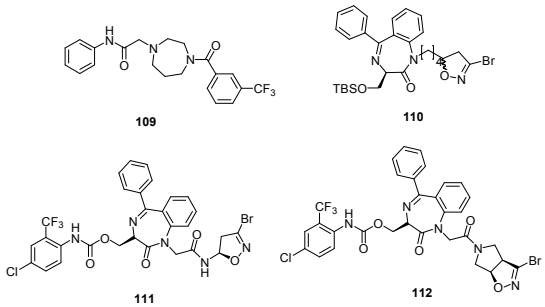

109 **110** **111** **112**

Fig. 15 Chemical structures of 1,4-diazepan based falcipain inhibitors

IX. Thiazolidine-2,4-diones

A series of 2,4-thiazolidinediones based on TZD 4 (thiazolidine-2,4-dione derivative), **113** was identified through structure-based virtual screening (Fig. 16). The compounds were synthesised and evaluated for their antimalarial potential which displayed low micromolar antiplasmodial activities against *P. falciparum* drug resistant W2 strain. FP-2 inhibition data revealed that compound **114** (IC_{50} = 11.23 μM) showed enhanced inhibitory activity in comparison to **113** (IC_{50} = 25.5 μM). In spite of significant antiparasitic activity, the most active compounds showed poor microsomal metabolic stability in the presence of human, rat and mouse hepatic microsomes. Molecular docking between FP-2 and **114** showed that chlorophenyl and the trimethoxyphenyl group occupied S2 and S1 subsites, respectively. The thiazolidine-2,4-dione scaffold was close to the active site of enzyme. His174 was shown to be in dipole-dipole interaction with the oxygen of inhibitor.[77]

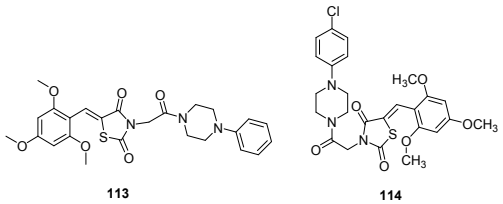

113 114

Fig. 16 Chemical structures of thiazolidine-2,4-diones based falcipain inhibitors

X. Triazine nitriles

Selective inhibitors of FP-2 and rhodesain from *P. falciparum* and *T. brucei* were identified through structure based drug design. FP-2 inhibition studies demonstrated preference for morpholine group in place of cyclopropylamine derivative or 2-methoxyethylamine groups in the S1 pocket and smaller size substituents were desired in the S2 pocket of the enzyme and 1,3-benzodioxol-5-yl and cyclohexyl substituents were preferred for S3 pocket. Compound **115**, with an unsubstituted cyclohexyl moiety and morpholine group with 1,3-benzodioxol-5-yl group in the S2 pocket of the enzyme was found to be more potent against FP-2 (*Ki* = 20 nM) and it showed *Ki* = 8.0 nM against rhodesain (Fig. 17). Another, lead compound **116** exhibited highest affinity against the rhodesain enzyme with *Ki* values of 2.0 nM. Some of the compounds showed affinity for human cathepsin L in the low nanomolar range while selectivity was observed against human cathepsin B and the viral cysteine proteases and α-chymotrypsin. Despite their excellent enzymatic activity and good selectivity, compounds displayed moderate antiplasmodial activity and marginal activity against *T. brucei rhodesiense*, thus studies are required to improve its inhibition potential in the cell-based assays. [78]

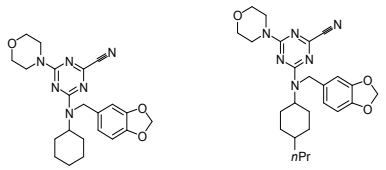

115 116

Fig. 17 Chemical structures of triazine nitriles based falcipain inhibitors

XI. Miscellaneous

Khanye *et al.* studied the inhibitory effect of gold (I) thiosemicarbazone complexes on FP-2 enzyme. The antiparasitic activity as well as enzyme inhibition revealed that coordination of gold (I) to thiosemicarbazone ligand enhanced their efficacy against *P. falciparum* as well as FP-2. The most potent inhibitor was gold (I) complex **117** with IC_{50} value of 0.87μM. The improved activity of thiosemicarbazone gold (I) complexes may be due to the geometry adopted by gold (I) by holding thiosemicarbazones that allows favourable interactions of thiosemicarbazones with the target enzyme. Although no correlation existed between antiplasmodial activity and enzyme inhibition which suggests that the antiplasmodial activity of these complexes may be due to the inhibition of more than one target. [79]

Langolf *et al.* developed a new class of potent and reversible cysteine protease inhibitors based on *N*-protected-guanidino-furan and -pyrrole motifs (Fig. 18). The most potent inhibitor, **118** exhibited IC_{50} = 1.06 μM, while other active compounds showed IC_{50} in the range of 1.38-8.09 μM against *P. falciparum*. The excellent antiparasitic activity clearly emphasizes on the presence of guanidine moiety and the nonpolar aromatic part of the aniline building block. The enzymatic inhibition data revealed that compound **119** showed potent activity with *Ki* = 0.52 μM against FP-2. These derivatives also showed excellent activity against African trypanosomiasis and rhodesain. Moreover these compounds exhibited low or moderate cytotoxicity against mammalian cells. [80]

Micale *et al.* evaluated some structurally varied gold complexes for the FP-2 inhibition as well as for *P. falciparum* growth inhibition. The results obtained from both inhibition studies failed to establish any correlation between the two, thus supporting the findings by Khanye *et al.* [79] Out of these gold complexes, $K[Au(Sac)_2]$, **120** displayed 66% inhibition of FP-2 which might be due to binding of Au (I) to the catalytic active site cysteine while auranofin was found to be potent inhibitor in growth assay with IC_{50} value of 0.142 μM. [81]

Shah *et al.* designed and synthesised combinatorial library comprising benzothiazole and triazole scaffolds based on core-hopping strategy. These compounds were evaluated for their inhibition potential of FP-2 which revealed fifteen analogues of both series with moderate inhibition of FP-2. Among these, two compounds, **121** and **122** with protonated amino groups from the benzthiazole series were found to inhibit both the enzymes: FP-2 and FP-3 which was well correlated with the results obtained by docking studies. Compounds possessing bulkier substituents, **123**, **124** and **125** from the triazole series afforded moderate inhibition of FP-2 while none of the compounds, except **123** from the triazole series inhibited FP-3 (Fig. 18). Compound **121** also exhibited potency against chloroquine-resistant cultured *P. falciparum* with IC_{50} value in the lower micromolar range. Both these compounds, **121** and **122** also inhibited mammalian cysteine proteases of papain family suggesting that the polar residues present in the S2 pocket may not be critical to the selective inhibition of falcipain. [82]

Kumar *et al.* designed and synthesized 3-methylene-substituted indolinones and evaluated them as FP inhibitors and antiplasmodial agents. The enzymatic inhibition results revealed that indolinones containing a Leu-isoamyl recognition moiety were having moderate inhibition potential against FP-2 while none was active against FP-3. These compounds exhibited antiplasmodial activity in the low micromolar range against the chloroquine-resistant W2 strain of *P. falciparum*. Coupling of 7-chloroquinoline to 3-methylene-substituted indolinone resulted into potent antiplasmodial agents with no effect on FP-2 inhibition suggesting a different mode of action for these compounds. Thus, 3-methylene-indolinone-2-ones being potent lead compounds can be further developed into new antimalarial therapeutics. Molecular docking studies of **126** with FP-2 showed interactions with Cys42. [83]

Oliveira *et al.* designed and synthesised a novel class of tetraoxane-vinyl sulfone based hybrid compounds possessing high potency against chloroquine-sensitive and chloroquine-resistant *P. falciparum* strains in the low nanomolar range. Although these demonstrate weak to moderate inhibition of FP-2 with IC_{50} values ranging from 1.0 to 10 µM but the ability of efficient delivery of vinyl sulfones (FP-2 inhibitor) in the presence of iron (II) bromide in the parasite digestive vacuole makes them promising candidate with nanomolar protease inhibitory activity. Mechanistic aspect of these compounds were studied with **127** which indicated the presence of intact parent vinyl sulfone, **128** in the infected erythrocytes even after 48 h of post treatment with the hybrid compounds suggesting its long lasting effect. These results clearly indicated that masking of tetraoxane partner offers efficient strategy for diminishing the off-target effects of known drugs (Fig. 18). [84]

Gibbons *et al.* extended their combination chemotherapy approach through a single prodrug entity utilizing 1,2,4-trioxolane as protease inhibitor carbonyl masking group. They synthesized carbonyl based protease inhibitors and their endoperoxide hybrids. These were evaluated for recombinant FP-2 and FP-3 inhibition and antimalarial activity against 3D7 *P. falciparum* strain. Aldehydes **129** and **130** displayed potent and selective inhibition of FP-2 in low nanomolar range while only *α*-phenoxy analogue, compound **131** among the keto series inhibited both the FP-2 and FP-3 with low nanomolar activity. **129** and **130** also displayed low nanomolar activity against 3D7 *P. falciparum* strain. Among the endoperoxides hybrids, aldehyde prodrugs, **132**, **133**, **134** and ketone prodrugs, **135** and **136** were the most potent where **133** and **134** exhibited IC_{50} value of 55 and 35 nM against 3D7 strain (Fig. 18). Although there is more than 400 times difference in the FP-2 inhibitory potency between aldehyde **129** and endoperoxide **133**, but similar activity against cultured parasites could be explained due to contribution from the activation and inhibitor release. Mechanistic approach was studied through ferrous mediated decomposition of these molecules which suggested that these compounds degrade to form carbonyl inhibitor along with C-radical formation. [85]

Singh *et al.* reported a new class of phthalimides functionalized with cyclic amines as antiparasitic agent and FP-2 inhibitor. Of all the synthesized derivatives, compound **137**, bearing piperazine linker was found to be the most potent antimalarial agent with IC_{50} values of 5.97, 2.0 and 1.1 µM on incubation period of 42, 60 and 90 h, respectively, thus effectiveness is increased with increase in exposure time of the parasite to the compound. The compound **137** was also found to be effective against chloroquine resistant strain (*Pf*7GB) with IC_{50} value of 7.21 µM. The enzymatic assay revealed that compound **138** was the most active compound against FP-2 thus suggesting that phenylalanine residue play a critical role in FP-2 inhibition. [86]

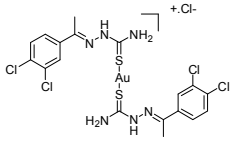

117

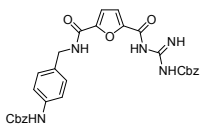

118

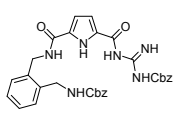

119

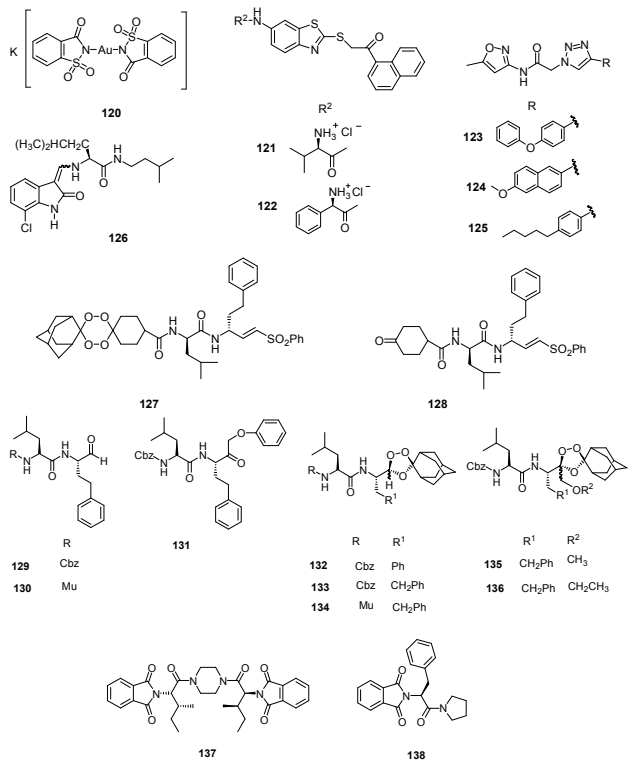

Fig. 18 Chemical structures of various falcipain inhibitors

2.1.3. Metalloaminopeptidases (MAPs) The neutral aminopeptidases M1 alanyl aminopeptidase (*Pf*A-M1), M17 leucine aminopeptidase (*Pf*A-M17) and M18 aminopetidase play an essential role in the growth and propagation of *Plasmodium* as these act during terminal stages of hemoglobin digestion by degrading small peptide fragments into free amino acids during the symptomatic erythrocytic stage of infection. [87] Another study has revealed that *Pf*A-M17 is associated with some other role in addition to hemoglobin digestion and found to be essential in the early life cycle of the parasite before the beginning of hemoglobin digestion. These are metalloenzymes which bear distinct arrangement of Zn^{2+} ion in their active site, therefore chelation of the metal ion in either enzyme inhibits its activity. Hence, those inhibitors which can effectively bind the metal ions will prove as a boon in malaria eradication campaign. [88] Several groups have synthesized inhibitors incorporating metal binding scaffolds which have proven their potency by reducing the enzyme activity thus affecting parasite growth.

A diverse library of bestatin derivatives was synthesised that varied at the side chain of either the *α*-hydroxy-*β* amino acid (P1) or the adjacent natural *α*-amino acid (P1') (Fig. 20). Screening of the library against *Pf*A-M1 showed the Tyr(OMe) derivative (**139**) was the most potent inhibitor (*Ki* = 43 nM) suggesting that S1 pocket could accommodate large aromatic side chains as well. The derivatives were evaluated against *P. falciparum* which showed moderate potency with IC_{50} values in the micromolar range. The most potent inhibitor **139** exhibited IC_{50} of 6.4 μM which was slightly less potent than bestatin, **140** (IC_{50} = 3.2 μM) might be due to lowered permeability because of methoxy group. [89]

The antimalarial potential of CHR-2863, **141** and its acid analogue CHR-6768 (**142)** was evaluated. Enzymatic assay against *Pf*A-M1 and *Pf*A-M17 demonstrated that **141** was almost two-fold more potent (*Ki* = 1.4 μM) than its acid derivative (*Ki* = 2.4 μM) while found to be equipotent as **140** (*Ki* = 1.6 μM) against *Pf*A-M1 enzyme. Both the ester and acid were found to be more potent (20 to 100 fold) against *Pf*A-M17 than *Pf*A-M1 while found to be 8-fold and 24-fold more potent, respectively against r*Pf*A-M17 than bestatin. The acid, **142** (*Ki* = 0.025 μM) displayed three times greater inhibition constant than **141** (*Ki* = 0.075 μM). The *in vitro* antiparasitic evaluation demonstrated that ester (IC_{50} = 370 nM) exhibited 5-fold greater potency than the acid (IC_{50} = 2.0 μM) while bestatin showed IC_{50} value of 5.0 μM. Analysis of parasite morphology after treatment with **141** showed that it induces vacuolization in *P. falciparum* parasites similar to **140**. Treatment of mice infected with murine malaria species *P. chabaudi* with **141** at the oral dose of 25 mg/kg daily reduced the peak parasitemia in all groups compared to the controls, with increased doses showed enhanced effect on parasite growth. [90]

SAR of a selective family of hydroxamate *Pf*A-M1 inhibitors based on malonic scaffold was evaluated. Introduction of steric constraints at the malonic position led to the identification of **143** which exhibited nanomolar selective inhibition of *Pf*A-M1 with IC_{50} value of 6.0 nM. It showed good physicochemical, *in vitro* plasma stability and potent *in vitro* antiplasmodial activity. "Fluoro-scanning" performed around hit molecule **143** and **144** identified para position on benzylamido group as the key position of halogen for activity (Fig. 20). The compound **143** was stable in microsomes, in plasma. The *in vivo* distribution study revealed that compound **143** reaches its site of action. Nonetheless, it was unable to kill the parasite at the conc. needed for enzyme inhibition. Thus, the results can be concluded that pharmacological activity of an inhibitor should not only be dependent upon its binding to the target molecule and its inhibitory potency but its ability to reach the target at an enough conc. for ample period of time. Docking study of compound **143** with *Pf*A-M1 showed that S1 pocket undergo major conformational change on inhibitor binding and it can accommodate

larger groups by making hydrophobic interaction thus supported the observation made by Velmourogane *et al.* [89, 91].

Synthesis and structure-activity relationships of a small library of metal-chelating phosphonic acid arginine mimetics were reported that probe the S1 pocket of both enzymes. Evaluation of this library as inhibitors of the *Pf*A-M1 and *Pf*A-M17 aminopeptidases of *P. falciparum* found 1-amino-5-guanidinopentylphosphonic acid (**145**) potent against *Pf*A-M1 with *Ki* value of 11 µM while rigidification due to introduction of phenyl group or reduction in the length of carbon chain reported detrimental to inhibition potential. Guanidino groups played a very important role in retaining the inhibitory activity. The compound 4-(pyrazol-1-yl)phenyl) (amino) methylphosphonic acid (**146**) emerged as most potent inhibitor of *Pf*A-M17 with *Ki* value of 11 nM. It was also found to be modest inhibitor of *Pf*A-M1 with *Ki* value of 104 µM involved in few interactions with the large S1 pocket of the enzyme, thus providing additional advantage to be developed as dual *Pf*A-M1/M17 inhibitor. Further optimization of compound **146** in terms of increasing *Pf*A-M1 inhibition potential and its physicochemical properties for antiparasitic activity is desirable to develop it as lead antimalarial candidate. X-ray crystal structures of lead inhibitors bound to these enzymes showed essential interactions within the active sites and shed light on the structural modifications required for making them dual inhibitor. Crystal structures of **145** and **146**with the *Pf*A-M1 and *Pf*A-M17, respectively were reported. In the *Pf*A-M1-145 enzyme complex, N2 of guanidino group makes interactions with backbone oxygen of Glu572, a critical residue required for the formation of S1 pocket of *Pf*A-M1. In the *Pf*A-M17-146 complex, phosphate group of the inhibitor is involved in extensive interactions with the two metal ions and carbonate ion present in the active site of *Pf*A-M17. The amine group of the inhibitor is involved in hydrogen bonding interactions with Asp379 and 399. The 4-(1H-pyrazol-1-yl)phenyl group fitted efficiently in the hydrophobic S1 pocket by forming hydrophobic packing interactions (Fig 19). [88]

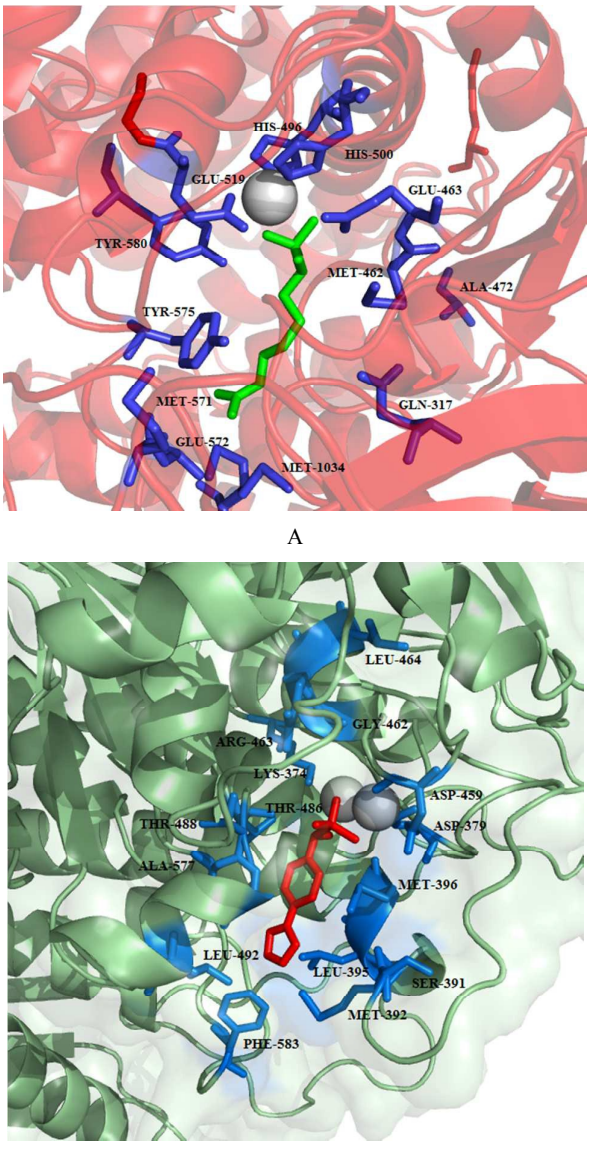

Fig. 19 Crystal structure of inhibitors bound to the active site of metalloaminopeptidases. Carbon atoms of *Pf*A-M1 are colored in red (A) and carbon atoms of *Pf*A-M17 are colored in green (B). Zinc is shown as grey sphere in *Pf*A-M1/ *Pf*A-M17. Inhibitors, **145** and **146** are colored in green and red, respectively. Figures were made in PyMol using PDB ID: 4K5L (*Pf*A-M1) and 4K3N (*Pf*A-M17)

To improve the membrane permeability and plasma safety profile, Mistry *et al.* replaced the phoshonic acid group with hydroxamic acid-based compounds as zinc binding groups. This approach led to the identification of **147** as potent dual inhibitor of *Pf*A-M1 (*Ki* = 0.8 µM / *Pf*A-M17 (*Ki* =0.03 µM). This inhibitor was found to be 100-fold active against *Pf*A-M1 than that of **145** while *Pf*A-M17 potency was comparable to **145**. This compound exhibited

selective inhibition of *Pf*A-M1 and *Pf*A-M17 over *Pf*M18AAP, another *P. falciparum* MAP. Crystal structure of both the enzyme with compound **147** revealed the reason behind improved potency that along with strong coordination to the zinc ion as well as probing the hydrophobic S1 pocket, *N*-Boc group was involved in binding within the S1' pocket. SAR of this molecule by incorporating *N*-acyl group in place of *N*-boc group identified compound **148** exhibiting *Ki* = 0.7 μM against *Pf*A-M1 comparable to that of compound **147** while same did not exist in case of *Pf*A-M17. Replacement of *N*-boc group by *N*-fluorobenzoyl group helped in regaining potency against *Pf*A-M17 but were unable to inhibit *Pf*A-M1. Such modification can be explored further for potent *Pf*A-M17 inhibition although it is unfavorable for *Pf*A-M1 inhibition. The compounds were further evaluated for their antiparasitic effect and compound **148** with IC_{50} of 227 nM emerged as potent inhibitor against 3D7 malaria parasites. Though compound **147** exhibited comparable enzyme inhibition potential, IC_{50} value of 783 nM suggested the less capability of cellular penetration of *N*-Boc group than the corrosponding *N*-acyl derivatives. Lack of toxicity suggested that this series has potential to be developed as potent MAP inhibitors. [87]

A Molecular Libraries Probe Production Centers Network collection comprising ~292000 compounds were screened to identify potent and selective *Pf*M18AAP inhibitors. This was done by developing a fluorescence enzymatic assay using recombinant *Pf*M18AAP enzyme and a fluorogenic peptide substrate (H-Glu-NHMec). This was further counter screened to identify compounds with nonspecific activity by cathepsin L1 (CTSL1) enzyme based assay. This high-throughput screening identified two structurally related compounds, CID 6852389, **149** and CID 23724194, **150** which exhibited micromolar potency and were inactive in CTSL1 titration experiments with IC_{50} > 59.6 μM (Fig. 20). Both compounds displayed non-competitive inhibition in micromolar range in *Pf*M18AAP enzyme assay with *Ki* values of 3.39 and 1.35 μM. The compounds were found active in whole cell assay with IC_{50} value of 4.0 μM and 1.3 μM, respectively. Thus, these compounds will provide the basis for the identification of small molecule *Pf*M18AAP inhibitors. [92]

A highly sensitive multiplex assay was developed for the rapid primary screening of "MMV 400" compounds against all the three metalloaminopeptidases of *P. falciparum*: *Pf*A-M1, *Pf*A-M17 and *Pf*M18AAP. The screening showed that the selected compounds were ineffective in inhibiting *Pf*M18AAP while three 'drug-like' and twenty one 'probe-like' compounds were identified targeting the *Pf*A-M1, *Pf*A-M17. A secondary assay performed over the 24 hit compounds identified seven compounds that inhibit the activity of *Pf*A-M1, *Pf*A-M17 by > 90% while two exhibited > 95% inhibition. MMV666023 (**151)** emerged as potent inhibitor of *Pf*A-M1 with 95% inhibition and reduced the activity of *Pf*A-M17 by 70%. Opposite specificity was observed with MMV020750 (**152**) which was able to reduce *Pf*A-M17 activity by 95% while reducing *Pf*A-M1 activity to only 75% of total enzyme activity. SAR analysis around **152** investigated the role of phenyl substituent which showed similar inhibition potential of ester and hydroxamic acid as that of parent compound with inhibitory activity in micromolar range against *Pf*A-M1 while > 10-fold reduction in activity was observed against *Pf*A-M17. The acid, **153** showed > 10-fold increase in activity against *Pf*A-M1. Molecular docking studies further confirmed that compound **151** and **152** are competitive inhibitors where compound **151** act by zinc coordination. [93]

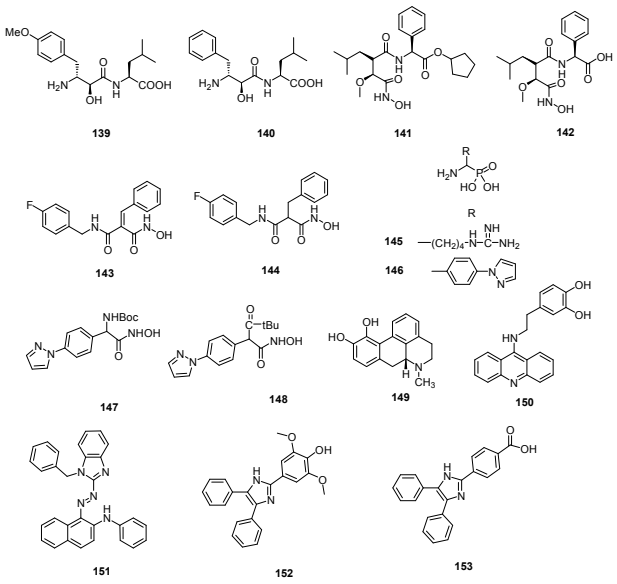

Fig. 20 Chemical structures of metalloaminopeptidase inhibitors

2.1.4. Dipeptidyl Aminopeptidase I (DPAP1) Three classes of endopeptidases like aspartic proteases, cysteine proteases and metalloproteases degrade hemoglobin to oligopeptides in the food vacuole. Although these classes of enzymes are potential targets to induce death of the parasites but the release of small peptides or amino acids from globin oligopeptides requires the services of exopeptidases such as dipeptidyl aminopeptidase 1 (DPAP1) which is located in the food vacuole. [94] The dipeptides generated from oligopeptides by DPAP1 forms the substrate for vacuolar aminopeptidase which is converted into single amino acids. Parasite genome encodes two more DPAP enzymes in which DPAP2 is mainly expressed in gametocytes whose function is yet to be

explored while DPAP3 is expressed during the erythrocytic cycle of *P. falciparum* in the active form where it played an essential role in parasite egress from RBCs. DPAPs are considered as potential targets as the closest human ortholog, human cathepsin C is not essential in mammals, although it is involved in activating a family of serine proteases which are involved in inflammation and immune response. [95] Since both DPAP1 and DPAP3 play an essential role in parasite life cycle, an inhibitor targeting these proteases will likely to disrupt multiple biological processes.

Validation of DPAP1 as a potentially valuable antimalarial drug target was further carried out. Activity based probes were utilized to reveal that small molecule inhibitors like Ala-4(I)Phe-DMK, **154** caused the formation of an immature trophozoite by specific inhibition of DPAP1 which leads to parasite death (Fig. 21). Although this compound showed potency *in vitro* but the overall lack of stability prohibited its use for *in vivo* studies. Therefore, computational methods were explored to design potent nonpeptidic inhibitors of DPAP1 that could be evaluated in mouse model of malaria. One of the compound, ML4118S (**155**) was found to be most potent than its R isomer as the cyclopentane moiety was deeply buried in the S2 pocket while in the R isomer, this group is partially exposed to the solvent. It was effective in killing *P. falciparum* at single-digit nanomolar conc., stable in mouse serum but toxic *in vivo* at 20 mg/kg and caused a decrease in parasite load in mouse model of malaria. Considering toxicity issues pertaining to this, related compound KB16 (**156**) which was designed to target *Trypanosoma cruzi* and known to have low toxicity in mice, showed significant decrease of parasitemia at a dose level of 20 mg/kg/day upto day 14. This compound targets berghepains (BP1) with IC_{50} value of 0.5 μM suggesting that the decrease in parasitemia was due to a combined effect of BP1 and DPAP1 inhibition. Although the compounds reported in this study are associated with lack of potency, poor pharmacokinetic properties and toxicity issues, these results evidenced DPAP1 as viable antimalarial drug target. [95]

Biochemical properties of DPAP1 were compared with that of human cathepsin C. A method was developed for the production of purified recombinant DPAP1 possessing features similar to those of native enzyme. DPAP1, like cathepsin C is activated by chloride ion and showed its high efficiency in catalysing amide bond hydrolysis at acidic pH values. DPAP1 exhibits monomeric quaternary structure which was different from the homotetrameric structure of cathepsin C. Positional scanning synthetic combinatorial library was profiled to determine S1 and S2 subsite preferences of DPAP1 and cathepsin C by utilizing fluorogenic dipeptidyl-7-amido-4-carbamoylcoumarin (dipeptide-ACC) PSL. The S1 preferences of DPAP1 were found to be similar to other C1-family cysteine peptidases while S2 subsite of both DPAP1 and cathepsin C favoured aliphatic hydrophobic residues, proline and some polar residues, thus exhibiting distinct specificity. Several fluorogenic dipeptide substrates were efficiently catalysed by DPAP1 except a substrate containing P2-phenylalanine residue which was found to be competitive inhibitor. Two reversible cathepsin C inhibitors containing nitrile pharmacophores, **157,** semicarbazide, **158** inhibited both recombinant and native DPAP1 (Fig. 21). Both enzymes were inhibited with sub-nanomolar *K*i values for semicarbazide and single-digit nanomolar *K*i values for peptide nitrile thus validating recombinant DPAP1 to be used for drug discovery campaign and characterization. [94]

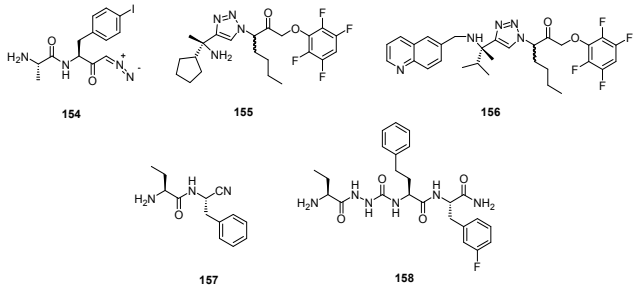

Fig. 21 Chemical structures of dipeptidyl aminopeptidase I inhibitors

3. Nucleus

Major pathways of nucleic acid metabolism of *Plasmodium* are well known targets against antimalarials. The genomic DNA or proteins regulating critical pathways for parasite growth and survival are attractive targets for designing antimalarial inhibitors. Some important enzymes and their inhibitors reported are discussed below.

3.1. Histone deacetylase (HDAC) Histone deacetylase enzymes are zinc-dependent enzymes that are required for catalyzing the removal of acetyl groups from the lysine residues located at the histone tail which results in chromatin condensation and transcriptional repression. Inhibition of this critical event in chromatin remodelling is lethal to the parasite as it alters the gene expression regulation. [96] All the *Plasmodium* species carry the HDAC gene homologues where *P. falciparum* genome encodes for five HDACs in which one of *Pf*HDAC exhibit homology to human class I (*Pf*HDAC1), two encoding homologues of class II HDACs (*Pf*HDAC2,3), whereas two genes showed homology to class III (*Pf*Sir2A and *Pf*Sir2B). [97] Among these, *P. falciparum* histone deacetylase 1 (*Pf*HDAC1) is a potential target in the malaria intervention strategies.

The effect of specific cap group substitution patterns and spacer-group chain lengths were accessed in enhancing the antimalarial and antileishmanial activity of aryltriazolylhydroxamates-based HDAC inhibitors (Fig. 22). The anti-parasitic effect of these compounds well correlated with their anti-HDAC activities. Many of the compounds were several folds cytotoxic selectively to *Plasmodium* parasite in comparison to standard HDAC inhibitors- SAHA and TSA. These results suggested an optimum length of methylene spacer group being 5 or 6 leading to high activity against protozoa. [98]

Several *Pf*HDAC inhibitors which were designed to bind the zinc and exterior surface around the active site of the enzyme were reported. 22 compounds possessed cinnamic acid derivatives or NSAID components as HDAC-binding groups while remaining were synthesised by substituting different amines in order to explore active-site space occupation by the 8-aminoquinoline group. Most of the compounds displayed potent antiplasmodial activity with IC_{50}<100 nM. All the selected compounds caused hyperacetylation of *Pf*histones with >10-fold, more cytotoxicity towards *P. falciparum* than a normal human cell type. Based on antimalarial and hyperacetylation data, compound **169** may be selected to serve as lead molecule. [96]

A piggy-back approach was utilised for anticancer histone deacetylase inhibitor SB939 (**170**) to be developed as potent antimalarial agent. In the biological evaluation against asexual-stage of *Plasmodium*, it exhibited IC_{50} values of 0.08 and 0.15 μM against chloroquine-sensitive (3D7) and chloroquine-resistant (Dd2) strains respectively, causing hyperacetylation of both histone and non-histone proteins of parasite. It exhibited additive effect in combination with the aspartic protease inhibitor lopinavir, **171** while antagonistic effect was observed with primaquine and piperaquine. It also displayed potency against *in vitro* growth of exoerythrocytic-stage *Plasmodium* in liver cells with IC_{50} of 155 nM thus providing additional benefit in targeting multiple life cycle stages of parasite. Evaluation of *in vivo* efficacy of this compound in an experimental cerebral malaria model revealed significant inhibition of *P. berghai* ANKA parasite growth with prevention of cerebral malaria-like symptoms. Thus, this study has provided a platform for the development of next-generation anticancer HDAC inhibitors as potential antimalarial drug leads. [99]

Lack of crystal structures of recombinant *Pf*HDAC made Hansen *et al.* to establish SAR based on known HDAC inhibitors. The SAR study revealed the importance of cap group, a connecting-unit linker region, as well as a zinc binding group (ZBG). Based on this data, they synthesized 16 HDAC inhibitors bearing alkoxyurea connecting-unit linker region, hydroxamic acid as ZBG and evaluated them for antiplasmodial potential against *Pf*3D7 strain. Based on the screening of compounds against sexual-stage *P. falciparum* parasites, hyperacylation tendency of histone H4 for the selected compounds, the compound **172** (*Pf*3D7 IC_{50} = 0.16 μm) emerged as most potent asexual stage inhibitor with >30-fold more cytotoxicity in comparison to normal mammalian cells. Thus, **172** can serve as lead for the future development of HDAC inhibitors with improved antiplasmodial activity and enhanced selectivity. [97]

Having identified the importance of hydroxamic acid as zinc binding group for potent inhibition of *Pf*HDAC, they used human HDAC4 and 5 inhibitor **173**, as a starting point for constructing mini-library of HDAC inhibitors containing alkoxyamide connecting-unit linker region. *In vitro* evaluation of these derivatives against asexual stage *P. falciparum* revealed IC_{50} in the range of 0.09-1.12 μM. When examined for HDAC inhibition as well as nuclear lysate % inhibition, compound **174** showed the highest potency with 93.3% and 82.6% inhibition, respectively. Five out of 21 compounds displayed potent inhibition of exo-erythrocytic stage of *P. berghai* mouse model with IC_{50} values in the range of 0.16-0.66 μM. Analysis of gametocytocidal data identified **173**, **174** and **175** as potent inhibitor with IC_{50} range 0.25-0.43 μM (Fig. 22). [100]

Two classes of HDAC inhibitors containing different zinc binding groups (hydroxamic acid vs thiol) were evaluated for the antiparasitic effect. Hydroxamic acid based HDAC inhibitors emerged as most potent antimalarial compounds with activity ranging from low double-digit to single-digit nanomolar range. Among three derivatives selected on the basis of *in vitro* evaluation, compound **176** exhibited 88% inhibition of parasitemia in *P. berghai* mouse model, presenting a new lead for further evaluation. [101]

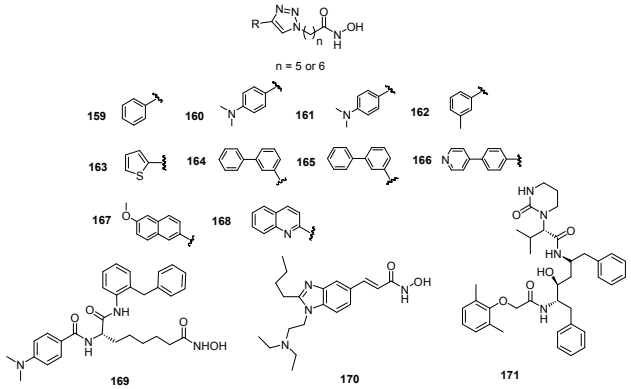

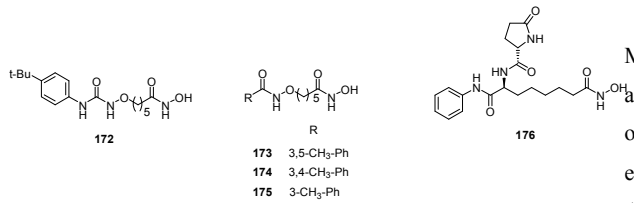

Fig. 22 Chemical structures of histone deacetylase inhibitors

3.2. Cyclin dependent kinases (CDK) *Plasmodium* cyclin dependent kinases are considered as an important therapeutic target for anti-malarial drug discovery because of their essential role in the growth and development of the parasite through the maintenance of cell cycle events taking place in the parasite. [102] Although CDKs (*Pf*mrk) can be targeted for a variety of diseases such as cancer, neurological disorders, microbial infection and cardiovascular disease, exploitation of minor differences in the amino acid sequences in the active-site pocket of both the human and *Plasmodium* CDKs can be explored for the development of specific inhibitors. [103]

Caridha *et al.* evaluated the potential of substituted thiophene and benzene sulphonamides against malarial and mammalian cyclin dependent protein kinases. Many of the compounds exhibited inhibition of *Pf*mrk at low to sub-micromolar concentrations. Selected compounds demonstrated specificity for human CDK7 over CDK1, CDK2 and CDK6 with IC_{50} values in the sub-micromolar range, might be due to the high sequence homology of *Pf*CDK with human CDK7. One of the sub-class of compounds, bromohydrosulfonylacetamides (**177**) was found to be selective for *Pf*CDK with IC_{50} value in the submicromolar range (Fig. 23). Compounds tested in the cross-reactivity studies against human CDK7 were also evaluated for antimalarial activity and cytotoxicity studies against mammalian cell lines. These compounds displayed moderate growth inhibition of drug resistant *P. falciparum* W2 strain as well as low toxicity profiles against mammalian cell lines. Further exploration of bromohydrosulfonylacetamide scaffold with variation in the thiophene and benzene ring substitutions may yield more potent *Pf*CDK inhibitors. [104]

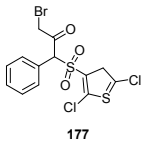

Fig. 23 Chemical structure of cyclin dependent kinase inhibitor

4. Mitochondria electron transport chain

Mitochondria play a crucial role in the survival of *P. falciparum*. Mitochondria can be a selective target for the development of antimalarial drugs as several differences exist among mitochondria of parasite and human at molecular as well as functional level. For example, mitochondrial electron transport chain is not essential for ATP production in parasite as their energy demands are met mainly by glycolysis in contrast to human enzyme where oxidative phosphorylation in mitochondria is an essential process for ATP production. [105] Mitochondrial electron transport chain is required by parasite for maintaining an intracellular pyrimidine pool for the synthesis of nucleic acids, glycoproteins and phospholipids. [106] The mitochondrial electron transport chain consists of five dehydrogenases: NADH: ubiquinone oxidoreductase (*Pf*NDH2), glycerol-3-phosphate dehydrogenase, succinate: ubiquinone oxidoreductase (Complex II or SDH), the malate:quinone oxidoreductase (MQO) and dihydroorotate dehydrogenase (DHODH). *Pf*NDH2 and MQO are absent in human mitochondria while human mitochondrial DHODH exhibit variations at molecular level. These dehydrogenases play a critical role in providing electrons to the downstream complexes: cytochrome bc_1 complex and cytochrome *c* oxidase (Complex IV) with ubiquinone (coenzyme Q) and cytochrome c functioning as electron carriers between the complexes. Although the ATP synthase (Complex V) is not involved in the generation of ATP in contrast to its mammalian counterpart, but is involved in the leaking of protons for electron transport chain. [107] These apparent differences between parasite and human mitochondria can be exploited for the development of novel chemical scaffolds with acceptable efficacy, pharmacokinetic, toxicity profiles and bioavailability.

4.1. Cytochrome bc_1 complex (Ubiquinol: cytochrome c oxidoreductase; complex III) Cytochrome bc_1 complex is a transmembrane protein whose electron transferring unit consists of three catalytic subunits (cytochrome *b*, the Reiske iron-sulphur protein, and cytochrome c_1). [108] This complex transports H^+ into the intermembrane space via the oxidation and reduction of ubiquinone in the modified Q cycle which requires distinct binding sites: Q_o and Q_i site. These sites are situated within cytochrome *b* where Q_o site is involved in the oxidation of ubiquinol near the intermembrane space while binding and reduction of ubiquinone takes place in the Q_i site near the mitochondrial matrix. [109] This complex provides the oxidized ubiquinone to DHODH for the biosynthesis of pyrimidines. The vital nature of this complex can be deduced by the fact that loss of *bc1* activity leads to collapse of mitochondrial function which

results in parasite death. [110] Atovaquone, is a front line antimalarial drug capable of inhibiting the cytochrome *bc1* complex of *P. falciparum* at Q_o site, thus authenticating this enzyme complex as a crucial target for the development of antimalarial chemotherapeutics. [111]

Twenty-six novel napthoquinone aliphatic esters (rhinacanthin analogues) were synthesised and evaluated them for their antiparasitic effect. Twenty-four esters exhibited substantial antimalarial effect with IC_{50} values in the range of 0.03-16.63 μM. Length of the chain played an important role in determining the activity as compounds bearing longer chain displayed strong antimalarial activity. Among these, compounds **178** (n = 7), **179** (n = 13) and **180** (n = 15) showed the best activity with IC_{50} values of 0.133, 0.032 and 0.030 μM, respectively (Fig. 24). Compounds **178** and **179** showed no toxicity against normal Vero cells with high potential therapeutic index of >1990 and 1826 respectively. They also inhibited *P. falciparum* 3D7 cyt bc_1 activity by binding to the Q_o site with IC_{50} values of 5.4 and 8.0 nM as compared to stigmatellin, **181** with IC_{50} value of 9.1 nM. The results of antiparasitic assay and cyt. bc_1 inhibition revealed the importance of 2'-substituents of propyl chain, the length of aliphatic chain, *α*-methyl substituent of side chain and ester moiety. [112]

Historical antimalarial compound endochin, **182** was utilised as a structural lead for optimization and adopted a novel chemical route to synthesize endochin-like quinolones (ELQ) i.e. 4(1*H*)-quinolone-3-diarylethers. Evaluation of these derivatives against multidrug resistant strains of *P. falciparum* and *in vivo* efficacy identified compound **183** (ELQ-300) as the most potent inhibitor of *P. falciparum* strains D6, Dd2, Tm90-C2B. Moreover, compound **183** exhibited excellent *in vivo* potency against *P. yoelii* in mice with ED_{50} and ED_{90} values of 0.02 and 0.06 mg/kg/day, respectively, and a non-recrudescence cure dose of 0.3 mg/kg/day. Noteworthy feature of **183** was its 30-fold more potency than atovaquone against murine malaria. It was found to be ≥20000-fold more selective for parasite bc_1 complex over human enzyme with EC_{50} value of 0.56 nM thus exhibiting superiority over atovaquone (IC_{50} = 2.0 nM). Preclinical animal studies on **183** demonstrated nonlinear pharmacokinetics i.e. good to excellent oral bioavailability at low doses needed for therapeutic effect but fell off rapidly at higher doses. Further studies need to be carried out to identify clinical formulation in order to improve exposure at higher doses. Compound **183** displayed potential that might be carried forward for clinical studies. [113]

A series of 3-alkyl-2-hydroxy-1,4-naphthoquinones was evaluated for its antiparasitic effect. Four compounds exhibited IC_{50} in the mid micromolar range with one of them, **184** displayed IC_{50} in the nanomolar range (IC_{50} = 443 nM). This most active inhibitor reportedly disrupted mitochondrial membrane potential with $IC_{50\Delta\Psi mt}$ = 16 μM and displayed low cytotoxicity against human cells which advocate its potential as an antimalarial agent. [114]

A new class comprising tetracyclic benzothiazepines (BTZs) was discovered as highly active and selective antimalarials with potency in nanomolar range. SAR trend among these derivatives (**185-190**) exhibited the importance of small hydrophobic substituents at R^2 site and non-polar aliphatic groups at R^1 site in enhancing antimalarial activity (Fig. 24). Synergistic studies of **185** with proguanil produced results comparable to that of atovaquone. Validation of cytochrome bc_1 as the target for this class was established on the basis of the combined approach employing genetically modified parasites, biochemical profiling, and resistance selection. As the resistance to atovaquone is reducing its efficacy, this class, being able to retain its potential against atovaquone resistant parasites, can be used as an alternative to atovaquone in combination therapy. [115]

A series of hydroxy-naphthoquinones possessing a methyl group on the benzene ring was synthesised and tested for interaction with the nuclear encoded rieske iron-sulphur protein (Fig. 24). Evaluation of these compounds against yeast and bovine cytochrome bc_1 complex as a model of parasite and human enzyme respectively identified **191** as a potential inhibitor. The metabolic instability associated with cytochrome bc_1 inhibitor, S-10576 (**192**) has been reported to overcome by introducing the trifluoromethyl function at the terminal end. The specificity of inhibitors for yeast bc_1 complex over bovine bc_1 revealed less selectivity than **192** but higher as compared to atovaquone. [116]

Cowley *et al.* prepared a series of quinolones substituted at 6- and 7- position utilizing Gould-Jacobs approach. The 7-substituted analogues expressed activity at as lower range as 0.46 nM against *P. falciparum*. SAR data of this series of compounds suggested the importance of ester functionality at 3 position and the presence of benzyl linker. The exceptional potency of compound **193** was further explored as cytochrome bc_1 inhibitor. Cytochrome *c* reductase assay revealed that potency of this compound (EC_{50} = 1.3 nM) lies in the same region as that of atovaquone (3.0 nM). Although the compounds displayed high potency, the problem associated with their solubility needs to be addressed. [108]

A novel class of conjugated quinoline-indoles which exhibited potent activity against *P. falciparum* was reported. Compounds bearing quaternary nitrogen on the quinoline (**194** and **195**) showed enhanced activity against the chloroquine-resistant K1 strain while

compounds possessing non-quaternerized nitrogen (**196**) are somewhat less active against K1 strain but these showed improved potency against chloroquine sensitive 3D7 strain in comparison to their analogues (Fig. 24). The antimalarial data clearly focused on the importance of conjugated indole ring in maintaining its antimalarial potential. It was suggested that quinoliniums showed less potency when parasites were exposed to target compounds for a short period of time. The mechanism of action of these compounds was reportedly due to the disruption of mitochondrial potential as evident from the structural relationship between these compounds and pyrivinum pamoate, which is supposed to act via dissipating mitochondrial function. These compounds disrupted mitochondrial potential at the conc. similar or even less than that required for parasite killing. [117]

Nam *et al.* identified decoquinate, **197** through a high-throughput screening of an annotated compound library comprising >28,000 compounds possessing drug-like characteristics. *In vitro* evaluation of decoquinate against blood stage *P. falciparum* exhibited activity in the single-digit nanomolar range with IC_{50} value of 4.3 nM. A chemical genomic analysis of decoquinate-resistant line revealed that resistance was conferred by mutations in cytochrome *b*. In addition to that, decoquinate was also found active *in vitro* against liver stage *P. yoelii* with IC_{50} value of 177 pM and when adminstered to mice at dose level of 50 mg kg^{-1} provided partial prophylaxis protection. The insensitivity of transgenic parasites expressing yeast dihydroorotate dehydrogenase to decoquinate further evidenced that actual target of this drug is mitochondrial electron transport chain. Molecular modelling studies revealed distinct mode of binding within the ubiquinol-binding site of cytochrome *b* for both decoquinate and atovaquone which formed the basis for limited cross-resistance of decoquinate to a panel of atovaquone-resistant parasites. [118]

da Cruz *et al.* also identified **197** via the screening of a library containing 1037 existing drugs with the ability of inhibiting *Plasmodium* hepatic development. Compound **197** displayed highest potency against liver stages, both *in vitro* and *in vivo*. Besides the ability to inhibit *Plasmodium* liver stages, it was also reported to be effective in killing the parasite's replicative blood stages and is potent against developing gametocytes inhibiting its transmission. The mode of action was demonstrated by exploring *Plasmodium* transfected with yeast DHODH which revealed that it causes selective and specific inhibition of parasite's mitochondrial bc_1 complex with an IC_{50} of 0.002 μM and selectivity index of >5000 in comparison to human bc_1 complex and showed little cross-resistance with antimalarial drug atovaquone. Single dose of decoquinate (**197**) is highly effective in preventing the appearance of the disease when administered orally thus presenting a highly potent and highly effective antimalarial drug targeting multiple stages of the parasite. [119]

A new family of plasmodial cytochrome bc_1 inhibitors was reported based on 4(*1H*)-pyridone scaffold which displayed potent antimalarial activity against *P. falciparum in vitro* and *in vivo*. The mechanism of action of this new family was found to be selective inhibition of electron-transport chain of *P. falciparum* targeting mainly cytochrome bc_1 complex. Inspite of similar mechanism of action to that of atovaquone, 4(*1H*)-pyridones did not exhibit cross-resistance with the former indicating that two exert different binding interactions in the cytochrome bc_1 complex. The lead optimization studies focused on improving potency and physicochemical properties, discovered a highly active antimalarial candidate, GSK932121 (**198**) which has been carried forward for human trials. Nonetheless, soluble phosphate prodrug, **199** of the candidate produced toxicity in the rat which led to the termination of **198** in human trials demonstrating a possibly narrow therapeutic index (Fig. 24). [106]

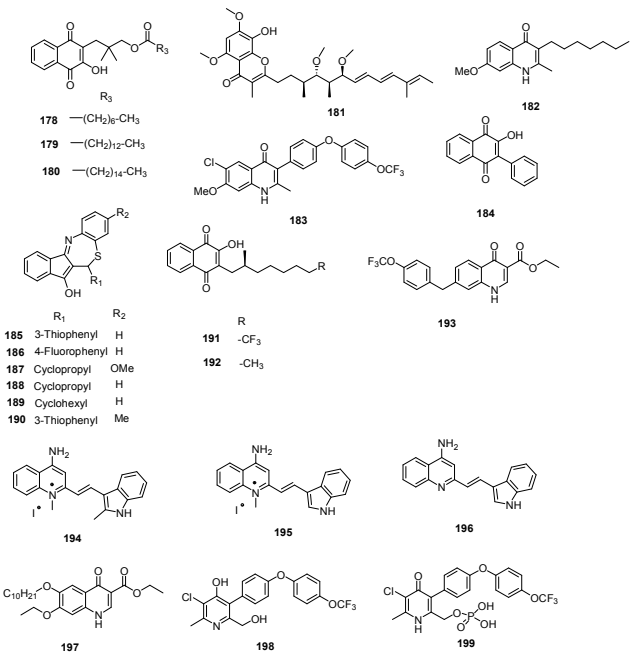

Fig. 24 Chemical structures of cytochrome *bc*1 complex inhibitors

4.2. Dihydroorotate dehydrogenase (DHODH) *P. falciparum de novo* pyrimidine biosynthetic pathway is required for nucleic acid

biosynthesis and cell proliferation that play key role in parasite survival. In contrast to *Plasmodium* which is reliant only upon *de novo* enzymes for the synthesis of pyrimidines, most cells including human utilize both the *de novo* biosynthesis and salvage pathway to synthesize pyrimidines. [120] Dihydroorotate dehydrogenase (*Pf*DHDOH), located on the inner mitochondrial membrane, catalyses the rate-limiting fourth step of this pathway and oxidises dihydroorotate (DHO) to orotate (ORO) with flavin mononucleotide (FMN) as a cofactor. [121] Mitochondrial electron transport chain comes to a halt due to inhibition of *Pf*DHODH activity which thereby leads to disruption of critical metabolic pathways and hence parasite death as a consequence of inhibition of pyrimidine biosynthesis. Since this enzyme is significantly different from that of human analog at the level of amino-acid sequences in the inhibitor-binding domain, it can be attractive target for the development of species-specific inhibitors for malaria treatment. [122]

The effect of substituents within the *N*-arylaminomethylene malonate inhibitors was studied in terms of *Pf*DHODH affinity and selectivity over that of human enzyme. Further the effect of flexibility associated with the diethyl portion of the molecules was also studied by conversion of free alkyl groups of ester groups into a rigid cyclic framework. Analysis of enzyme inhibition results along with molecular modelling predictions suggested the importance of diester head groups where both the ester groups bind in a conformation in which the alkyl groups of the ester moiety have opposite orientations. [123]

A series of *N*-alkyl-5-(1H-benzimidazol-1-yl)thiophene-2 carboxamides was identified which exhibited inhibition of *Pf*DHODH in low nanomolar range and selectivity over hDHODH (Fig. 26). These compounds also displayed antiparasitic effect against 3D7 and Dd2 strains as well as good tolerability and oral exposure in the mouse with ED_{50} values of 13-21 mg/kg/day in the 4-day murine *P. berghei*. Although compound Genz-667348 (**204**) was found active, it exhibited considerable inhibition of CYP2D6 as well as the cardiac hERG channel that makes it less desirable to be developed as antimalarial candidate. Analogs Genz-668857 (**205**) and -669178 (**206**), based on equipotency and favourable cytochrome P450 and hERG inhibition can be further tested to determine their candidature for preclinical development. [124]

Gujjar *et al.* carried out the optimization studies on the lead inhibitor possessing triazolopyrimidine core that has been identified previously. [125] Lead optimization study result in the identification of inhibitors, **207**, **208** bearing 4-SF_5 and 3,5-di-F-4-CF_3 substituted aniline moieties coupled to triazolopyrimidine ring, respectively. These inhibitors were superior to previously reported inhibitors [125] in terms of plasma exposure and efficacy in the *P. berghei* mouse model. [126]

*Pf*DHODH inhibitors were identified through structure-guided lead optimization around previously identified triazolopyrimidine scaffold. These derivatives were modified at the C2 position of the basic core. Two compounds, **209** and **210** were found to be potent against both sensitive and drug resistant strains of the parasite. The compound **210** showed similar potency to chloroquine in the humanized SCID mouse *P. falciparum* model. The compounds demonstrated excellent oral bioavailability, long half-life and low clearance. Based on enhanced *in vivo* efficacy as well as more linear pharmokinetics, **210** has been chosen to be developed as clinical candidate. High resolution crystal structure of DHODH bound to **210** revealed that inhibitor **210** forms two hydrogen bonds with Arg265 and His185 in the binding pocket located between FMN and the N-terminal α-helix (Fig 25). [121]

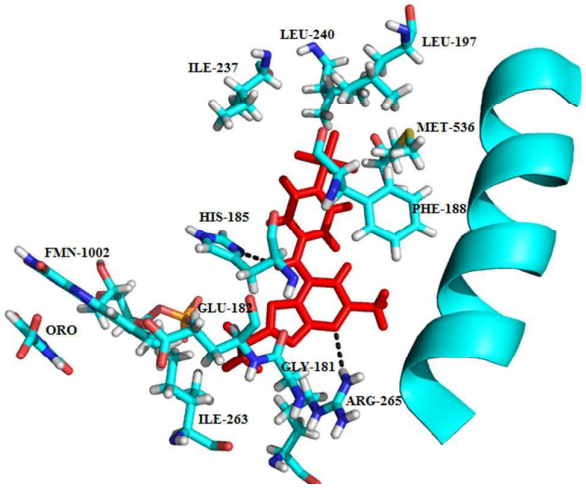

Fig. 25 X-ray structure of inhibitor binding site of *Pf*DHODH bound to **210.** Protein, falvin mononucleotide (FMN) (carbons in cyan); **210** is shown in red and hydrogen bonds are shown in black broken lines. The figure was made by using PyMol (PDB ID: 5BOO).

Skerlj *et al.* synthesized and optimised a series of 5-(2-methylbenzimidazol-1-yl)-*N*-alkylthiophene-2-carboxamides, that are reported as promising *Pf*DHODH inhibitors for the development of potent antimalarial agents (Fig. 26). The selectivity over human enzyme, efficacy in the three mouse models, acceptable safety pharmacology risk assessment and safety toxicology profile in rodents, lack of potential drug-drug interactions, acceptable ADME/pharmacokinetic profile, and projected human dose formed

the basis for the selection of compound **211** to be developed as potential candidate. [127]

A series of *N*-substituted salicylamides was synthesised and evaluated for *Pf*DHODH inhibition potential. The enzymatic assay revealed that selectivity as well as potency can be increased by introducing a 2,2-diphenylethyl substitution on the salicylamidic nitrogen (Fig. 26). The inhibition assay identified compound **212** as the most potent *Pf*DHODH inhibitor with IC_{50} of 7.0 μM. The active compounds were further tested for their potential in whole cell assay and compound **213** was found to inhibit parasite growth with EC_{50} value of 23 μM. [128]

Marwaha *et al.* identified imidazo[1,2-a]pyrimidines pharmacophore as potent *Pf*DHODH inhibitors based on bioisosteric transformations and permutations in the triazolopyrimidine scaffold reported previously. Depending upon the nature of amino aniline substitution, these compounds found to exhibit more potency than the triazolopyrimidines. The most potent candidate, **214** in this series displayed 4-fold better affinity (IC_{50} = 0.077 μM) compared to the equivalent triazolopyrimidine analog. The *in vivo* potential of the active candidate demonstrated 56% suppression of the parasites which was lower than the triazolopyrimidine analogs in the mouse model. This study showed the importance of N1, N4 and N5 functional sites which should be taken care of for the development of more effective antimalarial agents. [129]

A novel series of dihydrothiophenone derivatives as *Pf*DHODH inhibitors were identified through virtual screening. Further structural optimization and SAR analysis of dihydrothiophenone derivatives led to the discovery of various potent and specific *Pf*DHODH inhibitors. The most favorable compound **215**, comprising dihydrofuranone ring, exhibited selective inhibition of *Pf*DHODH (IC_{50} = 6.0 nM) with >14000-fold selectivity over hDHODH. The *in vitro* parasite growth inhibition provided encouraging results with IC_{50} of 15 and 18 nM against 3D7 and Dd2 cells, respectively. Furthermore, *in vivo* pharmacokinetics studies revealed 40% oral bioavailability for compound **215**. Further improvement of pharmacokinetic properties is required for this series to work on. [130]

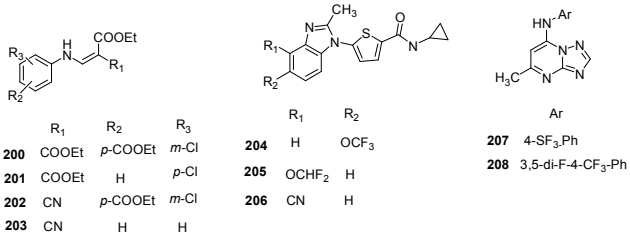

	R_1	R_2	R_3
200	COOEt	*p*-COOEt	*m*-Cl
201	COOEt	H	*p*-Cl
202	CN	*p*-COOEt	*m*-Cl
203	CN	H	H

	R_1	R_2
204	H	OCF_3
205	$OCHF_2$	H
206	CN	H

	Ar
207	4-SF_5-Ph
208	3,5-di-F-4-CF_3-Ph

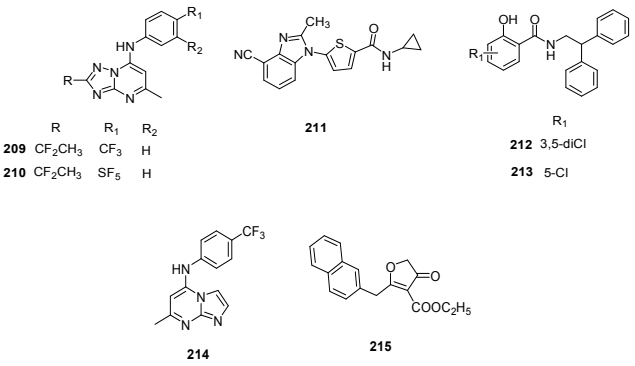

	R	R_1	R_2
209	CF_2CH_3	CF_3	H
210	CF_2CH_3	SF_5	H

211

	R_1
212	3,5-diCl
213	5-Cl

214

215

Fig 26 Chemical structures of dihydroorotate dehydrogenase inhibitors

4.3. NADH: ubiquinone oxidoreductase (NDH2) The mitochondrial electron transport chain of *P. falciparum* displays significant differences from that of human host as it is devoid of canonical protonmotive NADH:ubiquinone oxidoreductase (Complex I), and contains a single sub-unit, non-protonmotive NDH2 which is similar to that present in mitochondria of plants, fungi and some bacteria. [131] These differences among mitochondria make it a potential target for antimalarial chemotherapeutics. *P. falciparum* NDH2 in mitochondrion is a principal electron donor to the electron transport chain which catalyses the transfer of electrons from NADH to ubiquinone using a ping-pong mechanism for the maintenance of a constant pool of oxidized NADH which is required for several reductive metabolic pathways such as glycolysis and tricarboxylic acid cycle. [132] It also helps in generating mitochondrial electrochemical potential, a vital process for the parasite. Thus, targeting these enzymes will prove beneficial for the inhibition of the growth of malaria parasite. [133]

A range of ligand-based chemoinformatic methods were used to identify selective inhibitor of *P. falciparum* type II NADH:quinone oxidoreductase (*Pf*NDH_2). Extensive structural investigation led to the selection of series of 2-bisaryl 3-methyl quinolones for further antimalarial evaluation (Fig. 27). Several compounds of this series exhibited selective inhibition of *Pf*NDH_2 enzyme. The most potent compound **216** (CK-2-68) with IC_{50} of 36 nM against 3D7 strain of *P. falciparum*, is reported to selectively inhibit *Pf*NDH_2 enzyme as compared to other respiratory enzyme with IC_{50} of 16 nM. The most important feature of this lead compound is its low cytotoxicity as well as its high metabolic stability in the presence of human liver microsomes. The prodrug of lead compound **216** was also found to be effective at clearing parasitic infection after oral administration at 20 mg/kg in murine model of malaria. Other quinolones in this series (**217**, **218** and **219**) displayed dual targeting of key mitochondrial enzyme *Pf*NDH2 and *P. falciparum* cytochrome bc_1 in the low

nanomolar range presenting additional advantage over single-targeted inhibitors. [133] Lead optimization studies on compound **216** (CK-2-68) was carried out in order to reduce clog *P* and improve solubility by incorporating a variety of heterocycles within the side chain of quinolone core. This strategy led to the identification of a lead compound SL-2-25 **(220)** which exhibited both the enzyme inhibition (*Pf*NDH2) and whole cell antiparasitic activity (3D7 strain of *P. falciparum*) in the nanomolar range with IC_{50} 15 nM and 54 nM, respectively. It also displayed remarkable oral activity of ED_{50}/ED_{90} of 1.87/4.72 mg/kg against *P. berghei* (NS Strain) in murine model of malaria when administered as a phosphate salt. Some of the analogues in this series (**220, 221** and **222**) provided additional benefit being the dual inhibitor of *Pf*NDH2 and cytochrome bc_1 (Fig. 27). [134]

A potential inhibitor of *P. falciparum* cell proliferation, 1-hydroxy-2-dodecyl-4(1*H*) quinolone (HDQ), **223** that inhibited parasite bc_1 complex from both control and atovaquone-resistant strains TM90C2B with IC_{50} values in the submicromolar range (19 nM and 64 nM, respectively) was reported. The inhibition data clearly indicated that the drugs, atovaquone and HDQ targets different sites within the complex. In addition, HDQ also inhibited recombinant *Pf*NDH2 with IC_{50} value of 77 nM. To further determine the binding site of HDQ, yeast model was used to introduce point mutations into the Qi and Qo site. Point mutations introduced in the Qi site significantly reduced HDQ inhibition while it did not affect HDQ potency when inhibitor resistance mutations were introduced. This extensive study for the exploration of the mode of action of HDQ indicated that Qi site of the bc_1 complex can be a target for antimalarials. [110]

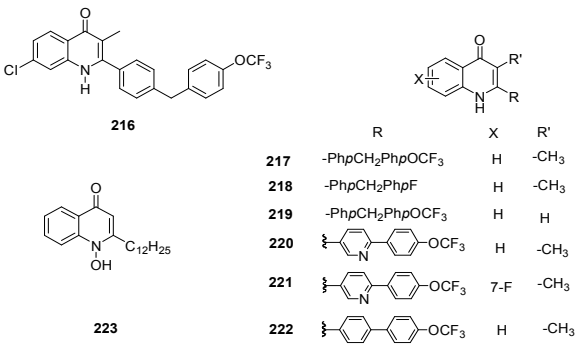

Fig. 27 Chemical structures of NADH: ubiquinone oxidoreductase inhibitors

5. Apicoplast

P. falciparum contains a characteristic non-photosynthetic plastid-like organelle called apicoplast. This organelle has homology with the chloroplasts of plants and algae and is surrounded by four membranes. *P. falciparum* apicoplast, like other plastids possess its own genome that encodes for transcription and translation related genes [135] and carries out crucial processes bearing similarities to those of plant plastids and cyanobacteria such as fatty acid synthesis type II (FAS II) pathway, a non-mevalonate (DOXP) pathway of isoprenoid biosynthesis, iron-sulphur clusters and heme synthesis. The metabolites and cofactors produced by these pathways are required for a variety of cellular processes and crucial for parasite survival thus, apicoplast is considered indispensable for parasite and can be exploited for antimalarial drug discovery campaign. [136]

5.1. Fatty acid synthesis type II (FAS-II) pathway Fatty acid biosynthesis is crucial for the liver stage of *P. falciparum*, as fatty acids constitutes the chief components of cell membranes and are involved in signal transduction, acylation of proteins and play important role in the growth, differentiation and maintenance of homeostasis in the parasite. The monofunctional enzymes involved in FAS-II pathway (dissociative pathway) are essentially different from the mammalian FAS-I pathway (associative pathway) which consists of dimer of a large multifunctional polypeptide. Although both the FAS-I and FAS-II involve same mechanistic steps, the enzymes of these pathways possess weak sequence similarity. [137] Thus, FAS-II pathway may prove a key target for malaria prophylaxis as the inhibition of FAS-II elongation enzymes such as *β*-ketoacyl-ACP reductase (FabG), *β*-hydroxacyl-ACP dehydratase (FabZ), and enoyl-ACP reductase (FabI, also known as ENR) prevents the emergence of the blood stage infection that prevents the clinical symptoms of the disease. [138]

Gupta *et al.* generated a common feature pharamcophore consisting of two hydrogen-bond acceptor and one aromatic hydrophobic feature using seven active flavonoids. *In vitro* evaluation of these compounds against FabI inhibition and growth inhibition of chloroquine sensitive (NF-54) *P. falciparum* strain suggested that (-)-catechin gallate, **224** was the most active compound with IC_{50} values of 0.3 μM and 3.2 μM, respectively (Fig. 29). Docking analysis also validates the pharmacophore model which is quite useful for the design of potent FAS-II inhibitors. [139]

Thirteen bromopyrrole alkaloids from marine sponges belonging to *Axinella* and *Agelas* genera were isolated and evaluated for their potential against four parasitic protozoa i.e. *T. brucei rhodesiense*, *T. cruzi*, *Leishmania donovani* and *P. falciparum* K1 strain. The results reported longamide B (**225**) (IC_{50} = 1.53 μg/mL) and dibromopalau'amine (**226**) (IC_{50} = 0.46 μg/mL) to be promising

trypanocidal agents (Fig. 29). Both these alkaloids exhibited exciting antileishmanial activities with IC_{50} values of 3.85 and 1.09 µg/mL, respectively. Dispacamide B (**227**) (IC_{50} = 1.34 µg/mL) and spongiacidin B (**228**) (IC_{50} = 1.09 µg/mL) exhibited selective antimalarial activity and SI values of >67.2 and 32.7, respectively. The inhibition assay against enzymes involved in fatty acid biosynthesis pathway identified bromopyrrolohomoarginin (**229**) as a potent inhibitor of *Pf*FabZ with IC_{50} = 0.28 µg/mL. Since its potential is identical to (-)-epigallocatechin gallate, **230** (IC_{50} = 0.32 µg/mL), it can be further explored as an antimalarial agent. [140]

2-hexadecynoic acid, **231** was reported as the novel inhibitor of plasmodial FAS-II enzymes having capability to arrest erythrocytic and liver stage *Plasmodium* infections. The *in vitro* evaluation of 2-, 5-, 6- and 9-hexadecynoic acids (HDAs) against erythrocytic stages of *P. falciparum* and liver stages of *P. yoelii* infections indicated highest antiplasmodial activity of 5-HDA, **232** (IC_{50} = 6.6 µg/ml) against blood stages of *P. falciparum*. Compound **231** was reported to be responsible for arresting the growth of liver stage *P. yoelii* infection indicated by both flow cytometric assay (IC_{50} **231** = 15.3 µg /ml, control drug atovaquone = 2.5 ng/ml) and immunofluorescence analysis (IC_{50} **231** = 4.88 µg /ml, control drug atovaquone = 0.37 ng/ml). The inhibitory activity of HDAs was also evaluated against multiple *P. falciparum* FAS-II (*Pf*FAS-II) elongation enzymes and reported that **231** displayed best inhibitory activity against the *Pf*FAS-II enzymes *Pf*FabI, *Pf*FabZ and *Pf*FabG with IC_{50} values ranging from 0.38- 3.50 µg/ml. Kinetic studies and molecular modelling studies predicted the inhibitory mechanism of 2-HDA. Kinetic studies revealed the inhibition of *Pf*FabI was non-competitive with respect to crotonyl-CoA and the cofactor NADH which implies the binding of 2-HDA to the enzyme at a different site that of substrate and the cofactor site. Thus, **231** could be developed as potent FAS-II inhibitor focusing mainly on the presence of a triple bond next to the carbonyl group which increases the conformational flexibility and dipole moment of 2-HDA, enabling it to interact with *Pf*FAS-II target enzymes more efficiently. [141]

Coumarin-based triclosan analogues were developed as novel inhibitors of *Pf*FabI. Among all the tested compounds, **233** and **234** exhibited the highest inhibitory activity with IC_{50} values of 0.25 and 0.27 µM, respectively**.** Compound **235** emerged as potent dual *Pf*FabI/*Pf*FabZ inhibitor, targeting two enzymes in the same pathway with IC_{50} value of 0.45/ 10 µM thus focusing on the importance of 2-hydroxy-4-chlorophenyl-based diaryl ether framework, as a capping fragment, for the inhibition of both *Pf* FabI and parasite growth. X-ray data revealed the interaction of coumarin-based triclosan analogues to the NADH binding pocket interacting with Ala219 backbone and Asn218 side chain (Fig 28). [142]

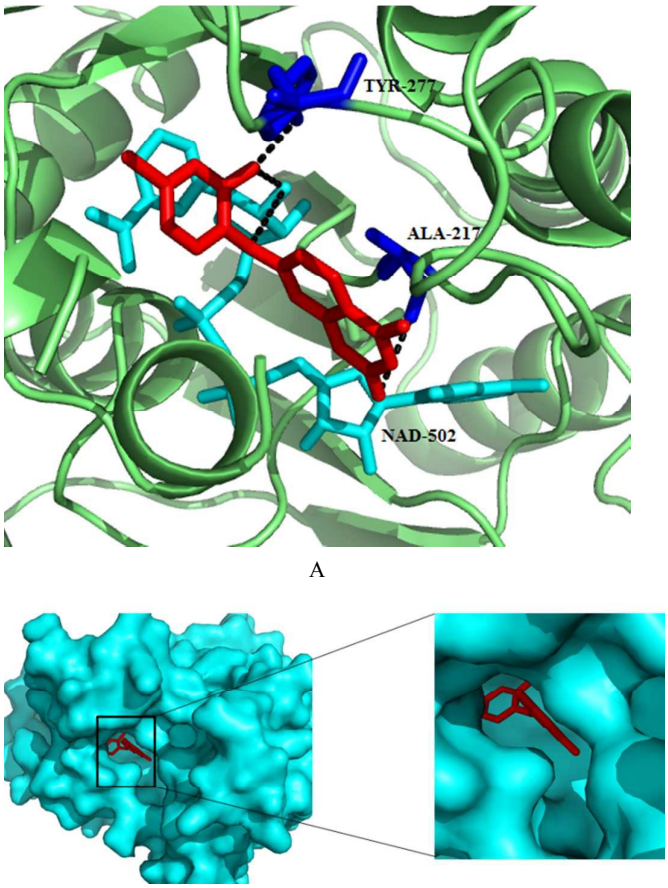

Fig. 28 Structural details of substrate/enzyme binding site. (A) Protein structure is shown in green colour. Catalytic site residues and cofactor NADH are depicted in blue and cyan colour, respectively while the inhibitor is shown in red colour. (B) Surface representation of protein (cyan colour) showing inhibitor in the active site. Figure was drawn in PyMol using PDB ID 4IGE.

A new methylene-bridged bisflavonoid, methylenebissantin (**237**) was isolated along with nine known compounds, including flavonoids, diterpenoids, and phenol derivatives from the aerial parts of *Dodonaea viscosa* Jacq. These isolates were evaluated for the *Pf*ENR inhibition in which **237** exhibited moderate inhibition of the enzyme with IC_{50} value of 91.13 µM. [143]

Lauinger *et al.* evaluated four lichen metabolites evernic acid, **238**, vulpic acid, **239** psoromic acid, **240** and (+)-usnic acid, **241** against FAS-II enzymes (Fig. 29) in which evernic acid emerged as potent *Pf* FabZ inhibitor with IC_{50} value of 10.7 µM and compound **241** was found to be most potent against LS activity and also

displayed stage specificity (LS IC_{50} value 2.3 µM and BS IC_{50} value 47.3 µM). Lichen acid binding to allosteric site affected the enzyme conformation thus, influencing the enzyme activity. [137]

Marchantin A, **242,** a macrocyclic bisbibenzyl ether, was isolated from the liverwort *Marchantia polymorpha*, and tested its potential against the three recombinant enzymes (*Pf*FabI, *Pf*FabG and *Pf*FabZ) of the *Pf*FAS-II pathway of *P. falciparum*. The results demonstrated moderate inhibiton against *Pf*FabZ (IC_{50} = 18.18 µM) while *Pf*FabI, *Pf*FabG enzymes were not affected. The cytotoxicity results against primary L6 rat cells with CC_{50} value of 6.64 µM suggested low selectivity index (SI) *in vitro*. Inspite of that, it has been found to have low toxicity *in vivo* and can be considered for further investigation and development to improve the selectivity and activity against the FAS-II enzyme pathway. Docking study predicted that in comparison to small molecule inhibitors which can enter narrow active site tunnel of the enzyme, marchantin A, (**242**) being bulky, supposed to block the entrance of the tunnel thus inhibiting the substrate from reaching the active site tunnel. [138]

Based on the virtual screening of *iResearch* database by molecular docking, a new class of phenylaminoacetic acid benzylidene hydrazines as inhibitor of *Pf*ENR was developed by Samal *et al.* [144] The spectrophotometric assay to screen the compounds *in vitro* against recombinant *Pf*ENR enzyme revealed **243** and **244** as potent *Pf*ENR inhibitor with IC_{50} values 8.0 and 7.0 µM, respectively followed by compound **245** (IC_{50} = 10 µM) and **246** (IC_{50} = 12 µM) (Fig. 29). This suggests that the presence of electron withdrawing group at *para* position is more preferred over electron releasing group that correlates to the greater inhibition potential.

The work on 2-alkynoic fatty acids was extended further for the search of more potent inhibitor of plasmodial FAS-II enzymes and reported 2-octadecynoic acid, **247,** as best inhibitor of *P. berghei* parasites with ten times higher potency (IC_{50} = 0.34 µg/ml) than the control drug primaquine. It was also found to be most active against blood stages of *P. falciparum* with IC_{50} value of 6.0 µg/ml thus acted as dual life stages inhibitor of *Plasmodium* species. The target determination studies revealed that the same compound effectively inhibited three *P. falciparum* FAS-II (*Pf*FAS-II) elongation enzymes *Pf*FabI, *Pf*FabZ, and *Pf*FabG with the lowest IC_{50} values (0.28–0.80 µg/ ml). The better inhibitory potential of compound **247** against *Pf*FAS-II enzymes than **231** laid emphasis on right alkyl chain length (longer) coupled with triple bond at C-2 seems to be important for the inhibition of both liver stage parasites growth and target enzyme activity. [145] Celastrol, **248** a triterpene quinone methide was isolated from the roots of the celastraceae *Tripterygium wilfordi*. Enzymatic assay revealed that celastrol inhibits *Pf*ENR in a non-competitive manner with average IC_{50} values of 5.9 and 4.7 µM with and without NAD+ preincubation, respectively. [146]

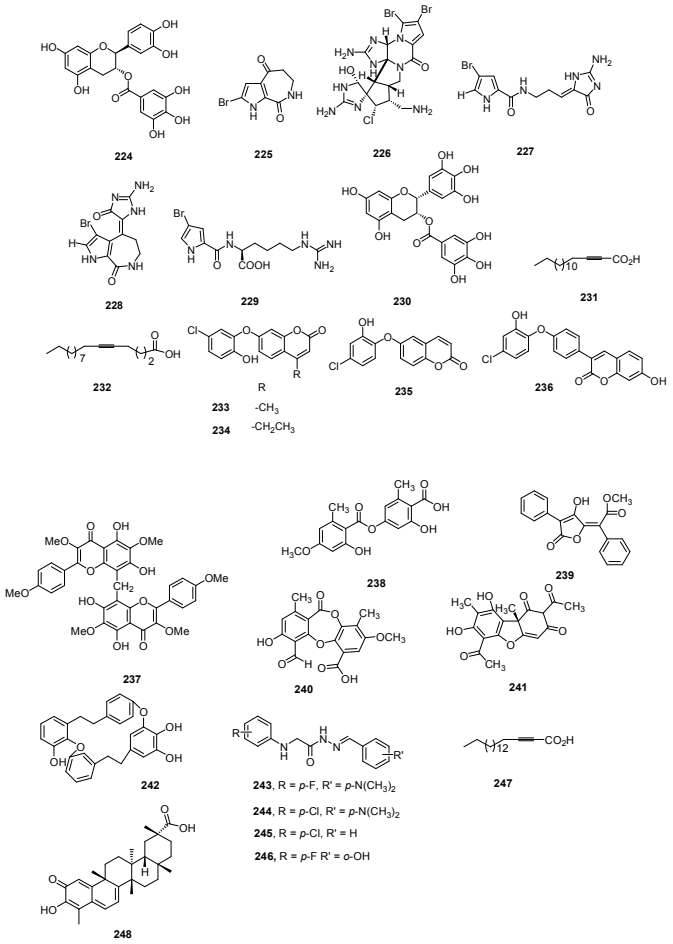

Fig. 29 Chemical structures of FAS-II pathway inhibitors

5.2. Isoprenoid biosynthesis pathway Isoprenoid biosynthesis pathway is crucial for the growth of all the organisms generating very important isoprenoid precursors such as isopentenyl diphosphate (IPP) and its isomer dimethylallyl diphosphate (DMAPP). [147] Synthesis of these vital building blocks is possible via two pathways– Mevalonate and non-mevalonate (or methylerythritol phosphate, MEP) pathways. *P. falciparum* utilizes the MEP pathway, which is absent in humans and animals, making it an appealing drug target. [148] 1-Deoxy-D-xylulose-5-phosphate reductoisomerase (DXR), a key enzyme which catalyses the Mg^{2+} (or Mn^{2+}) and NADPH triggered reductive isomerisation of 1-deoxy-D-xylulose 5-phosphate (DXP) into 2-methyl-D-erythritol-4-

phosphate (MEP) is the most attractive target for antimalarial drug development. [149] Although natural metabolite fosmidomycin (**249**), a structural analogue of DXP and its acetyl derivative FR-900098 (**250**) are available for *Pf*DXR inhibition, but due to short half-life in plasma as well as poor oral availability and low lipophilicity of **249** [150], several new analogues of **249** are required with optimum lipophilicity as well as hydrophilicity to allow it to permeate into *Plasmodium* cells with enhanced pharmokinetic and pharmacodynamics features.

Reverse analogues of **249** displaying high activity and selectivity for *Pf*DXR inhibition were evaluated for recombinant DXR inhibition as well as *in vitro* antiplasmodial activity against the multidrug-resistant K1 strain of *P. falciparum. N*-methyl substituted hydroxamic acid **251** emerged as most potent *Pf*DXR inhibitor with IC_{50} value of 3.1 nM, even more potent inhibitor than the reference fosmidomycin (**249**) and FR900098 (**250**) (Fig. 31). These compounds were found to be non-cytotoxic on human MRC-5 cells. Thus, the high potency of these compounds shed light on the importance of α-phenyl substitution and the reverse orientation of the hydroxamic acid group. [151]

Reverse fosmidomycin derivatives as inhibitors of DXR (IspC) were synthesized and biologically evaluated by Behrendt *et al*. Most of the compounds inhibited the target protein (*Pf*DXR) with IC_{50} values in the low nanomolar range. The most active compounds **252**, **253** exhibited the IC_{50} value of 3.0 nM against DXR enzyme as well as strong potency against *P. falciparum* replication in erythrocytes *in vitro* thus emphasizing the importance of free as well as *N*-methyl substituted hydroxamic acid and the correct selection of aryl substituents in the α-position. *In vivo* studies on *P. berghei* mouse model have shown that the compound **253** displayed 78% suppression of infected RBCs but with low % of survival rate. While the compound **252** with 89% suppression of infected RBCs with almost 60% survival rate has shown some potential and can be developed as promising drug candidate by further structural modifications and pharmacological studies. [152]

Brücher *et al.* developed α-aryl-substituted β-oxa isosteres of fosmidomycin with a reverse orientation of the hydroxamic acid group. These were evaluated for their inhibitory potential against recombinant *Pf*DXR (IspC) and *in vitro* antiplasmodial activity against chloroquine-sensitive and resistant strains of *P. falciparum*. Although oxa compounds showed weaker inhibitory activity as compared to cognate carba compounds, Compound **254** displayed high potency against DXR protein of *P. falciparum* with an IC_{50} value of 12 nM as well as potent *in vitro* antiplasmodial activity. In addition, lipophilic ester prodrugs of compound **254** demonstrated improved efficacy in *P. falciparum* growth assays with better IC_{50} values (0.013-0.031 µM) than **249**. Thus, the combination of methylene group in the β-position and methyl group at the hydroxamic acid motif produces inhibitors with the highest affinity (Fig. 31).[153]

Novel non-cytotoxic pyridine-containing fosmidomycin derivatives were developed as highly potent inhibitors of *Pf*DXR. They showed *Ki* values ranging from 1.9 to 13 nM, with the best compound **255** (K_i = 1.9 nM) possessing an acetyl and a pyridin-3-yl group which was 11 times more active than fosmidomycin. A 2.3 Å crystal structure of *Pf*DXR in complex with one of the inhibitors **256** has been reported, showing that conformational changes takes place especially in the flexible loop at the active site of the enzyme upon ligand binding (Fig. 30). Moreover, a hydrogen bond along with favorable hydrophobic interactions between the pyridine group and the *Pf*DXR account for the enhanced activity. Thus, these novel inhibitors emphasized the importance of the presence of an electron-deficient aromatic ring, such as a pyridine, at the α-position of the phosphonate group. [149]

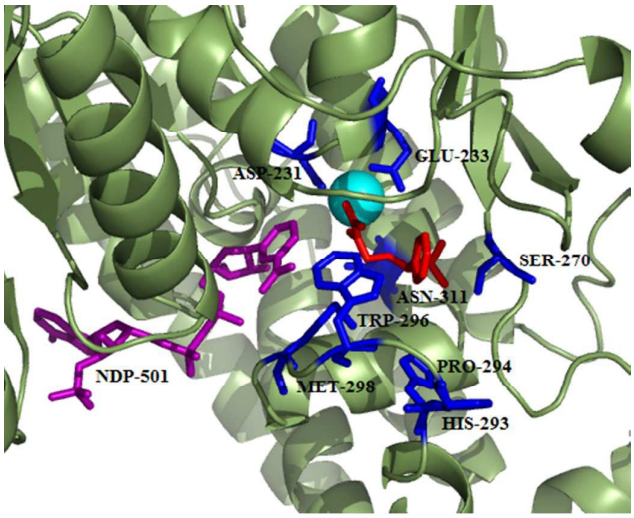

(A)

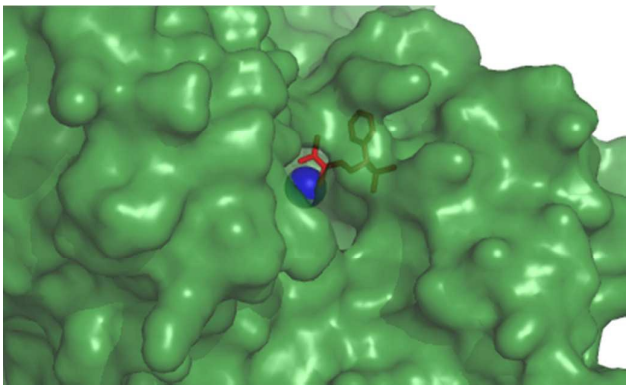

(B)

Fig. 30 (A) Crystal structure of *Pf*DXR in complex with Mn^{2+} (cyan sphere), **256** (red in colour) showing close-up view of the active site of *Pf*DXR: 256. Active site residues and the cofactor are shown in blue and purple colour, respectively (B) Surface representation of *Pf*DXR: 256 complex with Mn^{2+} (blue sphere). Figures were drawn using PyMol (PDB ID: 4GAE).

A series of aryl and heteroarylcarbamoylphosphonic acids, their diethyl esters and disodium salts as analogues of the potent DXR inhibitor fosmidomycin has also been reported. They were evaluated for the inhibitory potential against *Pf*DXR as well as against *Pf*3D7 strain growth and for human cell toxicity. Out of these, **257** was found to inhibit the activity of both *Pf*DXR, *Ec*DXR enzymes and *Pf*3D7 strain; and also non-toxic against human cell line Hst578T. Enzyme inhibition assay as well as docking studies indicated optimal linker length of two methylene units. [150] Thia isosters of reverse hydroxamic acid analogues of fosmidomycin were synthesised and found that *N*-methyl substituted hydroxamates are more potent than their respective unsubstituted hydroxamic acids, supporting the previous observation by other groups. In comparison to its oxa and carba compounds, thia isosters were found to be less potent inhibitor of *Pf*DXR. The results of *in vitro* antiplasmodial activity were not well correlated with that of enzyme inhibition due to the fact that the compounds have to cross several parasitic membranes to reach its site in apicoplast. The crystal structure determined with **258** was similar to the previously reported *Pf*DXR structures. It predicted that loop region over the active site can accommodate more bulky residues like phenyl and naphthyl group due to high mobility. To clarify the long unresolved question pertaining to the stereochemistry of chiral IspC ligands, enantiomers of most active compound **258** were separated by chiral HPLC and tested for enzyme inhibition potential against *Pf*DXR found to possess high degree of enantioselectivity towards enantiomer ***S*-(+)-258** with IC_{50} value of 9.4 nM (Fig. 31). [154]

To gain insights into the SAR of reverse fosmidomycin analogues, Konzuch *et al.* synthesized fosmidomycin analogues with reverse orientation by modifying key regions. The synthesised compounds were evaluated for their enzyme inhibition potential as well as their growth inhibitory effect on asexual stage *P. falciparum*. Reverse carba- and oxa-analogs were found to be more potent *P. falciparum* growth inhibitors. The enzyme inhibition results clearly indicated the importance of aryl group at *α*-position of fosmidomycin in increasing the potency against *Pf*DXR. The most active compound **259** exhibited IC_{50} in low nanomolar range. Crystallographic studies revealed the enantioselectivity of *S*-enantiomers of *α*-aryl substituted carba- and oxa-analogs of fosmidomycin in the active site of *Pf*DXR. [155]

To investigate the effect of *N*-acyl substitution on the *Pf*DXR, Cobb *et al.* carried out enzymatic biosynthesis of FR-900098 (**250**) analogues and based on the co-crystal structures of *Pf*DXR with fosmidomycin and FR-900098, *N*-propionyl derivative FR-900098P, **260** was selected for *Pf*DXR inhibition and it was found to be more potent than the parent compounds with *Ki* value of 0.92 nM. Based on the improved inhibition potential, *in vivo* biosynthetic platform was developed for its synthesis employing both mutasynthetic and metabolic engineering strategies representing a sustainable and environment compatible methodology. [156]

To further improve the pharmacodynamics and pharmacokinetics of **249**, Brücher *et al.* synthesized its prodrugs with reverse orientation. The modification of phosphonate moiety of fosmidomycin to its acyloxymethyl and alkoxycarbonyloxymethyl ester groups and esterification of hydroxamate moiety yielded double prodrugs. These prodrugs were evaluated for DXR inhibition potential as well as antiplasmodial *in vitro* activity against asexual blood stages of *P. falciparum*. None of the prodrugs (phosphonate and phosphonate-hydroxamate double prodrugs) exhibited considerable enzyme inhibition due to their bulkiness and inability of double prodrugs to chelate essential metal ion. The better part of the whole study was the improved antiplasmodial *in vitro* activity of the prodrugs in comparison to their parent compounds with IC_{50} value in the nanomolar range. Among all the studied compounds, the most potent prodrug was found to be **261** with IC_{50} value against *Pf*Dd2 was 4.0 nM and the best results were obtained with *n*-butyloxycarbonyloxymethyl group. Although the compounds displayed better *in vitro* efficacy but the selected compounds failed to produce significant *in vivo* results. [157]

To evaluate the effect of substituted aromatic groups at *β*-position of the propyl backbone of *N*-methyl substituted reverse

fosmidomycin analogue on DXR inhibition, Chofor *et al.* synthesized for the first time *β*-Substituted fosmidomycin analogues (Fig. 31). It was found that the direct substitution of aryl moiety at *β*-position produced poor inhibitor while the longer length of linker between the carbon backbone and the phenyl ring is responsible for better binding to the target enzyme. These derivatives were also evaluated for their *in vitro* schizontocidal activity against the *P. falciparum* K1 strain and the results were well correlated with the *Pf*DXR inhibitiory activity and recommends that four carbon chain (**262**) is optimal for enhanced *Pf*DXR inhibition. [148]

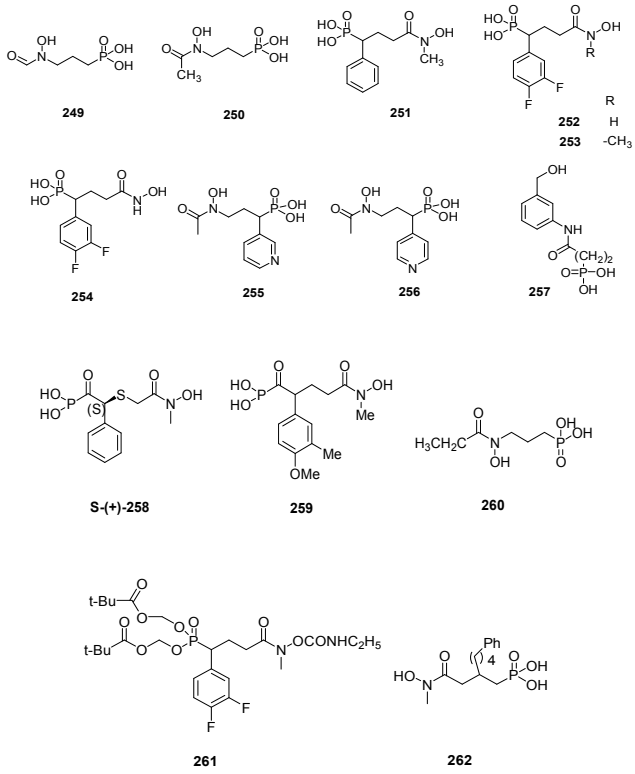

Fig. 31 Chemical structures of DXR inhibitors

5.3. *N*-myristoyltransferase (NMT) *P. falciparum* NMT, found in cytosol and ubiquitous in eukaryotes, carries out the essential processes of modification of protein substrates via the covalent attachment of myristate, a saturated 14-carbon fatty acid, to the N-terminal glycine of target proteins by the formation of amide linkage. [158,159] This enzyme plays key role in the sexual blood stage of the parasite and is essential for transmission. NMT follows a bi-bi catalytic reaction in which ordered binding of *S*-myristoyl-coenzyme A (Myr-CoA) to NMT occurs prior to the protein substrate which is followed by myristate transfer and ordered release of myristoylated protein and free CoA. [160] *N*-myristoylation of proteins modulates essential properties of protein such as lipophilicity, protein localization and stability causing protein-protein and protein-membrane interactions. Formation of inner membrane complex, a sub-cellular organelle vital for parasite red blood cells invasion is prevented by the inhibition of NMT leading to the death of the parasite. [161]

A set of diverse compounds were screened from the Pfizer corporate collection against *P. falciparum* and *L. donovani* NMTs. These selected hits were further tested for their selectivity over both human isoforms (*Hs*1 and *Hs*2) and for broad-spectrum anti-protozoan activity against *T. brucei* NMT. Analysis of screening results revealed the distinct SAR for *Leishmania* NMT from all other NMTs tested while a strong overlap was observed between SARs of *Plasmodium* NMT and both human NMTs posing challenge to achieve selectivity profile. Nonetheless, the group discovered two novel series targeting selectively *Plasmodium* NMT over other NMT orthologues and two structurally divergent series with selectivity over *Leishmania* NMT. [162]

Potent and selective inhibitors of *P. falciparum* NMT based on compound **266,** were designed and synthesized possessing benzofuran scaffold, identified by screening a focused library of NMT inhibitors of *C. albicans* NMT (*Ca*NMT) and *T. brucei* NMT (*Tb*NMT) by following "piggy-back" approach. Chemistry-driven optimization approach was carried out on compound **266** to identify two lead compounds **267** and **268** with submicromolar IC_{50} value of 0.27 and 2.0 μM, respectively (Fig. 32). These potent *Pf*NMT inhibitors have displayed highest antiparasitic activity as well as excellent selectivity over human NMT. These findings highly recommend the development of the optimized *Pf*NMT inhibitors into antimalarial therapeutics. The crystal structure data of *Pv*NMT in complex with compound **269** rationalizes the superiority of benzyl ester side chain and piperidine substituent as well as determines the interactions involved with the linker. This suggests that replacing the aromatic R^2 group by *N*-containing heterocycles can further improve the enzyme activity. [160]

In continuance to the discovery of *P. falciparum* and *P. vivax N*-myristoyltransferase inhibitors, Rackham *et al.* designed and synthesised novel benzo[*b*]thiophene-containing inhibitors by utilizing lead-hopping approach. Among all the compounds, **270** exhibited higher *Pf*NMT affinity, selectivity against *Hs*NMT, excellent ligand efficiency and markedly improved antiparasitic activity than benzo[*b*]furan analog. Analysis of SAR in the series yielded compound **271** which displayed potent *Pv*NMT enzyme affinity and 10-fold selectivity over *Pf*NMT but it was found to be

selective for *Hs*NMT. This was found to be the most potent antiplasmodial compound among the series with EC_{50} value of 2.0 μM. This observation was rationalized from the crystal structure of *Pv*NMT bound to **271** which shows the altered substitution pattern of benzothiophene which is deeply buried in the hydrophobic pocket. [163]

Benzo[*b*]thiophene scaffold based high affinity inhibitors of *P. falciparum* and *P. vivax* NMT based on Ligand Efficiency Dependent Lipophilicity (LELP) were further developed. This approach guided the discovery of compound **272** with 100-fold increase in enzyme affinity and 100-fold reduction in liphophilicity due to the addition of only two heavy atoms. This compound exhibited potency against resistant strains, blood and liver stage forms as well as selectivity over human liver host cells. [159]

Olaleye *et al.* developed peptidomimetic inhibitors of *Plasmodium* and *Leishmania* NMT based on *C. albicans* (*Ca*NMT) peptidomimetics, as *P. vivax* and *L. donovani* NMTs are reported to have 44% and 43% sequence identity with *Ca*NMT, respectively. Peptidomimetic scaffolds were designed by employing modifications at the C- and N-termini thereby exploiting both the ends. Among all the tested compounds, amine **273** displayed significantly improved potency against the NMTs of *P. vivax* (*Pv*NMT), *L. donovani* (*Ld*NMT) and *H. sapiens* (*Hs*NMT1). While the compound **274**, obtained by reduction in the length of alkyl chain (n=10 to 9), emerged as most potent inhibitor with IC_{50} = 0.68, 24.3, 0.024 μM against *Pv*NMT, *Pf*NMT, *Ld*NMT, respectively. The compound **274** is reported to be the most active inhibitor against *L. donovani* NMT till date with lower activity against *Hs*NMT1 (IC_{50} = 60 nM). The SAR has shed light on the importance of N-terminal moiety of peptidomimetic which is expected to be involved in strong electrostatic interaction with C-terminal carboxylate leucine of the enzyme which is crucial for activation of N-terminal amine of peptide substrate. Although these inhibitors display moderate selectivity against human NMT, the sequence alignment of residues as well as the structures of these inhibitors can facilitate a structure-guided design of more potent and selective parasitic inhibitors. [158]

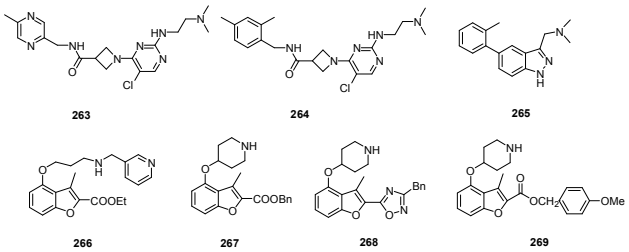

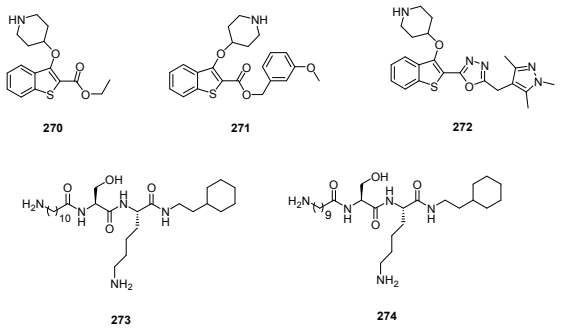

Fig. 32 Chemical structures of NMT inhibitors

6. Cytosol

Cytosol is the location of various enzymes involved in numerous metabolic pathways which are essential for parasite growth and propagation in both of its host, female anopheles mosquito and human being. It has been reported that due to the evolutionarily well conserved pathways, many of these parasite and host targets are quite similar that pose challenges to the design and development of inhibitors that selectively target parasite cytosolic enzymes. [26] The discussion of the inhibitors targeting particular enzymes involved in various pathways operating in cytosol such as folate metabolism, glycolysis, purine salvage and pyrimidine synthetic pathway etc. is given in this section:

6.1. Heat shock protein 90 (Hsp 90) *P. falciparum* Hsp 90 plays a crucial role in the development of asexual stage of the parasite during the intraerythrocytic cycle.[164] Specific inhibition studies of Hsp90 with inhibitor geldanamycin (GA) revealed its important contribution in regulation of ring to trophozoite stage transition in the parasite. [165] Although Hsp90, a cytosolic molecular chaperone essential for protein folding and gene regulation, exhibit a high degree of sequence similarity among different organisms ranging from bacteria to mammals, still there exists 40% difference between *Pf*Hsp90 and *Hs*Hsp90. [166] Hsp90 comprised of N terminus ATPase domain, a central acidic hinge region and a COOH-terminal substrate-binding domain that serves as a buffer for the regulation of heat shock stress. [164]

Shahinas *et al.* explored one of the most potent representatives of purine scaffold inhibitors, PU-H71 (**275**) as an antimalarial agent (Fig. 33). The compound exhibited high binding affinity to the *Pf*Hsp90 ATP-binding domain with K_d of 70.8 μM in comparison to GA derivative 17-AAG, **276** as positive control with K_d of 105 μM and it was suggested that Arg98 guanidinium group plays a key role in accommodating **275** in the *Pf*Hsp90 ATP binding pocket. It also

inhibited ATPase activity with an IC_{50} value of 511 nM while **276** displayed IC_{50} value of 146 nM. Compound **275** showed potent antiparasitic effect in cell culture with IC_{50} value of 111 nM as well as in the *P. berghei in vivo* mouse model of malaria. The synergistic effect of **275** shown with chloroquine displayed increase in activity. Based on biochemical and genetic studies, the group postulated that a direct association existed between *Pf*Hsp90 and *P. falciparum* chloroquine resistance transporter (*Pf*CRT) which is responsible for the mechanism of synergism. The synergism between **275** and chloroquine helped in reducing parasite load and improvement in the survival rate in the *P. berghei* BALB/c mouse model. The PU-H71 (**275**) and chloroquine is an appealing combination therapy to be used against malarial parasite. [167]

Hsp90 from *P. falciparum* were characterised by estimating its ATPase activity as well as drug (geldanamycin), **276** binding abilities and assessed its potential as an antimalarial drug target in mouse model. The studies demonstrated the highest ATPase activity of purified full length *Pf*Hsp90 among all known Hsp90s and it exhibited 6 fold higher ATPase activity than that of human Hsp90. Compound **276** showed vigorous inhibition of *Pf*Hsp90 ATPase activity (IC_{50} = 207 nM) in comparison to human Hsp90 (IC_{50} = 702 nM). Another derivative of GA, 17-(allylamino)-17-demethoxygeldanamycin, **277** showed efficacy in inhibiting parasite growth and increasing the survival rate in the mouse model of malaria. Both **276** and the derivative, **277** were also found to be effective against clinical resistant strains. Compounds **276** and **277** displayed IC_{50} values of 20 nM and 150 nM for complicated (RK1) respectively while they showed IC_{50} value of 5.0 nM and 50 nM for uncomplicated (DL1) malaria after 48 h of treatment. The effect of GA and its derivative in inhibiting *T. evansi* growth was also evaluated which potentially inhibit *T evansi* growth in the mouse model of trypanosomiasis. This biochemical characterization, drug interaction and *in vivo* studies advocated Hsp90 to be exploited as drug target and the potential of its inhibitors as antiprotozoal agents. [166]

A robotic high throughput screen (HTS) on 4000 small molecules from three different libraries comprising natural compounds, pharmacologically active scaffolds and FDA approved drugs was evaluated. These were evaluated for the competitive inhibitions of ATP-binding domain of *Pf*Hsp90. Hits were further evaluated for the specific competitive inhibition of ATP-binding domain of *Pf*Hsp90 over that of human Hsp90. Three compounds, (±)-2-amino-3-phosphonopropionic acid, **278** harmine, **279** acrisorcin, **280** were identified which exhibited ≥70% reduction in fluorescence for *Pf*Hsp90 while no significant reduction was observed for *Hs*Hsp90 (Fig. 33). When evaluated in the cell based antimalarial assay, all the three compounds displayed IC_{50} values in the nanomolar range against 3D7, W2 as well as multi-drug resistant clinical isolate 208432. The three compounds also demonstrated synergistic activity with chloroquine. This combination strategy is beneficial in counteracting the resistance associated with available antimalarial drugs. The substantial antimalarial effect and synergism with antimalarial agents make these compounds attractive candidate for further clinical development. [164]

In another study, the group further studied the selectivity of harmine, **279** for *Pf*Hsp90 ATP-binding pocket based on surface plasmon resonance studies. It also carried out synergistic activity of **279** with other antimalarials like artemisinin which showed an average Σ FIC_{50} of 0.1 for harmine and artemisinin, with the use of 3D7. *In vivo* synergistic data presented a combination of 75 mg/kg harmine and 5 mg/kg chloroquine as the lowest dose for achieving the synergistic activity which resulted in an average of 97.8% inhibition of parasitemia with no significant toxic effect. These results are encouraging for the development of novel chemotherapeutic combinations that are synergistic with existing antimalarials. [168]

Wang *et al.* exploited both the static and dynamic differences between the human and *Plasmodium* Hsp90s so as to develop pathogen-selective inhibitors. The exploration of the ATP-binding pocket showed that *Plasmodium* possesses a specific extension in the ATP-binding pocket whose sequence lining is identical to human Hsp90 but differ in their tertiary structure and dynamics. This understanding regarding the structure-based drug screen led to the discovery of 7-azaindole derivatives **281**, **282** and **283** that possess the ability to selectively bind to the recombinant N-terminal domain of *Pf*Hsp90 over that of human as well as *Pf*Hsp90 mutant with "human-like" dynamics. Furthermore, these compounds flaunted the preferential inhibition of the growth of yeast complemented by *Pf*Hsp90 and blockage of the growth of plasmodium in culture. [165]

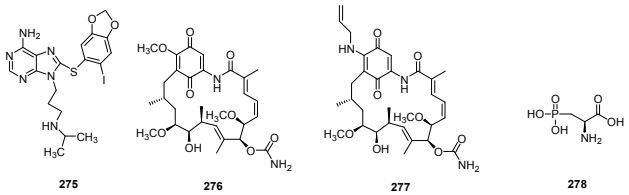

275 **276** **277** **278**

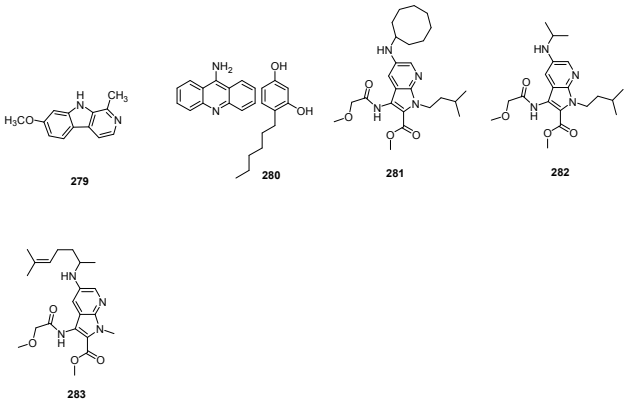

Fig. 33 Chemical structures of Hsp90 inhibitors

6.2. Lactate dehydrogenase (LDH) *P. falciparum* LDH enzyme plays an important role in glycolysis by catalysing the last step of energy production process which involves the interconversion of pyruvate to lactate.[169] This enzyme is expressed in the endoerythrocytic stage of the parasite which regenerate an important component, NAD^+ from NADH for the continuation of the glycolysis. This enzyme can be explored for selective inhibition as it exhibit different structural and kinetic properties compared to human LDH. [170] Since this enzyme is vital for metabolism, inhibitors targeting this enzyme present an exciting avenue in the malaria eradication campaign.

Molecular docking studies were performed to identify potential inhibitors of *Pf*LDH by using Molegro Virtual Docker software to analyse potential binding of selected compounds in the active site of *Pf*LDH. Selected compounds with the best binding energies: itraconazole, **284** atorvastatin, **285** and posaconazole, **286** were evaluated for their antiparasitic effect against *P. falciparum* chloroquine-resistant blood parasites (Fig. 34). All the three compounds exhibited potency in the immunoenzymatic assay carried out using monoclonals specific to *Pf*LDH or histidine rich protein (HRP2). Among three drugs tested, **286** showed lowest IC_{50} value of 2.6 and 5.3 µM respectively but was 40- and 100-folds less active than chloroquine in both *Pf*LDH and (HRP2) assays, respectively. These compounds were also found to be effective in reducing parasitemia in *P. berghei* treated mice. These results well supported the molecular docking analysis confirming it to be an important strategy for the discovery of new antimalarial drugs. [169]

Ethnopharmacological guided screening was done along with structure-based drug discovery approach for the identification of traditional herbs which caused specific inhibition of *Plasmodium* LDH. Effect of 8 plants in four different solvents was evaluated on the purified and recombinant *Pf*LDH and *Pv*LDH and aqueous extract of *Phyllanthus amarus* and chloroform extract of *Murraya koenigii* exhibited highest potency on r*Pf*LDH (IC_{50} = 11.2 µg/mL) and r*Pv*LDH (IC_{50} = 6.0 µg/mL), respectively without exerting any inhibitory effect on bovine heart and bovine muscle LDH. Aqueous extract of *Phyllanthus amarus* displayed its antiparasitic potential on the *P. falciparum* NE(chloroquine sensitive) and MRC-2 (chloroquine resistant) strains (IC_{50} = 7.1 µg/ml and 6.9 µg/ml, respectively).This type of study is beneficial and economical over high throughput screening, thus presenting an efficient approach for antimalarial drug discovery programmes. [170]

Sethiya *et al.* investigated the inhibitory effect of methanolic extract of *Evolvulus alsinoids* Linn. (*E. alsinoids*) on *Pf*LDH. The extract was characterized by thin layer chromatography which led to the identification of one marker compound, scopoletin, **287** and caused reduction in the *Pf*LDH activity (25.04%). [171] Bioactivity-guided isolation of antiplasmodial constituents from *Conyza sumatrensis* (Retz.) E.H. Walker (Cs) leaves which is used for the malaria treatment in Cameroon. The methanolic extract of *C. sumatrensis* exhibited IC_{50} value of 36 µg/mL which was fractionated into *n*-hexane, chloroform, ethyl acetate, *n*-butanol and water fractions. Antiplasmodial evaluation of these fractions revealed chloroform fraction to be most active (IC_{50}, 20 µg/ml) followed by n-hexane (IC_{50}, 36µg/ml), ethyl acetate (IC_{50}, 44 µg/ml), n-butanol (IC_{50}, 86 µg/ml) and water (IC_{50}, >100 µg/ml) fractions. The chromatographic separation of the hexane fraction led to the isolation of three homogeneous compounds: (2S)-1,2-di-*O*-[(9Z)-octadeca-9-enoyl]-3-*O*-β-D-galactopyranosyl glycerol (**288**) (IC_{50}, 34 µg/ml); (2S)-1,2-di-*O*-[(9Z,12Z,15Z)-octadeca-9,12,15-trienoyl]-3-*O*-(6-sulpho-α-D) quinovopyranosyl glycerol (**289**) (IC_{50}, 17.9 µg/ml) and 1-*O*-β-D-glucopyranosyl-(2S,3R,8E)-2-[(2′R)-2-hydroxy-palmitoylamino]-8-octadecene-1,3-diol (**290**) (IC_{50}, 18±0.12 µg/ml). Similarly, one homogeneous compound was obtained from the ethyl acetate fraction: 3-*O*-β-D-glucopyranosyl-3,4-dihydroxybenzoic acid (**291**) (IC_{50}, 25 µg/ml). Treatment of *P. berghei* K-173 infected mouse with these fractions showed chloroform fraction to be most effective in lowering parasitemia followed by n-butanol and ethylacetate fractions. These isolated constituents did not induce any toxicity to murine macrophages and erythrocytes. Compounds **289**, **290** and **291** exhibited the inhibition of LDH with IC_{50} values of 21, 39 and 42 µg/ml, respectively. [172]

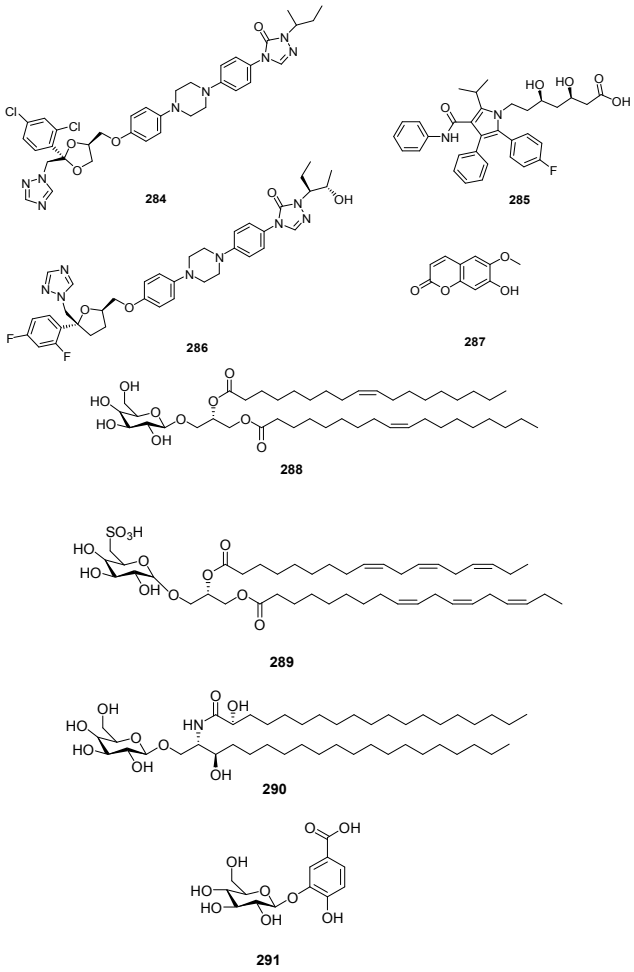

Fig. 34 Chemical structures of lactate dehydrogenase inhibitors

6.3. Purine nucleoside phosphorylase (PNP) PNP, a key enzyme of purine metabolism is considered as potential target for antimalarial chemotherapy as it is involved in salvage of extracellular purines since *P. falciparum*, being purine auxotrophs cannot synthesise purines via *de novo* pathway. This enzyme catalyses the essential process of phosphorolysis of inosine to ribose-1-phosphate and hypoxanthine, which is the main purine precursor for salvage pathway. [173] Disruption of this enzyme activity results in growth defects in *P. falciparum.* Moreover, metabolic pathways involved in the purine salvage are distinct among human and *Plasmodium* since *P. falciparum* PNP converts 5'-methylthioinosine (MTI) to hypoxanthine where MTI is produced by the action of adenosine deaminase over 5'-methylthioadenosine (MTA) while MTI is not produced in humans and human PNP is also not involved in the phosphorolysis reaction of methylthioinosine. [174] This specificity of plasmodial PNP can be explored for the designing of anti-malarial drugs.

Based on the observation that uridine can act as substrate for *Pf*PNP, Cui *et al.* synthesized two series of inhibitors where series one was based on human uridine phosphorylase (UP) inhibitors while series 2 comprised of uracil based analogues to mimic the PNP transition state. Enzyme inhibition results showed that human UP inhibitors were ineffective against *Pf*PNP while uracil based transition state analogues exhibited substantial inhibition with *K*i in the micromolar range with the most active one, **292** having *K*i value of 6.0 µM. Unfortunately, these compounds even the most active ones did not exert any significant antiparasitic effect which may be due to the low cellular permeability as indicated by low log *P*. [173]

A series of 8-aryl and 8-pyridylinosines by direct arylation reaction at position 8 of purine nucleosides was also reported. Hydrolytic stability of these compounds was studied at different pH values and inhibitory potential was assessed against *P. falciparum* PNP. Cytotoxic evaluation for these compounds against different types of cell cultures indicating no significant toxicity which supported the absence of metal-contaminants. Enzymatic evaluation against *Pf*PNP revealed compounds **293**, **294** and **295** inhibited the enzyme in the low micromolar range *K*i values (*K*i = 8.1, 3.7 and 5.3 µM, respectively) which is similar to that of *K*m of inosine (*K*m =5.9 µM) (Fig. 35). Compounds did not exert any inhibitory or substarte activity against human and prokaryotic PNP suggesting 8-arylinosines to be selective inhibitors of *Pf*PNP. Regrettably, lack of significant inhibitory activity against of growth of intraerythrocytic forms of the *P. falciparum* chloroquine-sensitive strain 3D7 hampered its suitability to be used as antimalarial agent. But the enzymatic potency associated with it makes it an appealing starting point to be developed further as specific inhibitors of the enzyme. [175]

Lautre *et al.* synthesized Zn(II), Co(II) and Cr(II) complexes of 2-amino-5-nitro-N-hydroxybenzamidine (**296**, **297** and **298**, respectively) and evaluated them for the inhibition of *Pf*PNP and growth of *P. falciparum*. The ligands as well as their metal complexes displayed good to excellent activity in which **297** showed the highest activity with EC_{50} of 65µM (87% inhibition) and **298** (EC_{50} = 70 µM (85% inhibition)), **296** (EC_{50} = 85 µM (67% inhibition)) were also active in growth assay. These ligand and complexes were evaluated for their *Pf*PNP inhibition potential and found that compound **297** with *K*i of 20 µM (IC_{50} = 65 µM) was most effective in the enzyme inhibition assay. The *K*i (IC_{50}) values for **296** and **298** were 35 (85) µM and 29 (70) µM, respectively.

Thus, such type of compounds can be exploited further for their multi-target effects. [176]

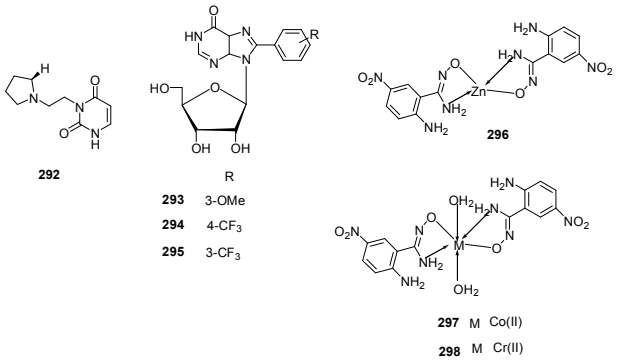

Fig. 35 Chemical structures of PNP inhibitors

6.4. Folate metabolism Folate metabolic pathway is crucial for the biosynthesis of RNA, DNA, and protein as numerous enzymes are involved in this pathway to synthesize folate cofactors required for nucleotide synthesis and amino acid metabolism. [177] Among these, dihydofolate reductase (DHFR), dihydopteroate synthase (DHPS), thymidylate synthase (TS) have been exploited as drug target in malaria chemotherapy and prophylaxis. The dihydrofolate reductase domain of *P. falciparum* bifunctional enzyme commonly known as dihydrofolate reductase-thymidylate synthase is one of the most crucial enzyme in the parasite life cycle as it catalyses the NADPH-dependent reduction of dihydrofolate to tetrahydrofolate which is required for DNA replication. [14,178] *Plasmodium* folate pathway is different from its mammalian counterpart as it is unable to absorb folate from the host system and has to exploit its own enzyme system for the synthesis of folate. [179] The development of antimalarial leads taking into account the specific differences between among human and *Plasmodium* folate biosynthesis enzymes will provide avenues for the treatment of malaria. [178]

A series of first generation small molecule dual inhibitors of FP-2 and DHFR based on lead compound **299** bearing sulfamide and amide moieties was randomly identified by screening FP-2 inhibitors (Fig. 37). Six compounds reportedly showed improved dual inhibitory activities as compared to lead compound **299** while the inhibitory potential of compound **300** containing thiazole group on amide moiety against FP-2 (IC_{50} = 7.0 μM) and DHFR (IC_{50} = 6.3 μM) were increased ~8 and ~6 times than that of compound **299**, respectively. Moreover, compound **300** displayed moderate *in vivo* antimalarial activity in a dose dependent fashion, its safety and survival rate were slightly better than that of positive control, chloroquine diphosphate salt. Thus, these dual inhibitors may provide alternate 'combination therapy' by linking two pharmacophores in a single structure thereby avoiding the pharmacokinetic disadvantages of two separate agents. [180]

Adane *et al* reported potent *Plasmodium* DHFR inhibitors based on guanylthiourea scaffold, synthesized mainly from the guanylthiourea and alkyl bromides. *In vitro* evaluation demonstrated that two compounds, **301** and **302** were potent with the IC_{50} value of 100 μM and 400 nM respectively (Fig. 37). The enzyme inhibition data clearly showed the importance of meta-substitution with a bulky atom and bisubstituted guanylthiourea compound also exhibited good activity. This enhanced activity might be due to increase in the hydrogen bond interactions in the active site of *Pf*DHFR enzyme. Thus, the mono-substituted and bi-substituted guanylthiourea derivatives can be explored further in order to improve the activity of this class of compounds. [181]

Yuthavong *et al.* reported development of highly selective and efficacious drug candidate to preclinical stage based on the co-crystal structures with inhibitors and substrates along with efficacy and pharmokinetic profiling. Due to low bioavailability and gastrointestinal toxicity associated with triazine based drug, 2,4-diaminopyrimidine scaffold was chosen for further chemical exploration and this strategy led to the development of **303** which was found to be low nanomolar range inhibitor of wild-type and quadruple mutant *Pf*DHFR as well as exhibited superior oral bioavailability in comparison to triazine based drugs. To increase the tighter binding and DHFR selectivity, fourteen molecules were synthesized and among them, **304** emerged as the most potent compound which was synthesized by replacing trichlorophenyl group of **303** by 2′-carboxyethylphenyl group. Compound **304** showed slow-off tight binding to the wild-type and quadruple mutant DHFR in the subnanomolar range. It exhibited potency against PYR-resistant *P. falciparum* with quadruple mutant *Pf*DHFR *in vitro*. *In vivo* studies against *P. chabaudi* in CD-1 mice and against quadruple mutant *P. falciparum* in SCID mice (ED_{50} = 0.3 mg⁄kg, ED_{90} = 1 mg⁄kg) indicated high potency. Compound **304** is now in preclinical trial, the inhibitor carboxylate group showed H-bond interaction with Arg122 of *Pf*DHFR-TS (Fig 36). Thus, the factors such as good pharmacokinetic profile in preliminary studies in mice and rats, good oral bioavailability (46%), reasonable half-life, safety profile presented **304** as a suitable candidate for further development. [182]

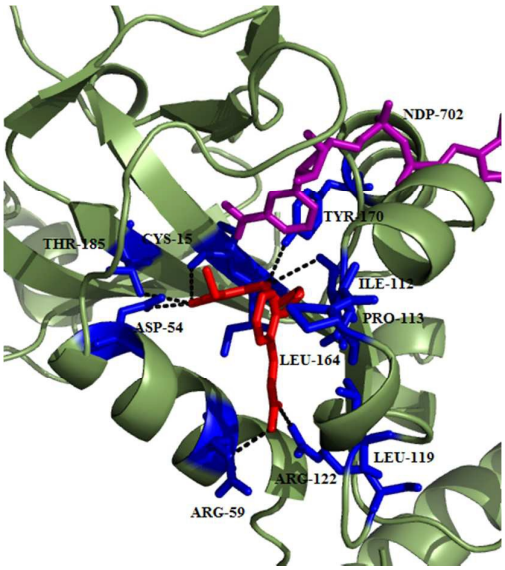

Fig. 36 Binding of 304 in the cavity of *Pf*DHFR-TS. Protein is shown in green colour which is making hydrogen bond interactions with **304** (red in colour). The image was created in PyMol using the PDB ID: 4DP3.

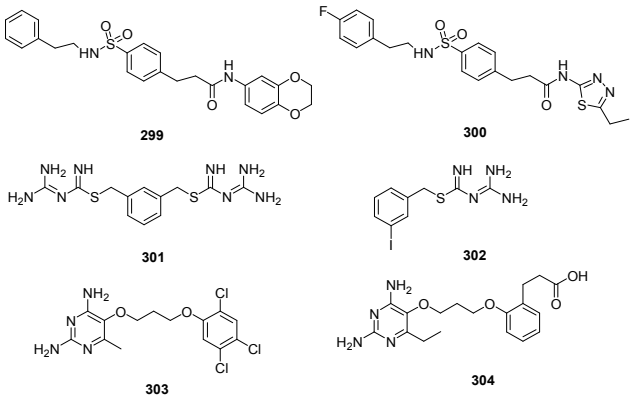

Fig. 37 Chemical structures of DHFR-TS inhibitors

6.5. Carbonic anhydrase (CA) Carbonic anhydrase enzymes are metalloenzymes which are responsible for catalysing the conversion of carbon dioxide to bicarbonate and protons in reversible manner ($CO_2 + H_2O \rightleftharpoons HCO_3^- + H^+$). [183] These enzymes are present in all life forms where six genetically distinct families of the enzymes have been reported to date: *α*-, *β*-, *γ*-, *δ*-, *ζ*-and *η*-classes. *Plasmodium* carbonic anhydrase belongs to *α*-CA class and it was discovered recently based on amino acid sequence studies that one more class, *η*- CA was also present in *Plasmodium* which although possesses similar structural features of that of *α*-class, their distinct zinc coordination mode make their catalytic site inimitable and different from other CAs. The active site of the *α*- and *η*- CA of *Plasmodium* contains zinc metal ion which is coordinated by three His residues and a nucleophile like water molecule/hydroxide ion as fourth ligand. [184] During intraerythrocytic stage, carbonic anhydrase plays a critical role in synthesizing pyrimidines by providing bicarbonate ion which along with adenosine 5'-triphosphate, glutamine, 5-phosphoribosyl-1-triphosphate and aspartate are involved in pyrimidine biosynthetic pathway. [185] Since the pyrimidine biosynthesis pathway displays key differences between the parasite and human host, novel antimalarials can be designed targeting the carbonic anhydrase.

The enzymatic activity of *Pf*CA in terms of CO_2 hydrase activity showed that *Pf*CA exhibited good CO_2 hydrase activity at pH 7.5 with a k_{cat} of 1.4×10^5 s^{-1} and a k_{cat}/K_M of 5.4×10^6 $M^{-1} \times s^{-1}$. Carbonic anhydrase inhibition potential for inorganic and complex anions and other molecules known to bind with zinc proteins was also studied and it was found that bicarbonate (HCO_3^-) **305,** carbonate (CO_3^{2-}) **306,** nitrate (NO_3^-) **307,** and selenite (SeO_4^-) **308,** were effective micromolar inhibitor of *Pf*CA (Ki = 0.66-0.90 mM) while less active against human isoforms I and II (Fig. 38). The most potent *Pf*CA inhibitors were sulfamide ($H_2NSO_2NH_2$) **309**, sulfamic acid (H_2NSO_3H), **310**, phenylboronic acid (Ph-$B(OH)_2$), **311** and phenylarsonic acid (Ph-AsO_3H_2) **312**, which exhibited inhibition constants in the low micromolar range with *K*i of 6.0–9.0 μM. The phylogenetic analysis and a deep investigation of sequence of *Pf*CA and other CAs from other *Plasmodium* species described that these protozoa encode for new genetic family of CAs designated as *η*-CA class which is elucidated in the report. [186]

Inhibition studies of the recently discovered *Plasmodium η*-CA from *Plasmodium* against a series of sulfonamides and sulfamates was performed. The potent inhibitors found were ethoxzolamide, **313** and sulthuame, **314** (K_i of 131–132 nM), followed by acetazolamide, **315** methazolamide, **316** and hydrochlorothiazide, **317** with K_i of 153–198 nM. Brinzolamide, **318** topiramate, **319** zonisamide, **320** indisulam, **321** valdecoxib, **322** and celecoxib, **323** also showed substantial inhibitory action against *Pf*CA, with K_i in the range of 217-308 nM. The potent *Pf*CA inhibitors identified so far can be arranged into a variety of chemical classes, ranging from aromatic primary sulfonamides, to monocyclic/bicyclic and heterocyclic derivatives on the basis of inhibition data. Thus, these chemical classes can be further explored to develop efficient, low nanomolar range inhibitors. [187]

A library of aromatic/heterocyclic sulfonamides bearing various scaffolds were evaluated bearing a wide variety of scaffolds against

*Pf*CA enzyme and *in vitro P. falciparum* growth as well as *in vivo* efficacy. Among all the compounds, 4-(3,4-dichlorophenylureido)thioureido-benzenesulfonamide, **324** was most potent *Pf*CA inhibitor (*K*i of 0.18 µM) with highest potency exhibited *in vitro P. falciparum* growth inhibition with IC_{50} of 1.0 µM. *In vivo* assay in *P. berghei* mouse model demonstrated its efficacy with ID_{50} of 10 mg/kg in comparison to chloroquine with ID_{50} of 5 mg/kg. Thus, these potential sulphonamides can be explored further for the development of novel chemotherapeutic agents against malaria. [183]

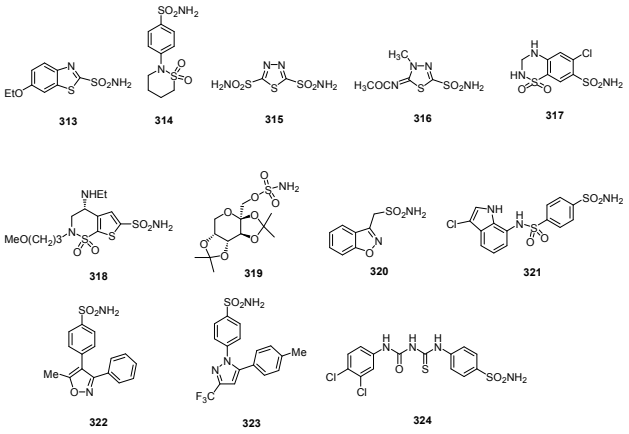

Fig. 38 Chemical structures of carbonic anhydrase inhibitors

6.6. Thioredoxin reductase (TrxR) The vulnerability of *P. falciparum* to attack by reactive oxygen species requires effective antioxidant and redox systems to inhibit damage caused by oxidative stress. [188] Low molecular weight thiol thioredoxin system present in the *P. falciparum* requires the services of thioredoxin reductase, associated to a class of pyridine dinucleotide oxidoreductases. This enzyme catalyses the NADPH dependent reduction of thioredoxin protein from its inactive disulfide state to an active dithiol form, acting as an electron donor that helps in maintaining a sufficient redox environment during intraerythrocytic stage and proliferation. This enzyme target can be explored as potential target as it is essential for the survival of malaria parasite for battling intraerythrocytic oxidative stress and proliferation. [189,190] Selective inhibitors can be designed as this enzyme of *P. falciparum* does not contain selenocysteine which is found in the active site of mammalian TrxR. [190]

About 133 structurally varied natural compounds from the MEGx® collection of AnalytiCon Discovery and three synthetic hispolone derivatives were screened for their binding potential against *Plasmodium* thioredoxin reductase (*Pf*TrxR) utilizing ultrafiltration (UF) and liquid chromatography (LC/MS) based ligand-binding assay. Nine compounds (yohimbine (**325**), catharanthine (**326**), vobasine (**327**), gnetifolin E (**328**), quinidine N-oxide (**329**), 11-hydroxycoronaridine (**330**), hispolone (**331**), hispolone methyl ether (**332**), and hernagine (**333**) exhibited binding to the *Pf*TrxR at 1.0 µM and their binding affinities ranked in the order as 331 >330 > 326 > 328 > 329 > 332 > 325 > 333 > 327 when tested individual (Fig. 39). When they were tested in an equimolar mixture of 1.0 µM conc., compounds **330**, **331**, **326** and **338** displayed specific binding to the active site of *Pf*TXR. The highest binding of **331** may be attributed to the presence of hydroxyl groups on the phenyl ring which were supposed to be involved in the hydrogen bonding to cysteine residue of the active site. [188]

LC/MS spectroscopy and ultrafiltration techniques were used for screening detannified methanolic extracts from *Guatteria recurvisepala*, *Licania kallunkiae* and *Topobea watsonii* to identify natural products for *Pf*TrxR inhibition. The % inhibition of *Plasmodium* growth of these plant extracts was found to be 57%, 86% and 58%, respectively. When incubated with 1.0 µM *Pf*TrxR, the extract of *Guatteria recurvisepala* displayed a relative binding affinity of 3.5-fold to the enzyme. The potential compound in the extract was identified as oleamide, **334** based on MS/MS experiments which exhibited *in vitro* antiparasitic effect against K1 strain with IC_{50} value of 4.29 µg/ml. [191]

A LC-MS based functional assay for evaluating the *Pf*TrxR inhibitory activity showed that out of curcumin, **335** demethoxycurcumin, **336** and bis-demethoxycurcumin, **337** inhibited *Pf*TrxR with IC_{50} value of 2.0 µM (Fig. 39). Antiplasmodial effect of **335** and demethoxycurcumin showed activity against the chloroquine sensitive D6 strain of *P. falciparum* and moderate activity against the chloroquine resistant W2 strain. Their cytotoxicity against Vero cells was found to be 64 µM and selectivity index of 4-6 folds and 1-fold against D6 and W2 respectively. [192]

Theobald *et al.* discovered and characterized seven molecules identified from an antimalarial set of 13533 compounds via single-target TrxR biochemical assays. They also produced highly pure recombinant, full-length, untagged enzymes from *P. falciparum*, *P. vivax*, *P. berghei*, and *P. yoelii* as well as Trx substrates from *P. falciparum* and *R. norvegicus*. The identified compounds exhibited specificity for *Pf*TrxR and the cytotoxicity <20% at 10 µM. Mechanism of action of these compounds, **338**, **339** was found to be non-competitive in nature with respect to both substrates, with *K*i values ranging from 1.3- 4.1 µM. Non-competitive inhibition

suggested that the inhibitor binds to the enzyme probably in the intersubunit region which is outside the 'substrates binding sites'. [190]

Aculeatin-like analogues were designed and synthesised by combining two sets of building blocks, many of which were active against *P. falciparum* whole cell assay. SAR around spirocyclohexadienone pharmacophoric scaffold revealed the preference of aliphatic long chain with optimized lipophilicity at position R5 and benzyl group. The presence of aculeatin-like scaffold was found to be of utmost importance in augmenting the antimalarial activity. The most active compounds in this series were **340** and **341** with the same appendages at R4 and R5 position having IC_{50} value of 1.35 and 2.29 μM, respectively. Among the selected compounds, compound **340** was slightly more selective against *P. falciparum* over human cell lines such as lymphoblast Jurkat and erythroblast K562 strains. Furthermore, a new aculeatin-like scaffold, **342** lacking Michael acceptor properties was identified, found active at 0.86 μM against *P. falciparum* 3D7 strain with selectivity index over 30. Enzyme inhibition data for these active compounds showed that (-)-aculeatin A completely blocked the transfer of electrons from *Pf*TrxR to the macromolecular acceptor Trx. They dramatically reducted the electron transfer from NADPH to the FAD active site by 68%, thus 32% residual activity was observed while compounds **340** and **342** exhibited 33% and 74% residual activity. These results strongly emphasized on the involvement of other plasmodial targets for the strong antiplasmodial activity of **342** that raises its potential to be developed as antimalarial agents with wide druggable spectrum. [193]

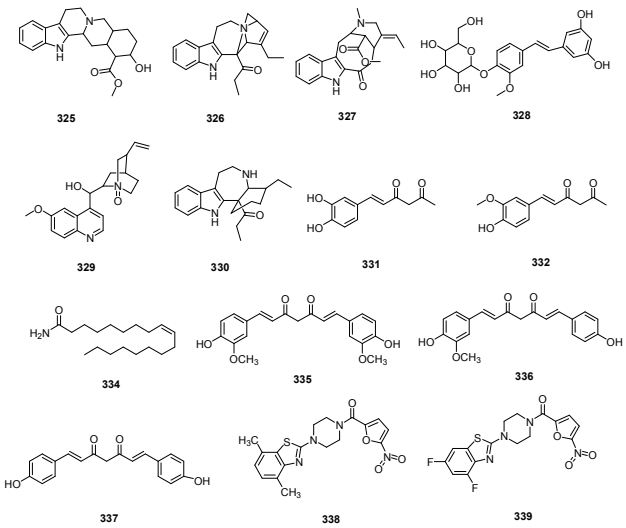

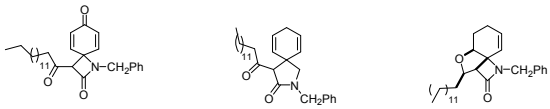

Fig. 39 Chemical structures of thioredoxin reductase inhibitors

6.7. Thymidylate kinase (TMK) *Plasmodium* is dependent on the de novo synthesis of pyrimidines as it lacks the ability to salvage preformed pyrimidines while humans carry out salvaging of preformed pyrimidine nucleosides thus making this pathway an exciting target for antimalarial chemotherapeutics. [194] Various enzymes are involved in the pyrimidine biosynthesis pathway such as DHFR and DHODH and in addition to these, *P. falciparum* TMK also get involved in pyrimidine biosynthesis. *P. falciparum* TMK is a potential drug target for malaria prophylaxis as it catalyses a key step of pyrimidine biosynthesis which involve the phosphorylation of thymidine monophosphate (TMP) to thymidine diphosphate (TDP) as well as that of deoxyguanosine monophosphate (dGMP) to give deoxyguanosine monophosphate (dGDP). [195,196] Moreover, *Plasmodium* parasite TMK displayed significant differences from that of human enzyme as elucidated by structural and kinetic studies. Inhibitors designed by the exploitation of structural differences will lead to selective inhibition of parasite TMK over that of human enzyme. Superposition of the structure of *Pf*TMPK-TMP-ADP with that of human TMPK complex found numerous important differences in the P-loop and the LID domain. [194]

Series of α-/β- thymidine analogues were designed, synthesised and evaluated for *Pf*TMK inhibition based on the report that a series of 5'-substituted *α*-thymidine derivatives have displayed submicromolar inhibition against *Mt*TMK and selectivity over hTMK. Both the 5'-urea-α- and β-thymidine derivatives exhibited moderate inhibition of the enzyme (*K*i = 50-200 μM) as well as moderate antiparasitic effect. The most active *α*-thymidine inhibitors among the series were 3-trifluoromethyl-4-chlorophenyl derivative **343** (*K*i = 31 μM) and the 4-nitrophenyl derivative **344** (Ki = 11 μM) while β-thymidine inhibitors, 3-trifluoromethyl-4-chlorophenyl derivatives **345** (Ki = 25 μM) and **346** (Ki = 27 μM) and the 4-nitrophenyl derivative **347** (Ki = 11 μM) showed slightly better efficacy in enzyme inhibition (Fig. 41). Despite poor enzyme inhibition, some of the derivatives exhibited potent antimalarial effect suggesting a different mode of action of these compounds. Optimisation of the 5'-para substituted phenyl urea α-thymidine derivatives identified a compound, **348** with potent antimalarial activity with selectivity over human ortholog (EC_{50} = 28 nM; CC_{50} =

29 µM). SAR analysis revealed the higher potency of α-anomers than β-anomers as well as preference for para substitution. Hydrophobic substituents at para position as well as presence of urea linker showed increased growth inhibition. *In vitro* DMPK studies on selected compounds showed reasonable microsomal stability in presence of hepatic microsomes except compound **348** which showed rapid turnover. Crystal structure of *Pf*TMK in complex with **345** revealed that thymidine ring mimics the natural TMP substrate. Deoxyribose ring acquires such orientation which allows thymidine to have maximum interactions within the binding pocket of the enzyme. (Fig. 40). [194]

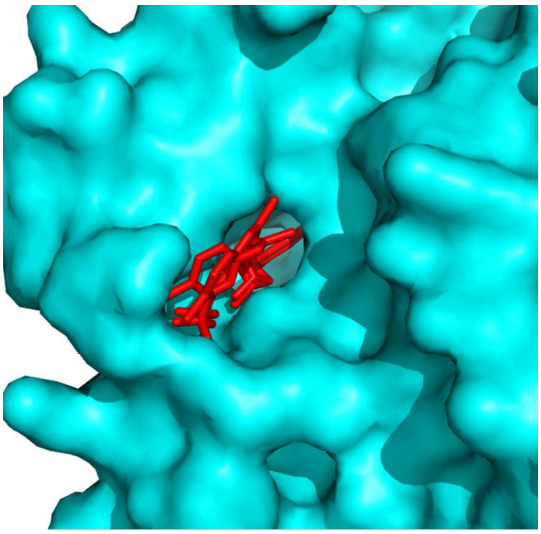

Fig. 40 Surface diagram of *Pf*TMK showing **345** (red colour) in the binding pocket. PyMol was used to draw the structure using PDB ID: 2YOF.

Inhibitory potential of seven carbocyclic analogues was screened against *Pf*TMK. The inhibitory results showed that 2',3'-dideoxycarbocyclic derivative of thymidine, ±**349** was the most potent inhibitor. When TMP and dGMP were used as substrate, it exhibited *Ki* value of 20 µM and 7.0 µM respectively. All the tested compounds displayed 3-4 fold more potency against deoxyguanylate kinase than the thymidylate kinase, indicating that thymidine derivatives were proficient of competing with guanylate for its active site. When compared with inhibition potential of other analogues, SAR studies suggested the preference for the 2'-deoxy or 2',3'-dideoxy carbocyclic derivatives over the 2',3'-dihydroxy derivatives. Since the inhibition was found in low micromolar range, further modifications are needed to produce more potent *Pf*TMK inhibitor. [195]

In order to improve the inhibitory activity of 2′,3′-dideoxycarbocyclic thymidine derivatives, Noguchi *et al.* synthesized enantioselective 2′,3′-dideoxycarbocyclic pyrimidine nucleosides and screened them for inhibitory activity against *Pf*TMK. The most potent inhibitor fluorinated dideoxy derivative (-)-**350** exhibited Ki^{TMP} and Ki^{dGMP} values of 14 and 20 µM, respectively as compare to the parent compound **(±-351)** (Ki^{TMP} and Ki^{dGMP} values of 20 and 7.0 µM respectively). Further modifications of **(-)-350** will produce much efficient inhibitors thus, presenting an effective strategy to develop safe and selective inhibitors. [197]

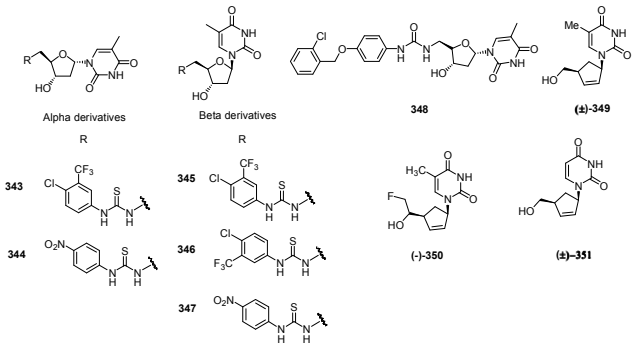

Fig.41 Chemical structures of thymidylate kinase inhibitors

Conclusion and future prospects

Increasing resistance to available malaria chemotherapeutics prompted the search of potential antimalarials that could overcome the shortcomings of the existing therapies. The whole genome sequence of *P. falciparum* has emerged as a powerful weapon for the discovery of new targets that helped in designing targeted inhibitors. Structure based drug design approach could provide the insight details of structure of the target protein, compound binding and inhibition mechanism. In this extensive review, we have discussed available key targets essential for the parasite survival and growth and their inhibitors derived from plant secondary metabolites, their modifications and synthetic routes following structure-guided drug discovery approach. It is conceivable that other (yet unknown) targets will be disclosed in near future which can be exploited by medicinal chemists for discovery and development of new drugs against malaria.

Abbreviations

AMA1	Apical membrane antigen 1
CA	Carbonic anhydrase
CDK	Cyclin dependent protein kinase
CPMG	Carr-Purcell-Meiboom-Gill

dGDP	deoxyguanosine monophosphate
dGMP	deoxyguanosine monophosphate
DHFR	Dihydrofolate reductase
DHODH	Dihydroorotate dehydrogenase
DHPS	Dihyropteroate synthase
DMAPP	Dimethylallyl diphosphate
DPAP	Dipeptidyl aminopeptidase
DXR	1-Deoxy-D-xylulose-5-phosphate reductoisomerase
DXP	1-deoxy- D-xylulose 5-phosphate
FabG	*β*-ketoacyl-ACP reductase
FabI/ENR	Enoyl-ACP reductase
FabZ	*β*-hydroxacyl-ACP dehydratase
FAS II	Fatty acid synthesis type II
FMN	Flavin mononucleotide
FP	Falcipain
HAP	Histo-aspartic protease
hCatD	Human cathepsin D
HDAC	Histone deacetylase
Hsp 90	Heat shock protein 90
IPP	Isopentenyl diphosphate
LDH	Lactate dehydrogenase
LE	Ligand efficiency
MAP	Metalloaminopeptidases
M1AAP	M1 alanyl aminopeptidase
M17LAP	M17 leucine aminopeptidase
MEP	2-methyl-D-erythritol-4-phosphate
MQO	Malate:quinone oxidoreductase
MSP	Merozoite surface proteins
NDH2	NADH: ubiquinone oxidoreductase
NMT	*N*-myristoyltransferase
PM	Plasmepsin
PNP	Purine nucleoside phosphorylase
PV	Parasitophorous vacuole
RBC	Red blood cells
RON	Rhoptry neck protein
SAR	Structure activity relationship
SDH	Succinate: ubiquinone oxidoreductase
SPR	Surface plasmon resonance
STD	Saturation transfer difference
SUB1	Subtilisin-like protease 1
TDP	Thymidine diphosphate
TMK	Thymidylate kinase
TMP	Thymidine monophosphate
TrxR	Thioredoxin reductase
TS	Thymidylate synthase
WHO	World Health Organization
ZBG	Zinc binding group

Conflicts of interest

Authors declare no competing interests

Acknowledgement

Mohammad Abid gratefully acknowledges the funding support in the form of Young Scientist from Science & Engineering Research Board (Grant No. SR/FT/LS-03/2011) and University Grant Commission (UGC), (Grant No. 41-277/2012 (SR)), New Delhi, Govt. of India. BA and BK acknowledge the fellowship support from UGC, INDIA.

References

1. U. R. Mane, D. Mohanakrishnan, D. Sahal, P. R. Murumkar, R. Giridhar and M. R. Yadav, *Eur. J. Med. Chem.*, 2014, **79**, 422–435.
2. WHO Report, 2014. http://apps.who.int/iris/bitstream/10665/144852/2/9789241564830_eng.pdf.
3. N. Boonyalai, P. Sittikul and J. Yuvaniyama, *Mol. Biochem. Parasitol.*, 2015, **201**, 5–15.
4. P. F. Salas, C. Herrmann and C. Orvig, *Chem. Rev.*, 2013, **113**, 3450–3492.
5. D. A. Fidock, P. J. Rosenthal, S. L. Croft, R. Brun and S. Nwaka, *Nature Reviews*, 2004, **3,** 509-520.
6. R. Gaur, M. P. Darokar, P. V. Ajayakumar, R. S. Shukla and R. S. Bhakuni, *Phytochemistry*, 2014, **107**, 135–140.
7. B. Dali, M. Keita, E. Megnassan, V. Frecer, and S. Miertus, *Chem. Biol. Drug. Des.*, 2012, **79**, 411–430.
8. P. J. Rosenthal, *J. Exp. Biol*., 2003, **206,** 3735-3744.
9. J. Held, A. Kreidenweiss, B. Mordmüller, *Expert Opin. Drug Discov.*, 2013, **8,** 1325-1337.
10. N. Drinkwater and S. McGowan, *Biochem. J.*, 2014, **461**, 349–369.
11. A. Yap, M. F. Azevedo, P. R. Gilson, G. E. Weiss, M. T. O'Neill, D. W. Wilson, B. S. Crabb and A. F. Cowman, *Cell. Microbiol.,* 2014, **16**, 642–656.
12. J. Valbuena, L. Rodríguez, R. Vera, A. Puentes, H. Curtidor, J. Cortés, J. Rosas and M. E. Patarroyo, *Biochimie*, 2006, **88**, 1447–1455.
13. S. S. Lim, C. O. Debono, C. A. MacRaild, I. R. Chandrashekaran, O. Dolezal, R. F. Anders, J. S. Simpson, M. J. Scanlon, S. M. Devine, P. J. Scammells and R. S. Norton, *Aust. J. Chem.*, 2013, **66**, 1530–1536.
14. A. Alam, M. Goyal, M. S. Iqbal, C. Pal, S. Dey, S. Bindu, P. Maity and U. Bandyopadhyay, *Expert Rev. Clin. Pharmacol.,* 2009, **2**, 469–489.
15. S. M. Devine, S. S. Lim, I. R. Chandrashekaran, C. A. MacRaild, D. R. Drew, C. O. Debono, R. Lam, R. F. Anders, J. G. Beeson, M. J. Scanlon, P. J. Scammells and R. S. Norton, *Med. Chem. Commun.*, 2014, **5**, 1500–1506.
16. E. F. Lee, S. Yao, J. K. Sabo, W. D. Fairlie, R. A. Stevenson, K. S. Harris, R. F. Anders, M. Foley and R. S. Norton, *Biopolymers*, 2011, **95**, 354–364.

17. B. V. Normand, M. L. Tonkin, M. H. Lamarque, S. Langer, S. Hoos, M. Roques, F. A. Saul, B. W. Faber, G. A. Bentley, M. J. Boulanger, M. Lebrun, *PLoS pathog*., 2012, **8**, e1002755.
18. A. Alam, *Malar. Res. Treat.*2014, 20–22.
19. P. Srinivasan, A. Yasgar, D. K. Luci, W. L. Beatty, X. Hu, J. Andersen, D. L. Narum, J. K. Moch, H. Sun, J. D. Haynes, D. J. Maloney, A. Jadhav, A. Simeonov and L. H. Miller, *Nat. Commun.*, 2013, **4**, 2261.
20. S. Giovani, M. Penzo, S. Brogi, M. Brindisi, S. Gemma, E. Novellino, L. Savini, M. J. Blackman, G. Campiani and S. Butini, *Bioorg. Med. Chem. Lett.*, 2014, **24**, 3582–3586.
21. S. Giovani, M. Penzo, S. Butini, M. Brindisi, S. Gemma, E. Novellino, G. Campiani, M. J. Blackman, and S. Brogi, *RSC Advances,* 2015, **5**, 22431-22448.
22. C. Withers-Martinez, C. Suarez, S. Fulle, S. Kher, M. Penzo, J. Ebejer, K. Koussis, F. Hackett, A. Jirgensons, P. Finn and M. J. Blackman, *Int. J. Parasitol.*, 2012, **42**, 597–612.
23. C. Withers-Martinez, M. Strath, F. Hackett, L. F. Haire, S. A. Howell, P. A. Walker, C. Evangelos, G. G. Dodson, M. J. Blackman, *Nat. Commun.*, 2014, **5,** 3726.
24. S. Gemma, S. Giovani, M. Brindisi, P. Tripaldi, S. Brogi, L. Savini, I. Fiorini, E. Novellino, S. Butini, G. Campiani, M. Penzo and M. J. Blackman, *Bioorg. Med. Chem. Lett.*, 2012, **22**, 5317–5321.
25. S. S. Kher, M. Penzo, S. Fulle, P. W. Finn, M. J. Blackman and A. Jirgensons, *Bioorg. Med. Chem. Lett.*, 2014, **24**, 4486–4489.
26. P. J. Rosenthal, *J. Exp. Biol.*, 2003, **206**, 3735–3744.
27. T. S. Skinner-Adams, C. M. Stack, K. R. Trenholme, C. L. Brown, J. Grembecka, J. Lowther, A. Mucha, M. Drag, P. Kafarski, S. McGowan, J. C. Whisstock, D. L. Gardiner and J. P. Dalton, *Trends in Biochem. Sci.*, 2009, **35**, 53–61.
28. Z. S. Saify, M. K. Azim, W. Ahmad, M. Nisa, D. E. Goldberg, S. A. Hussain, S. Akhtar, A. Akram, A. Arayne, A. Oksman and I. A. Khan, *Bioorg. Med. Chem. Lett.*, 2012, **22**, 1282–1286.
29. Y. Song, H. Jin, X. Liu, L. Zhu, J. Huang and H. Li, *Bioorg. Med. Chem. Lett.*, 2013, **23**, 2078–2082.
30. S. C. Mohapatra, H. K. Tiwari, M. Singla, B. Rathi, A. Sharma, K. Mahiya, M. Kumar, S. Sinha and S. C. Chauhan, *J. Biol. Inorg. Chem.*, 2010, **15**, 373–385.
31. T. Luksch, A. Blum, N. Klee, W. E. Diederich, C. A. Sotriffer and G. Klebe, *Chem. Med. Chem.*, 2010, **5**, 443–454.
32. W. Ahmed, M. Rani, I. A. Khan, A. Iqbal, K. M. Khan, M. A. Haleem and M. K. Azim, *J. Enzyme Inhib. Med. Chem.,* 2010, **25**, 673–678.
33. D. Gupta, R. S. Yedidi, S. Varghese, L. C. Kovari and P. M. Woster, *J. Med. Chem.*, 2010, **53**, 4234–4247.
34. Z. S. Saify, M. Nisa, K. F. Azhar, K. azim, H. Rasheed, N. Mushtaq, M. A. Arain, S. Haider, M. Khanum and W. Ahmed, *Nat. Prod. Res.,* 2011, **25**, 1965-1968.
35. N. Vaiana, M. Marzahn, S. Parapini, P. Liu, M. Dell'Agli, A. Pancotti, E. Sangiovanni, N. Basilico, E. Bosisio, B. M. Dunn, D. Taramelli and S. Romeo, *Bioorg. Med. Chem. Lett.* 2012, **22**, 5915–5918.
36. V. Aureggi, V. Ehmke, J. Wieland, W. B. Schweizer, B. Bernet, D. Bur, S. Meyer, M. Rottmann, C. Freymond, R. Brun, B. Breit and F. Diederich, *Chem. Eur. J.*, 2013, **19**, 155–164.
37. M. J. Meyers, M. D. Tortorella, J. Xu, L. Qin, Z. He, X. Lang, W. Zeng, W. Xu, L. Qin, M. J. Prinsen, F. M. Sverdrup, C. S. Eickhoff, D. W. Griggs, J. Oliva, P. G. Ruminski, E. J. Jacobsen, M. A. Campbell, D. C. Wood, D. E. Goldberg, X. Liu, Y. Lu, X. Lu, Z. Tu, X. Lu, K. Ding and X. Chen, *ACS Med. Chem. Lett.,* 2014, **5**, 89-93.
38. K. Jaudzems, K. Tars, G. Maurops, N. Ivdra, M. Otikovs, J. Leitans, I. Kanepe-Lapsa, I. Domraceva, I. Mutule, P. Trapencieris, M. J. Blackman and A. Jirgensons, *ACS Med. Chem. Lett.,* 2014, **5**, 373-377.
39. H. Jin, Z. Xu, K. Cui, T. Zhang, W. Lu and J. Huang, *Fitoterapia*, 2014, **94**, 55–61.
40. A. Nezami, I. Luque, T. Kimura, Y. Kiso and E. Freire, *Biochemistry,* 2002, **41**, 2273-2280;
41. A. Kiso, K. Hidaka, T. Kimura, Y. Hayashi, A. Nezami, E. Freire, Y. Kiso, *J. Pept. Sci.*, 2004, **10**, 641-647.
42. T. Miura, K. Hidaka, T. Uemura, K. Kashimoto, Y. Hori, Y. Kawasaki, A. J. Ruben, E. Freire, T. Kimura and Y. Kiso, *Bioorg. Med. Chem. Lett*., 2010, **20**, 4836–4839.
43. T. Miura, K. Hidaka, Y. Azai, K. Kashimoto, Y. Kawasaki, S. Chen, R. F. de Freitas, E. Freire and Y. Kiso, *Bioorg. Med. Chem. Lett.*, 2014, **24**, 1698–1701.
44. A. Mahindra, R. P. Gangwal, S. Bansal, N. E. Goldfarb, B. M. Dunn, A. T. Sangamwar and R. Jain, *RSC Adv.*, 2015, **5**, 22674–22684.
45. J. M. Coterón, D. Catterick, J. Castro, M. J. Chaparro, B. Diaz, E. Fernández, S. Ferrer, F. J. Gamo, M. Gordo, J. Gut, L. de las Heras, J. Legac, M. Marco, J. Miguel, V. Muñoz, E. Porras, J. C. de la Rosa, J. R. Ruiz, E. Sandoval, P. Ventosa, P. J. Rosanthal and J. M. Fiandor, *J. Med. Chem.,* 2010, **53**, 6129–6152.
46. R. Ettari, A. Pinto, L. Tamborini, I. C. Angelo, S. Grasso, M. Zappalà, N. Capodicasa, L. Yzeiraj, E. Gruber, M. N. Aminake, G. Pradel, T. Schirmeister, C. De Micheli and P. Conti, *Chem. Med. Chem.*, 2014, **9**, 1817–1825.
47. B. Rathi, A. K. Singh, R. Kishan, N. Singh, N. Latha, S. Srinivasan, K. C. Pandey, H. K. Tiwari and B. K. Singh, *Bioorg. Med. Chem.*, 2013, **21**, 5503-5509.
48. R. Löser, J. Gut, P. J. Rosenthal, M. Frizler, M. Gütschow and K. T. Andrews, *Bioorg. Med. Chem. Lett.*, 2010, **20**, 252–255.
49. L. Rizzi, S. Sundararaman, K. Cendic, N. Vaiana, R. Korde, D. Sinha, A. Mohmmed, P. Malhotra and S. Romeo, *Eur. J. Med. Chem.*, 2011, **46**, 2083–2090.
50. B. Somanadhan, S. R. Kotturi, C. Y. Leong, R. P. Glover, Y. Huang, H. Flotow, A. D. Buss, M. J. Lear and M. S. Butler, *J. Antibiot. (Tokyo)*., 2013, **66**, 259–264.
51. T. Conroy, J. T. Guo, N. Elias, K. M. Cergol, J. Gut, J. Legac, L. Khatoon, Y. Liu, S. McGowan, P. J. Rosenthal, N. H. Hunt and R. J. Payne, *J. Med. Chem*., 2014, **57**, 10557-10563.
52. S. K. Chakka, M. Kalamuddin, S. Sundararaman, L. Wei, S. Mundra, R. Mahesh, P. Malhotra, A. Mohmmed and L. P. Kotra, *Bioorg. Med. Chem.*, 2015, **23**, 2221–2240.
53. F. Bova, R. Ettari, N. Micale, C. Carnovale, T. Schirmeister, C. Gelhaus, M. Leippe, S. Grasso and M. Zappalà, *Bioorg. Med. Chem.*, 2010, **18**, 4928–4938.
54. V. Ehmke, F. Kilchmann, C. Heindl, K. Cui, J. Huang, T. Schirmeister and F. Diederich, *Med. Chem. Commun.*, 2011, **2**, 800–804.
55. R. Ettari, M. Zappalà, N. Micale, T. Schirmeister, C. Gelhaus, M. Leippe, A. Evers and S. Grasso, *Eur. J. Med. Chem.,* 2010, **45**, 3228–3233.
56. D. J. Weldon, F. Shah, A. G. Chittiboyina, A. Sheri, R. R. Chada, J. Gut, P. J. Rosenthal, D. Shivakumar, W. Sherman, P. Desai, J. Jung and M. A. Avery, *Bioorg. Med. Chem. Lett.*, 2014, **24**, 1274–1279.
57. Y. Liu, W. Lu, K. Cui, W. Luo, J. Wang and C. Guo, *Arch. Pharm. Res.*, 2012, **35**, 1525–1531.
58. Y. Liu, K. Cui, W. Lu, W. Luo, J. Wang, J. Huang and C. Guo, *Molecules*, 2011, **16**, 4527–4538.
59. W. Luo, W. Lu, K. Cui,Y. Liu, J. Wang and C. Guo, *Med. Chem. Res.,* 2012, **21**, 3073–3079.
60. E. M. Guantai, K. Ncokazi, T. J. Egan, J. Gut, P. J. Rosenthal, P. J. Smith, K. Chibale, *Biorg. Med. Chem*., 2010, **18**, 8243-8256.

61. E. M. Guantai, K. Ncokazi, T. J. Egan, J. Gut, P. J. Rosenthal, R. Bhampidipati, A. Kopinathan, P. J. Smith and K. Chibale, *J. Med. Chem.*, 2011, **54**, 3637–3649.
62. B. Pérez, C. Teixeira, J. Gut, P. J. Rosenthal, J. R. B. Gomes and P. Gomes, *Chem. Med. Chem.*, 2012, **7**, 1537-1540.
63. M. Akhter, R. Saha, O. Tanwar, M. M. Alam, M. S. Zaman, *Med. Chem. Res.*, 2014, **24**, 879-890.
64. T. Waag, C. Gelhaus, J. Rath, A. Stich, M. Leippe and T. Schirmeister, *Bioorg. Med. Chem. Lett.*, 2010, **20**, 5541–5543.
65. L. Wang, H. He, Y. Di, Y. Zhang and X. Hao, *Tetrahedron Lett.*, 2012, **53**, 1576–1578.
66. S. C. Stolze, E. Deu, F. Kaschani, N. Li, B. I. Florea, K. H. Richau, T. Colby, R. A. L. van der Hoorn, H. S. Overkleeft, M. Bogyo and M. Kaiser, *Chem. Biol.*, 2012, **19**, 1546–1555.
67. E. Salas-Sarduy, A. Cabrera-Muñoz, A. Cauerhff , Y. González-González, S. A. Trejo, A. Chidichimo, M. de los Angeles Chávez-Planes and J. J. Cazzulo, *Exp. Parasitol.*, 2013, **135**, 611–622.
68. L. Wang, S. Zhang, J. Zhu, L. Zhu, X. Liu, L. Shan, J. Huang, W. Zhang and H. Li, *Bioorg. Med. Chem. Lett.*, 2014, **24**, 1261–1264.
69. R. G. Kamkumo, A. M. Ngoutane, L. R. Y. Tchokouaha, P. V. T. Fokou, E. A. K. Madiesse, J. Legac, J. J. B. Kezetas, B. N. Lenta, F. F. Boyom, T. Dimo, W. F. Mbacham, J. Gut and P. J. Rosenthal, *Malar. J.*, 2012, 11, 382-389.
70. R. Oliveira, R. C. Guedes, P. Miereles, I. S. Albuquerque, L. M. Gonçalves, E. Pires, M. R. Bronze, J. Gut, P. J. Rosenthal, M. Prudêncio, R. Moreira, P. M. O'Neill and F. Lopes, *J. Med. Chem.*, 2014, **57**, 4916-4923.
71. U. R. Mane, H. Li, J. Huang, R. C. Gupta, S. S. Nadkarni, R. Giridhar, P. P. Naik and M. R. Yadav, *Bioorg. Med. Chem.,* 2012, **20**, 6296–6304.
72. R. H. Hans, J. Gut, P. J. Rosenthal and K. Chibale, *Bioorg. Med. Chem. Lett.*, 2010, **20**, 2234–2237.
73. N. Tadigoppula, V. Korthikunta, S. Gupta, P. Kancharla, T. Khaliq, A. Soni, R. K. Srivastava, K. Srivastava, S. K. Puri, K. S. R. Raju, Wahajuddin, P. S. Sijwali, V. Kumar and I. S. Mohammad, *J. Med. Chem.*, 2012, **56**, 31-45.
74. J. B. Bertolodo, L. D. Chiaradia-Deatorre, A. Mascarello, P. C. Leal, M. N. S. Cordeiro, R. J. Nunes, E. S. Sarduy, P. J. Rosenthal and H. Terenzi, *J. Enzyme Inhib. Med. Chem.*, 2014, **30**, 299-307.
75. R. Mahesh, S. Mundra, T. Devadoss and L. P. Kotra, *Arab. J. Chem.*, 2014 (Article in press).
76. R. Ettari, L. Tamborini, I. C. Angelo, S. Grasso, T. Schirmeister, L. Lo Presti, C. De Micheli, A. Pinto,and P. Conti, *Chem. Med. Chem.*, 2013, **8**, 2070-2076.
77. R. K. Sharma, Y. Younis, G. Mugumbate, M. Njoroge, J. Gut, P. J. Rosenthal and K. Chibale, *Eur. J. Med. Chem.*, 2015, **90**, 507–518.
78. V. Ehmke, C. Heindl, M. Rottmann, C. Freymond, W. B. Schweizer, R. Brun, A. Stich, T. Schirmeister and F. Diederich, *Chem. Med. Chem.,* 2011, **6**, 273–278.
79. S. D. Khanye, G. S. Smith, C. Lategan, P. J. Smith, J. Gut, P. J. Rosenthal and K. Chibale, *J. Inorg. Biochem.*, 2010, **104**, 1079–1083.
80. S. Langolf, U. Machon, M. Ehlers, W. Sicking, T. Schirmeister, C. Büchhold, C. Gelhaus, P. J. Rosenthal and C. Schmuck, *Chem. Med. Chem.* 2011, **6**, 1581–1586.
81. N. Micale, M. A. Cinellu, L. Maiore, A. R. Sannella, C. Severini, T. Schirmeister, C. Gabbiani and L. Messori, *J. Inorg. Biochem.*, 2011, **105**, 1576–1579.
82. F. Shah, Y. Wu, J. Gut, Y. Pedduri, J. Legac, P. J. Rosenthal and M. A. Avery, *Med. Chem. Commun*. 2011, **2**, 1201–1207.
83. S. P. Kumar, J. Gut, R. C. Guedes, P. J. Rosenthal, M. M. M. Santos and R. Moreira, *Eur. J. Med. Chem.*, 2011, **46**, 927–933.
84. R. Oliveira, A. S. Newton, R. C. Guedes, D. Miranda, R. K. Amewu, A. Srivastava, J. Gut, P. J. Rosenthal, P. M. O'Neill, S. A. Ward, F. Lopes and R. Moreira, *Chem. Med. Chem.* 2013, **8**, 1528–1536.
85. P. Gibbons, E. Verissimo, N. C. Araujo, V. Barton, G. L. Nixon, R. K. Amewu, J. Chadwick, P. A. Stocks, G. A. Biagini, A. Srivastava, P. J. Rosenthal, J. Gut, R. C. Guedes, R. Moreira, R. Sharma, N. Berry, M. L. S. Cristiano, A. E. Shone, S. A. Ward and P. M. O'Neill, *J. Med. Chem.*, 2010, **53**, 8202–8206.
86. A. K. Singh, V. Rajendran, A. Pant, P. C. Ghosh, N. Singh, N. Latha, S. Garg, K. C. Pandey, B. K. Singh and B. Rathi, *Bioorg. Med. Chem.*, 2015, **23**, 1817–1827.
87. S. N. Mistry, N. Drinkwater, C. Ruggeri, K. K. Sivaraman, S. Loganathan, S. Fletcher, M. Drag, A. Paiardini, V. M. Avery, P. J. Scammells and S. McGowan, *J. Med. Chem*., 2014, **57**, 9168-9183.
88. K. K. Sivaraman, A. Paiardini, M. Siénczyk, C. Ruggeri, C. A. Oellig, J. P. Dalton, P. J. Scammells, M. Drag, S. McGowan, *J. Med. Chem*., 2013, **56**,. 5213-5217.
89. G. Velmourougane, M. B. Harbut, S. Dalal, S. McGowan, C. A. Oellig, N. Meinhardt, J. C. Whisstock, M. Klemba and D. C. Greenbaum, *J. Med. Chem*., 2011, **54**, 1655–1666.
90. T. S. Skinner-Adams, C. L. Peatey, K. Anderson, K. R. Trenholme, D. Krige, C. L. Brown, C. Stack, D. M. M. Nsangou, R. T. Mathews, K. Thivierge, J. P. Dalton and D. L. Gardiner, *Antimicrob. Agents Chemother.,* 2012, **56**, 3244–3249.
91. R. Deprez-Poulain, M. Flipo, C. Piveteau, F. Leroux, S. Dassonneville, I. Florent, L. Maes, P. Cos and B. Deprez, *J. Med. Chem.,* 2012, **55**, 10909-10917.
92. T. Spicer, V. Fernandez-Vega, P. Chase, L. Scampavia, J. To, J. P. Dalton, F. L. Da Silva, T. S. Skinner-Adams, D. L. Gardiner, K. R. Trenholme, C. L. Brown, P. Ghosh, J. L. Wang, D. A. Whipple, F. J. Schoenen and P. Hodder, *J. Biomol. Screen.,* 2014, **19**, 1107-1115.
93. A. Paiardini, R. S. Bamert, K. Kannan-Sivaraman, N. Drinkwater, S. N. Mistry, P. J. Scammells and S. McGowen, *PLoS One*, 2015, **2**, e0115859.
94. F. Wang, P. Krai, E. Deu, B. Bibb, C. Lauritzen, J. Pedersen, M. Bogyo and M. Klemba, *Mol. Biochem. Parasitol.*, 2011, **175**, 10–20.
95. E. Deu, M. J. Leyva, V. E. Albrow, M. J. Rice, J. A. Ellman and M. Bogyo, *Chem. Biol.*, 2010, **17**, 808–819.
96. N. C. Wheatley, K. T. Andrews, T. L. Tran, A. J. Lucke, R. C. Reid and D. P. Fairlie, *Bioorg. Med. Chem. Lett.*, 2010, **20**, 7080–7084.
97. F. K. Hansen, T. S. Skinner-Adams, S. Duffy, L. Marek, S. D. M. Sumanadasa, K. Kuna, J. Held, V. M. Avery, K. T. Andrews and T. Kurz, *Chem. Med. Chem.*, 2014, **9**, 665–670.
98. V. Patil, W. Guerrant, P. C. Chen, B. Gryder, D. B. Benicewicz, S. I. Khan, B. L. Tekwani and A. K. Oyelere, *Bioorg. Med. Chem.*, 2010, **18**, 415–425.
99. S. D. M. Sumanadasa, C. D. Goodman, A. J. Lucke, T. Skinner-Adams, I. Sahama, A. Haque, T. A. Do, G. I. McFadden, D. P. Fairlie and K. T. Andrews, *Antimicrob. Agents chemother.*, 2012, **56**, 3849–3856.
100. F. K. Hansen, S. D. M. Sumanadasa, K. Stenzel, S. Duffy, S. Meister, L. Marek, R. Schmetter, K. Kuna, A. Hamacher, B. Mordmüller, M. U. Kassack, E. A. Winzeler, V. M. Avery, K. T. Andrews and T. Kurz, *Eur. J. Med. Chem.*, 2014, **82**, 204–213.
101. G. Giannini, G. Battistuzzi and D. Vignola, *Bioorg. Med. Chem. Lett.*, 2015, **25**, 459–461.
102. J. A. Geyer, S. M. Keenan, C. L. Woodard, P. A. Thompson, L. Gerena, D. A. Nichols, C. E. Gutteridge and N. C. Waters, *Bioorg. Med. Chem. Lett.*, 2009, **19**, 1982–1985.

103. C. L. Woodard, S. M. Keenan, L. Gerena, W. J. Welsh, J. A. Geyer and N. C. Waters, *Bioorg. Med. Chem. Lett.*, 2007, **17**, 4961–4966.
104. D. Caridha, A. K. Kathcart, D. Jirage and N. C. Waters, *Bioorg. Med. Chem. Lett.*, 2010, **20**, 3863–3867.
105. P. A. Stocks, V. Barton, T. Antoine, G. A. Biagini and S. A. Ward and P. M. O'Neill, *Parasitology*, 2013, **141**, 50-65.
106. J. M. Bueno, E. Herreros, I. Angulo-Barturen, S. Ferrer, J. M. Fiandor, F. J. Gamo, D. Gargallo-Viola and G. Derimanov, *Future Med. Chem.*, 2012, **4**, 2311–2323.
107. G. L. Nixon, C. Pidathala, A. E. Shone, T. Antoine, N. Fisher, S. A. Ward, P. M. O'Neill, S. A. Ward and G. A. Biagini, *Future Med. Chem.*, 2013, **5**, 1573–1591.
108. R. Cowley, S. Leung, N. Fisher, M. Al-Helal, N. G. Berry, A. S. Lawrenson, R. Sharma, A. E. Shone, S. A. Ward, G. A. Biagini and P. M. O'Neill, *Med. Chem. Commun*., 2012, **3**, 39–44.
109. M. J. Capper, P. M. O'Neill, N. Fisher, R. W. Strange, D. Moss, S. A. Ward, N. G. Berry, A. S. Lawrenson, S. S. Hasnain, G. A. Biagini and S. V. Antonyuk, *Proc. Natl. Acad. Sci. U.S.A*., 2015, **112**, 755-760.
110. C. Vallières, N. Fisher, T. Antoine, M. Al-Helal, P. Stocks, N. G. Berry, A. S. Lawrenson, S. A. Ward, P. M. O'Neill, G. A. Biagini and B. Meunier, *Antimicrob. Agents chemother.*, 2012, **56**, 3739–3747.
111. P. Zhao, L. Wang, X. Zhu, X. Huang, C. Zhan, J. Wu and G. Yang, *J. Am. Chem. Soc.,* 2010, **132**, 185–194.
112. N. Kongkathip, N. Pradidphol, K. Hasitapan, R. Grigg, W. Kao, C. Hunte, N. Fisher, A. J. Warman, G. A. Biagini, P. Kongsaeree, P. Chuawong and B. Kongkathip, *J. Med. Chem.*, 2010, **53**, 1211–1221.
113. A. Nilsen, G. P. Miley, I. P. Forquer, M. W. Mather, K. Katneni, Y. Li, S. Pou, A. M. Pershing, A. M. Stickles, E. Ryan, J. X. Kelly, J. S. Doggett, K. L. White, D. J. Hinrichs, R. W. Winter, S. A. Charman, L. N. Zakharov, I. Bathurst, J. N. Burrows, A. B. Vaidya and M. K. Riscoe, *J. Med. Chem.*, 2014, **57,** 3818-3834..
114. D. C. Schuck, S. B. Ferreira, L. N. Cruz, D. R. da Rocha, M. S. Moraes, M. Nakabashi, P. J. Rosenthal, V. F. Ferreira and C. R. S. Garcia, *Malar. J.*, 2013, **234**, 1-6.
115. C. K. Dong, S. Urgaonkar, J. F. Cortese, F. Gamo, J. F. Garcia-Bustos, M. J. Lafuente, V. Patel, L. Ross, B. I. Coleman, E. R. Derbyshire, C. B. Clish, A. E. Serrano, M. Cromwell, R. H. Barker, J. D. Dvorin, M. T. Duraisingh, D. F. Wirth, J. Clardy and R. Mazitschek, *Chem. Biol.*, 2011, **18**, 1602–1610.
116. L. M. Hughes, C. A. Lanteri, M. T. O'Neil, J. D. Johnson, G. W. Gribble, and B. L. Trumpower, *Mol. Biochem. Parasitol.* 2011, **177**, 12-19.
117. S. C. Teguh, N. Klonis, S. Duffy, L. Lucantoni, V. M. Avery, C. A. Hutton, J. B. Baell and L. Tilley, *J. Med. Chem.*, 2013, **56,** 6200-6215.
118. T. Nam, C. W. McNamara, S. Bopp, N. V. Dharia, S. Meister, G. M. C. Bonamy, D. M. Plouffe, N. Kato, S. McCormack, B. Bursulaya, H. Ke, A. B. Vaidya, P. G. Schultz and E. A. Winzeler, *ACS Chem. Biol.,* 2011, **6**, 1214–1222.
119. F. P. da Cruz, C. Martin, K. Buchholz, M. J. Lafuente-Monasterio, T. Rodrigues, B. Sönnichsen, R. Moreira, F. J. Gamo, M. Marti, M. M. Mota, M. Hannus and M. Prudêncio, *J. Infect. Dis.*, 2012, **205**, 1278–1286.
120. X. Deng, D. Matthews, P. K. Rathod and M. A. Phillips, *Acta. Cryst.,* 2015, **F71**, 553–559.
121. J. M. Coteron, M. Marco, J. Esquivias, X. Deng, K. L. White, J. White, M. Koltun, F. El Mazouni, S. Kokkonda, K. Katneni, R. Bhamidipati, D. M. Shackleford, I. Angulo-Barturen, S. B. Ferrer, M. B. Jiménez-Díaz, F. Gamo, E. J. Goldsmith, W. N. Charman, I. Bathurst, D. Floyd, D. Matthews, J. N. Burrows, P. K. Rathod, S. A. Charman and M. A. Phillips, *J. Med. Chem.*, 2011, **54**, 5540–5561.
122. P. K. Ojha, I. Mitra, S. Kar, R. N. Das and K. Roy, *Mol. Inf.,* 2012, **31**, 711–718.
123. D. Cowen, P. Bedingfield, G. A. McConkey, C. W. G. Fishwick and A. P. Johnson, *Bioorg. Med. Chem. Lett.*, 2010, **20**, 1284–1287.
124. M. L. Booker, C. M. Bastos, M. L. Kramer, R. H. Barker, R. Skerlj, A. B. Sidhu, X. Deng, C. Celatka, J. F. Cortese, J. E. G. Bravo, K. N. C. Llado, A. E. Serrano, I. Angulo-Barturen, M. B. Jiménez-Diaz, S. Viera, H. Garuti, S. Wittlin, P. Papastogiannidis, J. Lin, C. J. Janse, S. M. Khan, M. Duraisingh, B. Coleman, E. J. Goldsmith, M. A. Phillips, B. Munoz, D. F. Wirth, J. D. Klinger, R. Wiegand and Edmund Sybertz, *J. Biol. Chem.,* 2010, **285**, 33054–33064.
125. R. Gujjar, A. Marwaha, F. El Mazouni, J. White, K. L. White, S. Creason, D. M. Shackleford, J. Baldwin, W. N. Charman, F. S. Buckner, S. Charman, P. K. Rathod and M. A. Phillips, *J. Med. Chem.,* 2009, **52**, 1864-1872.
126. R. Gujjar, F. El Mazouni, K. L. White, J. White, S. Creason, D. M. Shackleford, X. Deng, W. N. Charman, I. Bathurst, J. Burrows, D. M. Floyd, D. Matthews, F. S. Buckner, S. A. Charman, M. A. Phillips, and P. K. Rathod, *J. Med. Chem.*, 2011, **54**, 3935-3949.
127. R. T. Skerlj, C. M. Bastos, M. L. Booker, M. L. Kramer, R. H. Barker Jr, C. A. Celatka, T. J. O'Shea, B. Munoz, A. B. Sidhu, J. F. Cortese, S. Wittlin, P. Papastogiannidis, I. Angulo-Barturen, A. B. Jimenez-Diaz and E. Sybertz, *ACS Med. Chem. Lett.*, 2011, **2**, 708-713.
128. I. Fritzson, P. T. P. Bedingfield, A. P. Sundin, G. McConkey, and U. J. Nilsson, *Med. Chem. Comm.,* 2011, **2**, 895-898.
129. A. Marwaha, J. White, F. El Mazouni, S. A. Creason, S. Kokkonda, F. S. Buckner, S. A. Charman, M. A. Phillips and P. K. Rathod, *J. Med. Chem.*, 2012, **55**, 7425-7436.
130. M. Xu, J. Zhu, Y. Diao, H. Zhou, X. Ren, D. Sun, J. Huang, D. Han, Z. Zhao, L. Zhu, Y. Xu and H. Li, *J. Med. Chem.*, 2013, **56**, 7911-7924.
131. G. A. Biagini, N. Fisher, A. E. Shone, M. A. Mubaraki, A. Srivastava, A. Hill, T. Antoine, A. J. Warman, J. Davies, C. Pidathala, R. K. Amewu, S. C. Leung, R. Sharma, P. Gibbons, D. W. Hong, B. Pacorel, A. S. Lawrenson, S. Chareonsutthivarakul, L. Taylor, O. Berger, A. Mbekeani, P. A. Stocks, G. L. Nixon, J. Chadwick, J. Hemingway, M. J. Delves, R. E. Sinden, A. Zeeman, C. H. M. Kocken, N. G. Berry, P. M. O'Neill and S. A. Ward, *Proc. Natl. Acad. Sci. U.S.A*., 2012. **109**, 8298-8303.
132. C. K. Dong, V. Patel, J. C. Yang, J. D. Dvorin, M. T. Duraisingh, J. Clardy and D. F. Wirth, *Bioorg. Med. Chem. Lett.*, 2009, **19**, 972–975.
133. C. Pidathala, R. Amewu, B. Pacorel, G. L. Nixon, P. Gibbons, W. D. Hong, S. C. Leung, N. G. Berry, R. Sharma, P. A. Stocks, A. Srivastava, A. E. Shone, S. Charoensutthivarakul, L. Taylor, O. Berger, A. Mbekeani, A. Hill, N. E. Fisher, A. J. Warman, G. A. Biagini, S. A. Ward and P. M. O'Neill, *J. Med. Chem.*, 2012, **55**, 1831-1843.
134. S. C. Leung, P. Gibbons, R. Amewu, G. L. Nixon, C. Pidathala, W. D. Hong, B. Pacorel, N. G. Berry, R. Sharma, P. A. Stocks, A. Srivastava, A. E. Shone, S. Charoensutthivarakul, L. Taylor, O. Berger, A. Mbekeani, A. Hill, N. E. Fisher, A. J. Warman, G. A. Biagini, S. A. Ward and P. M. O'Neill, *J. Med. Chem.,* 2012, **55**, 1844-1857.
135. N. Arisue and T. Hashimoto, *Parasitol. Int.*, 2015, **64**, 254–259.
136. M. J. Shears, C. Y. Botté and G. I. McFadden, *Mol. Biochem. Parasitol.*, 2015, **199**, 34–50.
137. I. L. Lauinger, L. Vivas, R. Perozzo, C. Stairiker, A. Tarun, M. Zloh, X. Zhang, H. Xu, P. J. Tonge, S. G. Franzblau, D. Pham,

C. V Esguerra, A. D. Crawford, L. Maes and D. Tasdemir, *J. Nat. Prod.*, 2013, 76, 1064-1070.
138. S. Jensen, S. Omarsdottir, A. G. Bwalya, M. A. Nielsen, D. Tasdemir and E. S. Olafsdottir, *Phytomedicine*, 2012, **19**, 1191–1195.
139. A. K. Gupta, S. Saxena and M. Saxena, *Bioorg. Med. Chem. Lett.*, 2010, **20**, 4779–4781.
140. F. Scala, E. Fattorusso, M. Menna, O. Taglialatela-Scafati, M. Tierney, M. Kaiser and D. Tasdemir, *Mar. Drugs*, 8, 2010, 2162–2174.
141. D. Tasdemir, D. Sanabria, I. L. Lauinger, A. Tarun, R. Herman, R. Perozzo, M. Zloh, S. H. Kappe, R. Brun and N. M. Carballeira, *Bioorg. Med. Chem.*, 2010, **18**, 7475–7485.
142. F. Belluti, R. Perozzo, L. Lauciello, F. Colizzi, D. Kostrewa, A. Bisi, S. Gobbi, A. Rampa, M. L. Bolognesi, M. Recanatini, R. Brun, L. Scapozza and A. Cavalli, *J. Med. Chem.,* 2013, **56**, 7516-7526.
143. A. Muhammad, I. Anis, Z. Ali, S. Awadelkarim, A. Khan, A. Khalid, M. R. Shah, M. Galal, I. A. Khan and M. I. Choudhary, *Bioorg. Med. Chem. Lett.*, 2012, **22**, 610–612.
144. R. P. Samal, V. M. Khedkar, R. R. S. Pissurlenkar, A. G. Bwalya, D. Tasdemir, R. A. Joshi, P. R. Rajamohanan, V. G. Puranik and E. C. Coutinho, *Chem. Biol. Drug Des.,* 2013, **81**, 715-729.
145. N. M. Carballeira, A. G. Bwalya, M. A. Itoe, A. D. Andricopulo, M. L. Cordero-Maldonado, M. Kaiser, M. M. Mota, A. D. Crawford, R. V. C. Guido and D. Tasdemir, *Bioorg. Med. Chem. Lett.*, 2014, **24**, 4151–4157.
146. L. Tallorin, J. D. Durrant, Q. G. Nguyen, J. A. McCammon and M. D. Burkart, *Bioorg. Med. Chem.*, 2014, **22**, 6053–6061.
147. A. S. Murkin, K. A. Manning, and S. A. Kholodar. *Bioorg. Chem.,* 2014, **57**, 171-185.
148. R. Chofor, S. Sooriyaarachchi, M. D. P. Risseeuw, T. Bergfors, J. Pouyez, C. Johny, A. Haymond, A. Everaert, C. S. Dowd, L. Maes, T. Coenye, A. Alex, R. D. Couch, T. A. Jones, J. Wouters, S. L. Mowbray and S. Van Calenbergh, *J. Med. Chem.*, 2015, **58**, 2988-3001.
149. J. Xue, J. Diao, G. Cai, L. Deng, B. Zheng, Y. Yao and Y. Song, *ACS Med. Chem. Lett.* 2013, **4**, 278-282.
150. T. Bodill, A. C. Conibear, M. K. M. Mutorwa, J. L. Goble, G. L. Blatch, K. A. Lobb, R. Klein and P. T. Kaye, *Bioorg. Med. Chem.*, 2013, **21**, 4332–4341.
151. C. T. Behrendt, A. Kunfermann, V. Illarionova, An. Matheeussen, T. Gräwert, M. Groll, F. Rohdich, Adelbert Bacher, W. Eisenreich, M. Fischer, L. Maes and Thomas Kurz, *Chem. Med. Chem.*, 2010, **5**, 1673–1676.
152. C. T. Behrendt, A. Kunfermann, V. Illarionova, An. Matheeussen, M. K. Pein, T. Gräwert, J. Kaiser, A. Bacher, W. Eisenreich, B. Illarionov, M. Fischer, L. Maes, M. Groll and T. Kurz, *J. Med. Chem.*, 2011, **54**, 6796–6802.
153. K. Brücher, B. Illarionov, J. Held, S. Tschan, A. Kunfermann, M. K. Pein, A. Bacher, T. Gräwert, , L. Maes, B. Mordmüller, M. Fischer and T. Kurz, *J. Med. Chem.*, 2012, **55**, 6566-6575.
154. A. Kunfermann, C. Lienau, B. Illarionov, J. Held, T. Gräwert, C. T. Behrendt, P. Werner, S. Hähn, W. Eisenreich, U. Riederer, B. Mordmüller, A. Bacher, M. Fischer, M. Groll and T. Kurz, *J. Med. Chem.*, 2013, **56**, 8151-8162.
155. S. Konzuch, T. Umeda, J. Held, S. Hähn, K. Brücher, C. Lienau, C. T. Behrendt, T. Gräwert, A. Bacher, B. Illarionov, M. Fischer, B. Mordmüller, N. Tanaka and T. Kurz, *J. Med. Chem.*, 2014, **57**, 8827-8838.
156. R. E. Cobb, B. Bae, Z. Li, M. A. DeSieno, S. K. Nair and H. Zhao, *Chem. Commun.*, 2015, **51**, 2526–2528.
157. K. Brücher, T. Gräwert, S. Konzuch, J. Held, C. Lienau, C. Behrendt, B. Illarionov, L. Maes, A. Bacher, S. Wittlin, B. Mordmüller, M. Fischer and T. Kurz, *J. Med. Chem.*, 2015, **58**, 2025-2035.
158. T. O. Olaleye, J. A. Brannigan, S. M. Roberts, R. J. Leatherbarrow, A. J. Wilkinson, and E. W. Tate. *Org. Biomol. Chem.*, 2014, **12**, 8132-8137.
159. M. D. Rackham, J. A. Brannigan, K. Rangachari, S. Meister, A. J. Wilkinson, A. A. Holder, R. J. Leatherbarrow and E. W. Tate, *J. Med. Chem.*, 2014, **57**, 2773-2788.
160. Z. Yu, J. A. Brannigan, D. K. Moss, A. M. Brzozowski, A. J. Wilkinson, A. A. Holder, E. W. Tate and R. J. Leatherbarrow, *J. Med. Chem.*, 2012, **55**, 8879-8890.
161. M. H. Wright, B. Clough, M. D. Rackham, K. Rangachari, J. A. Brannigan, M. Grainger, D. K. Moss, A. R. Bottrill, W. P. Heal, M. Broncel, R. A. Serwa, D. Brady, D. J. Mann, R. J. Leatherbarrow, R. Tewari, A. J. Wilkinson, A. A. Holder and E. W. Tate, *Nature Chem.*, 2013, **6**, 112-121.
162. A. S. Bell, J. E. Mills, G. P. Williams, J. A. Brannigan, A. J. Wilkinson, T. Parkinson, R. J. Leatherbarrow, E. W. Tate, A. A. Holder and D. F. Smith, *PLoS Negl. Trop. Dis.*, 2012, **6**, e1625.
163. M. D. Rackham, J. A. Brannigan, D. K. Moss, Z. Yu, A. J. Wilkinson, A. A. Holder, E. W. Tate and R. J. Leatherbarrow, *J. Med. Chem.*, 2013, **56**, 371–375.
164. D. Shahinas, M. Liang, A. Datti and D. R. Pillai, *J. Med. Chem.*, 2010, **53**, 3552-3557.
165. T. Wang, W. H. Bisson, P. Mäser, L. Scpozza and D. Picard, *J. Med. Chem.*, 2014, **57**, 2524-2535.
166. R. Pallavi, N. Roy, R. K. Nageshan, P. Talukdar, S. R. Pavithra, R. Reddy, S. Venketesh, R. Kumar, A. K. Gupta, R. K. Singh, S. C. Yadav and U. Tatu, *J. Bio. Chem.,* 2010, **285**, 37964–37975.
167. D. Shahinas, A. Folefoc, T. Taldone, G. Chiosis, I. Crandall and D. R. Pillai, *PLoS one,* 2013, **8,** e75446.
168. D. Shahinas, G. MacMullin, C. Benedict, I. Crandall and D. R. Pillai, *Antimicrob. Agents Chemother.*, 2012, **8,** 4207-4213.
169. J. Penna-Coutinho, W. A. Cortopassi, A. A. Oliveira, T. C. C. França and A. U. Krettli, *PLoS one,* 2011, **6**, e21237.
170. P. Keluskar and S. Ingle, *J. Ethnopharmacol.*, 2012, **144**, 201–207.
171. N. Sethiya, P. Keluskar, S. Ingle, and S. Mishra, *Asian Pac. J. Trop. Dis.* 2014, **4**, 489-491.
172. P. K. Boniface, S. Verma, A. Shukla, H. S. Cheema, S. K. Srivastava, F. Khan, M. P. Darokar, and A Pal, *Parasit. Int.,* 2015, **64**, 118-123.
173. H. Cui, G. F. Ruda, J. Carrero-Lérida, L. M. Ruiz-Pérez, I. H. Gilbert and D. González-Pacanowska, *Eur. J. Med. Chem.*, 2010, **45**, 5140–5149.
174. T. M. Donaldson, L. Ting, C. Zhan, W. Shi, R. Zheng, S. C. Almo and K. Kim, *PLoS one,* 2014, **9**, e84384.
175. A. Gigante, E. Priego, P. Sánchez-Carrasco, L. M. Ruiz-Pérez, J. V. Voorde, M Camarasa, J. Balzarini, D. González-Pacanowska, and M. Pérez-Pérez. *Eur. J. Med. Chem.*, 2014, **82**, 459-465.
176. H. K. Lautre, K. Patil, H. Youssouffi, T. Ben Hadda, V. Bhatia and A. K. Pillai, *World. J. Pharma. Pharmaceut. Sci.*, 2014, **3**, 1053–1068.
177. J. E. Hyde, *Acta Tropica,* 2005, **94**, 191-206.
178. S. Abbat, V. Jain and P. V. Bharatam, *J. Biomol. Struct. Dyn.*, 2014, 1–16 (Ahead-of-print).
179. C. Capasso and C. T. Supuran, *J. Enzyme Inhib. Med. Chem.,* 2013, **29**, 379-387.
180. H. Huang, W. Lu, X. Li, X. Cong, H. Ma, X. Liu, Y. Zhang, P. Che, R. Ma, H. Li, X. Shen, H. Jiang, J. Huang and J. Zhu, *Bioorg. Med. Chem. Lett.*, 2012, **22**, 958–962.

181. L. Adane, S. Bhagat, M. Arfeen, S. Bhatia, R. Sirawaraporn, W. Sirawaraporn, A. K. Chakraborti and P. V Bharatam, *Bioorg. Med. Chem. Lett.*, 2014, **24**, 613–617.
182. Y. Yuthavong, B. Tarnchompoo, T. Vilaivan, P. Chitnumsub, S. Kamchonwongpaisan, S. A. Charman, D. N. McLennan, K. L. White, L. Vivas, E. Bongard, C. Thongphanchang, S. Taweechai, J. Vanichtankul, R. Rattanajak, U. Arwon, P. Fantauzzi, J. Yuvaniyama, W. N. Charman and D. Matthews, *Proc. Natl. Acad. Sci. U.S.A.*, 2012, **109**, 16823–16828.
183. S. R. Krungkrai and J. Krungkrai, *Asian Pac. J. Trop. Biomed.*, 2011, **1**, 233–242.
184. G. De Simone, A. Di Fiore, C. Capasso and C. T. Supuran, *Bioorg. Med. Chem. Lett.*, 2015, **25**, 1385–1389.
185. J. Krungkrai, A. Scozzafava, S. Reungprapavut, S. R. Krungkrai, R. Rattanajak, S. Kamchonwongpaisan and C. T. Supuran, *Bioorg. Med. Chem.* 2005, **13**, 483–489.
186. S. D. Prete, D. Vullo, G. M. Fisher, K. T. Andrews, S. Poulsen, C. Capasso and C. T. Supuran, *Bioorg. Med. Chem. Lett.*, 2014, **24**, 4389–4396.
187. D. Vullo, S. D. Prete, G. M. Fisher, K. T. Andrews, S. Poulsen, C. Capasso and C. T. Supuran, *Bioorg. Med. Chem.*, 2015, **23**, 526–531.
188. R. Munigunti, V. Mulabagal and A. I. Calderón, *J. Pharm. Biomed. Anal.*, 2011, **55**, 265–271.
189. R. Munigunti, S. Gathiaka, O. Acevedo, R. Sahu, B. Tekwani and A. I. Calderón, *Chem. Cent. J.* 2013, **7**, 175.
190. A. J.Theobald, I. Caballero, I. Coma, G. Colmenarejo, C. Cid, F. Gamo, M. J. Hibbs, A. L. Bass and D. A. Thomas. *Biochemistry*, 2012, **51**, 4764-4771.
191. R. Munigunti, N. Nelson, V. Mulabagal, M. P. Gupta, R. Brun, and A. I. Calderón, *Plant. Med.,* 2011, **77**, 1749-1753.
192. R. Munigunti, S. Gathiaka, O. Acevedo, R. Sahu, B. Tekwani and A. I. Calderón, *Nat. Prod. Res*. 2014, **28**, 359-364.
193. M. Winkler, M. Maynadier, S. Wein, M. Lespinasse, G. Boumis, A. E. Miele, H. Vial, and Y. Wong. *Org. Biomol. Chem.,* 2015, **13**, 2064-2077.
194. H. Cui, J. Carrero-Lérida, A. P. G. Silva, J. L. Whittingham, J. A. Brannigan, L. M. Ruiz-Pérez, K. D. Read, K. S. Wilson, D. González-Pacanowska and I. H. Gilbert, *J. Med. Chem.*, 2012, **55**, 10948-10957.
195. A. Kato, Y. Yasuda, Y. Kitamura, M. Kandeel and Y. Kitade, *Parasitol. Int.*, 2012, **61**, 501–503.
196. P. K. Ojha and K. Roy, *BioSystems*, 2013, **113**, 177–195.
197. Y. Noguchi, Y. Yasuda, M. Tashiro, T. Kataoka, Y. Kitamura, M. Kandeel and Y. Kitade, *Parasitol. Int*., 2013, **62**, 368–371.
198. K. S. Harris, J. L. Casey, A. M. Coley, J. A. Karas, J. K. Sabo, Y. Y. Tan, O. Dolezal, R. S. Norton, A. B. Hughes, D. Scanlon and M. Foley, *J. Biol. Chem.,* 2009, **284**, 9361-9371.
199. S. Arastu-Kapur, E. L. Ponder, U. P. Fonović, S. Yeoh, F. Yuan, M. Fonović, M. Grainger, C. I. Phillips, J. C. Powers, and M. Bogyo, *Nat. Chem. Biol*., 2008, 4, 203-213.
200. G. S. Dow, Y. Chen, K. T. Andrews, D. Caridha, L. Gerena, M. Gettayacamin, J. Johnson, Q. Li, V. Melendez, N. Obaldia III, T. N. Tran and A. P. Kozikowski, *Antimicrob. Agents Chemother.,* 2008, **52**, 3467-3477.
201. P. Mukherjee, A. Pradhan, F. Shah, B. L. Tekwani, and M. A. Avery, *Bioorg. Med. Chem.* 2008, **16**, 5254-5265.
202. C. L. Woodard, Z. Li, A. K. Kathcart, J. Terrell, L. Gerena, M. Lopez-Sanchez, D. E. Kyle, A. K. Bhattacharjee, D. A. Nichola, W. Ellis, S. T. Prigge, J. A. Geyer and N. C. Waters, *J. Med. Chem*., 2003, **46**, 3877-3882.
203. K. Maity, B. S. Venkata, N. Kapoor, N. Surolia, A. Surolia, and K. Suguna, *J. Struct. Biol.*, 2011, **176**, 238-249.
204. D. Tasdemir, G. Lack, R. Brun, P. Rüedi, L. Scapozza, and R. Perozzo, *J. Med. Chem.*, 2006, **49**, 3345-3353.
205. R.Conners, F. Schambach, J. Read, A. Cameron, R. B. Sessions, L. Vivas, A. Easton, S. L. Croft, and R. L. Brady, *Mol. Biochem. Parasitol*., 2005, **142**, 137-148.
206. A. Cameron, J. Read, R. Tranter, V. J. Winter, R. B. Sessions, R. L. Brady, L. Vivas, A. Easton, H. Kendrick, S. L. Croft, D. Barros, J. L. Lavandera, J. J. Martin, F. Risco, S. G. Ochoa, F. J. Gamo, L. Sanz, L. Leon, J. R. Ruiz, R. Gabarró, A. Mallo and F. G. de Ias Heras, *J. Biol. Chem.*, 2004, **279**, 31429-31439.
207. D. C. Madrid, L. Ting, K. L. Waller, V. L. Schramm, and K. Kim, *J. Biol. Chem*., 2008, **283**, 35899-35907.
208. J. Yuvaniyama, P. Chitnumsub, S. Kamchonwongpaisan, J. Vanichtanankul, W. Sirawaraporn, P. Taylor, M. D. Walkinshaw and Y. Yuthavong, *Nat. Struct. Biol.*, 2003, **10**, 357-365.
209. T. Triglia, J. G. T. Menting, C. Wilson and A. F. Cowman. *PNAS*, 1997, **94**, 13944-13949.
210. L. Jiang, P. Lee, J. White and Pradipsinh K. Rathod, *Antimicrob. Agents Chemother*., 2000, **44**, 1047-1050.
211. S. Reungprapavut, S. R. Krungkrai and Jerapan Krungkrai, *J. Enzyme Inhib. Med. Chem.,* 2004, **19,** 249-256.
212. R. L. Krauth-Siegel and G. H. Coombs, *Parasitol. Today,* 1999, **15**, 404-409.

Structure guided drug-discovery approach towards identification of *Plasmodium* Inhibitors

Babita Aneja[a], Bhumika Kumar[a], Mohamad Aman Jairajpuri[b], Mohammad Abid[a]*

This article provides a comprehensive review of inhibitors from natural, semisynthetic or synthetic sources against key targets of *Plasmodium falciparum.*